

1
2
3 **The 2019 Methane Budget And Uncertainties At 1 Degree Resolution And Each Country**
4 **Through Bayesian Integration Of GOSAT Total Column Methane Data And A Priori**
5 **Inventory Estimates**

6
7 Authors: John R. Worden¹, Daniel Cusworth^{1,4}, Zhen Qu², Yi Yin³, Yuzhong Zhang^{2,6}, A.
8 Anthony Bloom¹, Shuang Ma¹, Brendan Byrne¹, Tia Scarpelli², Joannes D. Maasakkers⁵, David
9 Crisp¹, Riley Duren⁴, and Daniel J. Jacob²

- 10
11 1) Jet Propulsion Laboratory / California Institute for Technology
12 2) Harvard University
13 3) California Institute for Technology
14 4) University of Arizona
15 5) SRON Netherlands Institute for Space Research
16 6) Westlake University
17

18 Corresponding Author: john.r.worden@jpl.nasa.gov

Deleted: @2021 All Rights Reserved

19
20 **Abstract:** We use Optimal Estimation (OE) to quantify methane fluxes based on total column
21 CH₄ data from the Greenhouse Gases Observing Satellite (GOSAT) and the GEOS-Chem global
22 chemistry transport model. We then project these fluxes to emissions by sector at 1 degree
23 resolution and then to each country using a new Bayesian algorithm that accounts for prior and
24 posterior uncertainties in the methane emissions. These estimates are intended as a pilot dataset
25 for the Global Stock Take in support of the Paris Agreement. However, differences between the
26 emissions reported here and widely-used bottom-up inventories should be used as a starting point
27 for further research because of potential systematic errors of these satellite based emissions
28 estimates. We find that agricultural and waste emissions are ~263 +/- 24 Tg CH₄/yr,
29 anthropogenic fossil emissions are 82 +/- 12 Tg CH₄/yr, and natural wetland/aquatic emissions
30 are 180 +/- 10 Tg CH₄/yr. These estimates are consistent with previous inversions based on
31 GOSAT data and the GEOS-Chem model. In addition, anthropogenic fossil estimates are

Deleted: present

Deleted: 2019 global methane (CH₄) emissions and uncertainties, by sector, at 1-degree and country-scale resolution based on a Bayesian integration of satellite data and inventories.

Deleted: Globally, we find that agricultural and fire emissions are 227 +/- 19 Tg CH₄/yr, waste is 50 +/- 7 Tg CH₄/yr , anthropogenic fossil emissions are 82 +/- 12 Tg CH₄/yr, and natural wetland/aquatic emissions are 180 +/- 10 Tg CH₄/yr.

Deleted: . *Calculation of emissions and uncertainties:* We first apply a standard optimal estimation (OE) approach to quantify CH₄ fluxes using Greenhouse Gases Observing Satellite (GOSAT) total column CH₄ concentrations and the GEOS-Chem global chemistry transport model. Second, we use a new Bayesian algorithm that projects these posterior fluxes to emissions by sector to 1 degree and country-scale resolution. This algorithm can also quantify uncertainties from measurement as well as smoothing error, which is due to the spatial resolution of the top-down estimate combined with the assumed structure in the prior emission uncertainties. *Detailed Results:*

55 consistent with those reported to the United Nations Framework Convention on Climate Change
56 [80.4 Tg CH₄/yr for 2019]. Alternative priors can be easily tested with our new Bayesian
57 approach (also known as prior swapping) to determine their impact on posterior emissions
58 estimates. We use this approach by swapping to priors that include much larger aquatic emissions
59 and fossil emissions (based on isotopic evidence) and find little impact on our posterior fluxes.
60 This indicates that these alternative inventories are inconsistent with our remote-sensing
61 estimates and also that the posteriors reported here are due to the observing and flux inversion
62 system and not uncertainties in the prior inventories. We find that total emissions for
63 approximately 57 countries can be resolved with this observing system based on the degrees-of-
64 freedom for signal metric (DOFS > 1.0) that can be calculated with our Bayesian flux estimation
65 approach. Below DOFS of 0.5, estimates for a countries total emissions are more weighted to our
66 choice of prior inventories. The top five emitting countries (Brazil, China, India, Russia, USA)
67 emit about half of the global anthropogenic budget, similar to our choice of prior emissions but
68 with the posterior emissions shifted towards the agricultural sector and less towards fossil
69 emissions, consistent with our global posterior results. Our results suggest remote sensing based
70 estimates of methane emissions can be substantially different (although within uncertainty) than
71 bottom-up inventories, isotopic evidence, or estimates based on sparse in situ data, indicating a
72 need for further studies reconciling these different approaches for quantifying the methane
73 budget. Higher resolution fluxes calculated from upcoming satellite or aircraft data, such as the
74 Tropospheric Monitoring Instrument (TROPOMI) and those in formulation such as the
75 Copernicus CO₂M, MethaneSat, or Carbon Mapper can be incorporated in our Bayesian
76 estimation framework for the purpose of reducing uncertainty and improving the spatial
77 resolution and sectoral attribution of subsequent methane emissions estimates.

78

Deleted: However, our results are on the high side for agricultural and waste emissions and the low side for fossil and wetland as compared to top-down estimates from the 2017 Global Carbon Project (GCP) [205-246 Tg CH₄/yr], [91-121 Tg CH₄/yr], and [155-217 Tg CH₄/yr] respectively, that are primarily based on in situ measurements.

Deleted: test

Deleted: Changing priors to test recent bottom-up results reflecting much larger

Deleted: with much

Deleted: and isotopic evidence reflecting much

Deleted: larger

Deleted: than our choice of priors does not fundamentally change our posterior emissions

Deleted: , indicating

Deleted: that

Deleted: t

Deleted: 8

Deleted: metric

Deleted:

Deleted: We find the top five emitting countries (Brazil, China, India, Russia, USA) emit about half of the global anthropogenic budget, similar to our choice of prior emissions. However, posterior emissions for these countries are mostly from agriculture, waste and fires (~129 Tg CH₄/yr) with ~45 Tg CH₄/yr from fossil emissions, as compared to prior inventory estimates of ~88 and 60 Tg CH₄/yr respectively, primarily because the satellite observed concentrations are larger than expected in regions with substantive livestock activity. Differences are outside of 1-sigma uncertainties between prior and posterior for Brazil, India, and Russia but are consistent for China and the USA. The new Bayesian algorithm to quantify emissions from fluxes also allows us to “swap priors” if better informed or alternative priors and/or their covariances are available for testing. For example, recent bottom-up literature supposes greatly increased values for wetland/aquatic as well as fossil emissions. Swapping in priors that reflect these increased emissions results in posterior wetland emissions or fossil emissions that are inconsistent (differences greater than calculated uncertainties) with these increased bottom-up estimates, primarily because constraints related to the methane sink only allow total emissions across all sectors of ~560 Tg CH₄/yr and because the satellite based estimate well constrains the spatially distinct fossil and wetland emissions. Given that this observing system consisting of GOSAT ... [1]

Deleted: -

Deleted: offer the promise of much higher resolution fluxes relative to GOSAT assuming they can provide data wi... [2]

Deleted: in principal

Deleted: the

Deleted: demonstrated here

177 Table of Contents

178	<u>1.0 Introduction</u>	4
179	<u>1.1 Atmospheric Methane Background</u>	4
180	<u>1.2 Global Stock Take</u>	5
181	<u>1.3 Overview of Bottom-Up Emissions And Uncertainties</u>	6
182	<u>1.4 Use of Remote Sensing For Quantifying Emissions and Uncertainties</u>	7
183	<u>2.0 Approach for Quantifying “Top Down” Emissions Using Satellite Data</u>	10
184	<u>2.1 Top Down Flux Estimates</u>	11
185	<u>2.2 Projecting Fluxes To Emissions And Their Uncertainties</u>	16
186	<u>2.3 Generation of Prior Emissions, Covariances, and Uncertainties</u>	18
187	<u>3.0 Results</u>	25
188	<u>3.1 Global Methane Budget By Sector</u>	26
189	<u>3.2 Top 10 Emitting Countries</u>	29
190	<u>3.3 Results for all Countries</u>	32
191	<u>3.4 What Happens to (Top Down) Methane Budget if Priors for Wetland/Aquatic and Fossil Emissions are Substantially Increased?</u>	33
192		
193	<u>4.0 Summary and Future Directions</u>	35
194	<u>5.0 Data Repositories</u>	36
195	<u>6.0 Author Contributions</u>	37
196	<u>7.0 Acknowledgements</u>	37
197	<u>8.0 Appendix table of emissions for each country ordered by DOFS</u>	38
198	<u>9.0 References</u>	61
199		
200		
201		

Deleted: 1.0 → **Introduction** - 5¶
 1.1 → Atmospheric Methane Background - 5¶
 1.2 → Global Stock Take - 6¶
 1.3 → Overview of Bottom-Up Emissions And Uncertainties - 7¶
 1.4 → Use of Remote Sensing For Quantifying Emissions and Uncertainties - 8¶
2.0 Approach for Quantifying “Top Down” Emissions Using Satellite Data - 10¶
 2.1 → Top Down Flux Estimates - 11¶
 2.2 → Projecting Fluxes To Emissions And Their Uncertainties - 15¶
 2.3 → Generation of Prior Emissions, Covariances, and Uncertainties - 18¶
3.0 Results: Total Emissions and Emissions by Country - 23¶
 3.1 → Global Methane Budget By Sector - 24¶
 3.2 → Top 10 Emitting Countries - 26¶
 3.3 → Results for all Countries - 29¶
 3.4 → What Happens to (Top Down) Methane Budget if Priors for Wetland/Aquatic and Fossil Emissions are Substantially Increased? - 30¶
4.0 Summary and Future Directions - 31¶
5.0 Data Repositories - 32¶
6.0 Author Contributions - 33¶
7.0 Acknowledgements - 33¶
8.0 Appendix table of emissions for each country ordered by DOFS - 34¶
9.0 References - 57¶

230

231

1.0 Introduction

232

1.1 Atmospheric Methane Background

233

234 Atmospheric methane (CH_4) is the second most important anthropogenic greenhouse gas
 235 behind carbon dioxide (CO_2) and a contributor to poor surface air quality as it is an ozone
 236 precursor. Atmospheric methane has increased by nearly a factor 3 over its pre-industrial values
 237 largely due to anthropogenic emissions (e.g. [Dlugokencky et al. 2011](#); Ciais *et al.* 2013, and refs
 238 therein). Over the last two decades, methane has been increasing but for reasons that are still
 239 being assessed, although recent studies provide evidence that it is due to a combination of fossil
 240 and agricultural emissions with some role due to variations in the atmospheric sink of methane
 241 (e.g. Schaefer *et al.* 2016; Worden *et al.* 2017; Turner *et al.* 2019; Zhang *et al.* 2021). However,
 242 it is unclear which regions and which sectors are the cause of changes in atmospheric methane
 243 over the last twenty years because of substantial uncertainties in all components of the methane
 244 budget (Kirchke *et al.* 2013, Janssens *et al.* 2019; Sanoussi *et al.* 2020) from the global (Table 1)
 245 to local scale (Section 2). Methane has a relatively short lifetime of approximately 9 years
 246 making it an attractive target for emissions reduction as a decline in emissions will have a rapid
 247 impact on net radiative forcing and corresponding atmospheric heating (e.g. Shindell *et al.* 2009;



Deleted: ;

Deleted: Dlugokencky *et al.* 2011

Sector	Prior (Tg CH_4/yr)	Posterior (Tg CH_4/yr)
Wetlands / Aquatic Seeps	199.8+/-52.8 32.0+/-6.2	179.8+/-10.0 22.5+/-3.8
Livestock	87.6+/-17.2	146.1 +/ -10.3
Rice	36.9+/-12.9	67.6 +/- 6.8
Fires	15.1+/-2.5	13.3+/-2.2
Waste	57.7+/-11.9	49.6+/-7.1
Oil	41.6+/-9.7	28.8 +/- 4.7
Gas	24.5+/-4.7	28.0 +/- 3.6
Coal	31.4+/-9.8	25.3 +/- 3.9
Total	526+/-128	561 +/- 52

Table 1: Prior emissions and uncertainties are generated from various inventories or models (Section 2.3). Posterior emissions represent projection of satellite based fluxes back to emissions while accounting for the prior emissions distribution and covariances (Section 2.2). We conservatively assume uncertainties are 100% correlated so that the total reported prior and posterior uncertainties are the sum of the individual uncertainties.

250 Ganeson *et al.* 2019; Turner *et al.* 2019). Hence there is significant interest in accurately
251 quantifying methane emissions for identifying those emissions that can be efficiently reduced.

252

253 **1.2 Global Stock Take**

254

255 As part of the effort to reduce methane emissions and corresponding risk related to
256 changes in climate, the Paris Agreement resulted in a framework by which countries provide an
257 accounting of their emissions. A “Global Stock Take” (GST) to track progress in emission
258 reductions is conducted at five-year intervals, beginning 2023. To support the first GST, Parties
259 to the Paris Agreement are compiling inventories of GHG emissions and removals to inform
260 their progress. Inventories are generally estimated using “bottom-up” approaches, in which
261 emission estimates are generally based on activity data and emission factors. These bottom-up
262 methods can provide precise and accurate emission estimates when the activity data are well
263 quantified and emission factors are well understood. However, substantial uncertainties exist for
264 emissions in many parts of the globe where these measurements are not rigorously made or
265 tested across multiple sites. Even regions and emissions that are thought to be well measured can
266 have significant differences between independent assessments and official reports; for example,
267 Alvarez *et al.* (2018) demonstrates that 2015 oil and gas emissions are under estimated by the
268 United States Environmental Protection Agency by about 60%. These differences, if they are
269 representative for emissions across the globe indicate a need for an independent assessment of
270 emissions and their uncertainties to better evaluate if reported changes in emissions are in fact
271 occurring or if changes in the natural carbon cycle through wetlands and the methane sink are
272 substantively affecting atmospheric methane burden. Top down estimates of methane emissions
273 using atmospheric measurements provide an independent way of testing these inventories as
274 observed methane concentrations are compared against expected concentrations that result from
275 reported inventories. The objective of this paper is to demonstrate the use of satellite
276 observations for testing and updating emissions by sector for use with the Global Stock Take.
277 While these top-down atmospheric methane budgets cannot replace the detailed activity reports
278 used to generate bottom-up inventories, they can be combined with those bottom-up products to
279 produce a more complete and transparent assessment of progress toward greenhouse gas
280 emission reduction targets. They can also help determine if the natural part of the methane
281 budget is becoming a strong component of atmospheric methane increases. As discussed next, an

282 important component of this ~~assessment~~ is the evaluation of uncertainties from both bottom-up
283 inventories and in top-down approaches.

~~Deleted: effort~~

284
285

286 ***1.3 Overview of Bottom-Up Emissions And Uncertainties***

287
288 Bottom-up uncertainties are calculated for the methane budget by comparison between
289 independent methods or sources, evaluating multiple estimates from a single source, comparison
290 between models and remote sensing data, and expert opinion. For example, Saunois *et al.*
291 (2020) uses a range of results from different studies to quantify uncertainty in the different
292 sectors of the methane budget. However, these uncertainties are likely underestimated as they
293 suggest that total anthropogenic agricultural emissions, for example, are known to 10% or
294 better, whereas comparisons between different global inventories (e.g., Janssens-Maenhout *et al.*
295 2019) suggest a much larger range of estimates for the global totals (e.g., 129 to 219 Tg CH₄/yr
296 for agriculture, and 129 to 164 Tg CH₄/yr for fossil emissions). Uncertainties in national or
297 regional total emissions are even more challenging to estimate such that expert opinion is used:
298 Janssens-Maenhout *et al.* (2019) suggests that Annex 1 (developed) countries have
299 approximately 15% uncertainty in reported fossil emissions whereas Annex 2 countries have
300 ~30% uncertainties, essentially asserting that less informed inventories have double the
301 uncertainty of better informed emissions. Wetland emissions, which comprise ~30-45 % of the
302 methane budget also show significant differences of up to 40% across wetland models (e.g.
303 Melton *et al.* 2013; Poulter *et al.* 2017, Ma *et al.* 2021), depending on region. An example of
304 how these uncertainties are projected to the total methane budget for each of the main sectors is
305 presented in Table 1 using the prior emissions and their uncertainties for the analysis discussed
306 in this paper (Section 2.3).

307 However, recent studies challenge even these estimates of emission uncertainties;
308 emissions for lakes and rivers could be as large or larger than wetlands, with correspondingly
309 larger uncertainties of 50% or more (Saunois *et al.* 2020; Rosentreter *et al.* 2021). Primarily
310 because of this extra term from lakes and rivers, the total budget from bottom-up inventories
311 discussed in Saunois *et al.* (2020) ranges from 583 – 861 Tg CH₄/yr. Contrasting with this much
312 larger than expected biogenic source is isotopic evidence that suggests fossil emissions are also
313 much larger than expected, 160 +/- 40 Tg CH₄/yr (Schweitzke *et al.* 2017). These larger than

315 expected values from aquatic and fossil sources are challenging to reconcile with existing bottom
316 up estimates and with global estimates from the top down which are primarily constrained by the
317 methane sink. For example, the methane sink must approximately balance total methane
318 emissions, leading to total emissions of 560 ± 60 Tg CH₄/yr (e.g., Prather *et al.* 2012).
319 Consequently much larger values in either aquatic emissions or fossil emissions must be
320 balanced by much lower emissions in other sectors indicating that either our knowledge of the
321 processes controlling different components of the methane sink are fundamentally wrong or one
322 or both of these inflated emissions is incorrect, that is, well outside calculated uncertainties.
323

324 **1.4 Use of Remote Sensing For Quantifying Emissions and Uncertainties**
325

326 Top-down approaches using in situ or remote sensing measurements of atmospheric
327 methane can be used to evaluate and update bottom-up emissions (or inventories) by first
328 projecting bottom up emissions through a chemical transport model to atmospheric
329 concentrations and then comparing these modeled concentrations to observations (e.g.

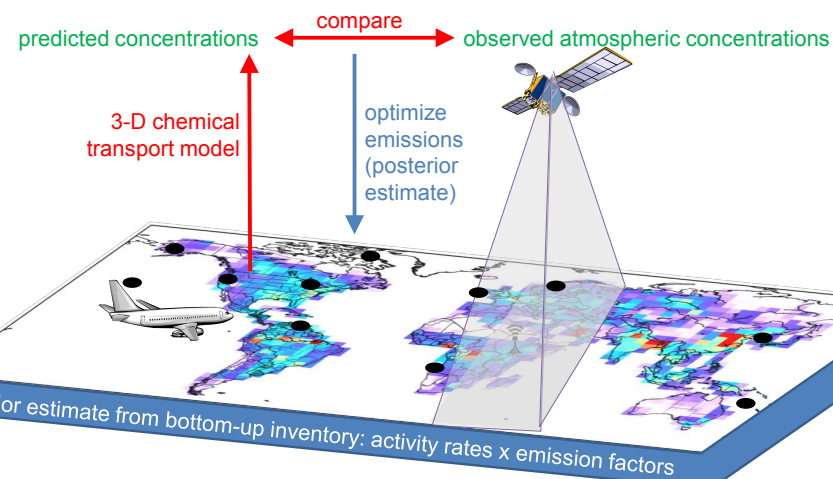


Figure 1: Schematic describing how observed atmospheric concentration data are used with a global chemistry transport model to quantify methane fluxes.

330 Frankenberg *et al.* 2005; Bergamaschi *et al.* 2013, Qu *et al.* 2021 and refs therein). An inverse
331 method is utilized to update the net flux (or total emissions and surface sinks) within a chosen
332 grid scale based on the mismatch between modeled and observed concentrations (Figure 1).
333 When the top-down quantified flux can be uniquely associated with a single source, these tests of
334 bottom-up inventories provide information about biases in the reported emission (e.g., Duren *et*
335 *al.* 2019, Varon *et al.* 2019, Pandey *et al.* 2019) which can be used to either update the emissions
336 or provide evidence that additional research is needed to improve the process knowledge used to
337 construct the emissions. However, top-down fluxes have other uncertainties that must be
338 accounted for when comparing to bottom-up inventories, these include 1) systematic and random
339 uncertainties in the data, 2) systematic errors in the model that relates observed methane
340 concentrations to fluxes, and 3) smoothing error related to uncertainty in the prior emissions
341 combined with the spatial resolution of the top-down estimate.

342 Top-down approaches can typically quantify the precision of the fluxes as it is directly
343 related to the uncertainties of the observations and the prior knowledge of the flux distribution.
344 However, the accuracy of the top-down fluxes related to data and model is more challenging to
345 quantify and recent results suggest that these errors can be substantive. For example, Qu *et al.*
346 (2021) demonstrates that systematic differences between total column CH₄ concentrations from
347 TROPOMI and GOSAT satellite data, likely related to poorly characterized surface albedo, can
348 lead to substantial differences when used to constrain top-down fluxes. For example, there is
349 almost a 100% difference between estimated livestock emissions in Brazil when comparing
350 TROPOMI versus GOSAT based fluxes, which Qu *et al.* (2021) attributes to biases in the
351 TROPOMI total column data due to surface albedo variations over Brazil.

352 Errors in model transport and chemistry are another significant uncertainty when
353 inverting concentration data to fluxes. For example, McNorton *et al.* (2020) finds that model
354 errors in atmospheric concentrations that result from atmospheric transport can be as large or
355 larger as uncertainties in the data, leading to almost a doubling of the uncertainty in top-down
356 fluxes. Schuh *et al.* (2019) demonstrates that transport errors can result in biases of up to 1.7
357 Petagrams of carbon in top-down CO₂ fluxes, about the same as the global net yearly carbon
358 sink. Jiang *et al.* (2013) also demonstrates that errors in convection can affect surface emissions
359 estimates of CO by up to 40% in regions of strong convection such as S.E. Asia. Unfortunately,
360 challenges remain in quantifying how model uncertainties project to flux uncertainty. One

Deleted:

Deleted: 2) smoothing error related to uncertainty in the prior emissions combined with the spatial resolution of the top-down estimate, and 3) systematic errors in the model that relates observed methane concentrations to fluxes.

Deleted: Similarly, McNorton *et al.* (2020) finds that model errors can be as large or larger as uncertainties in the data, which could lead to almost a doubling of the expected uncertainty in top-down fluxes.

370 approach is to use an ensemble of models for the inversion in which the same data and
371 constraints are used for the inverse model; a challenge here is to ensure that the inversion
372 approach used with each model is consistent. For example, the Global Carbon Project (Saunois *et*
373 *al.* 2020) uses an ensemble of model inversions using different data sets to evaluate flux
374 inversion errors; however, as shown in Section 2.2, this approach does not attempt to attribute
375 differences in results to either the model, data, or spatial resolution and hence it can be
376 challenging to identify approaches to reduce overall uncertainty. Another approach is to use
377 different data sets but the same model and inversion setup to quantify emissions, as different
378 sensitivities of the model to the different observed concentrations are affected by model error
379 (Jiang *et al.* 2015; Yin *et al.* 2021). A third approach is to mitigate model and transport error. For
380 example, Jiang *et al.* (2015) assimilates observed CO concentrations over ocean regions before
381 inverting for continental source emissions to ensure that model/data mismatch over the ocean
382 does not affect the emissions estimates. As discussed in the next section our flux inversion
383 jointly estimates OH (the primary methane sink) with methane emissions to mitigate the impact
384 of OH variability on CH₄ emissions estimates. A latitudinal correction is also applied to both
385 data and model to ensure that errors in stratospheric chemistry and transport have less of an
386 impact on the estimated fluxes. However, the residual systematic errors from model transport
387 and chemistry are not characterized although there is no evidence to suspect significant
388 systematic errors based on comparing posterior concentrations with independent data as
389 discussed in the next section. Nonetheless, as stated in the abstract, differences between top-
390 down emissions reported in this manuscript with those from bottom-up efforts should be
391 considered as a starting point for new investigation as opposed to confirmation or falsification of
392 the top-down or bottom up estimate.

393 Smoothing error is also a significant but challenging component of the emissions error
394 budget to quantify for top-down estimates.. This uncertainty depends on the spatial and temporal
395 resolution of the top-down estimate combined with the prior uncertainty of the emissions
396 (Rodgers 2000). The spatial resolution of the estimate in turn depends on the sampling, pixel
397 size, measurement uncertainty, and lifetime of the gas. As typical top-down estimates do not
398 quantify the terms needed to quantify smoothing error, smoothing error is not usually represented
399 in top-down error budgets. However, this term can be the largest of the error sources, as
400 discussed further in Section 2.1, especially if the *a priori* uncertainties for emissions are poorly

Deleted: Smoothing error, is also challenging to quantify for top-down estimates.

403 characterized. Our Bayesian, optimal estimation approach (Rodgers 2000) described here allows
404 us to quantify smoothing error for the sectoral emissions presented here (Sections 2.2. and 2.3).
405 Furthermore, by reporting the averaging kernel matrices and fluxes we can remove smoothing
406 error in comparisons between top-down fluxes and bottom-up models (Ma *et al.* 2021) or greatly
407 reduce the smoothing error component in comparisons between two different instruments (e.g.
408 Cusworth *et al.* 2021).

409 Related to the problem of calculating smoothing error is that many top-down fluxes are
410 projected back to emissions by assuming that all emissions within a grid can be uniformly scaled
411 by the ratio of posterior to prior flux (e.g., Maasakkers *et al.* 2019 and references therein). This
412 method, while computationally expedient, diverts from the Bayesian assumptions used with top-
413 down inversions, potentially adding poorly characterized uncertainty and potentially unphysical
414 biases (Cusworth *et al.* 2021) to the emissions estimates, because it does not account for the
415 structure of the errors or their correlations and instead assumes that different types of emissions
416 within a grid cell (e.g. fires, fossil, livestock, wetlands) are 100% correlated. Shen *et al.* (2021)
417 addresses this problem by weighting the posterior emissions estimate by their prior uncertainty.
418 Our approach used here is derived in Cusworth *et al.* (2021) and summarized in Section 2.2,
419 addresses this problem by accounting for the structure of the errors, following a Bayesian
420 methodology from the start of the problem (calculation of fluxes using observations) to the end
421 (calculation of emissions from fluxes).

422

423 **2.0 Approach for Quantifying “Top Down” Emissions Using Satellite Data**

424 Our emission quantification approach is described in this section. First optimal estimation
425 is used (Section 2.1) to quantify methane fluxes on a 2x2.5 grid using the GEOS-Chem global
426 chemistry transport model with GOSAT satellite data for the year 2019. For our purposes of
427 emissions attribution, this first inverse step must report the prior as well as the posterior flux
428 error covariance (or Hessian) matrices (Zhang *et al.* 2021, Qu *et al.* 2021). The posterior error
429 covariance (or Hessian) can be computationally challenging to calculate so is typically not
430 reported with variational or adjoint based top-down estimates and instead ensemble approaches
431 are used to approximate flux uncertainties (e.g. Janadarnan *et al.* 2020). However in our
432 approach, this first step uses analytic Jacobians derived from the GEOS-Chem model that relate
433 emissions to concentrations and hence has been traditionally computationally expensive as

Deleted: Our Bayesian, optimal estimation approach (Rodgers 2000) described here allows us to either remove the effect of smoothing error in comparisons between top-down fluxes and wetland models such as demonstrated in Ma *et al.* (2021) or to explicitly quantify it for sectoral emissions (Section 2.2 and 2.3).[§]

Deleted: et al

441 compared to ensemble or adjoint based inversion methods, but does allow for a straightforward
442 calculation of the Hessian. The second step (Section 2.2) uses the prior fluxes, the corresponding
443 constraint and Hessian covariance matrices, and priors and prior covariances for emissions by
444 sector, to linearly project the fluxes to emissions by sector at 1 degree resolution while
445 accounting for the prior uncertainty distributions, correlations in the posterior covariance, and
446 varying spatial resolution. This step can use different prior emissions and prior covariances from
447 that of the flux inversion as the information from the flux inversion is preserved (Rodgers and
448 Connor 2003). Critical to this second step is that prior uncertainties and their correlations are
449 provided for the emissions for the desired sector and spatial resolution (Section 2.3).

450
451 **2.1 Top Down Flux Estimates**
452

453 We estimate top-down fluxes based on the approach and results described in Maasakkers *et*
454 *al.* (2021), Zhang *et al.* (2021) and Qu *et al.* (2021) and the reader is referred to these papers for
455 a more extensive description of the approach and validation of these methane fluxes. To
456 summarize, we optimize a state vector that consists of (1) 2019 methane emissions from all
457 sectors on a global $2^\circ \times 2.5^\circ$ grid (4020 elements); and (2) tropospheric OH concentrations in
458 northern and southern hemispheres (2 elements). We assume the seasonal variations of methane
459 emissions to be correct in the prior inventory and apply posterior/prior ratio equally to all months
460 in each grid cell. The optimization of annual hemispheric OH concentrations avoids propagating
461 biases in the simulated interhemispheric OH gradient to the solution for methane emissions
462 (Zhang *et al.*, 2018). We solve this Bayesian problem analytically, which yields a best posterior
463 estimate for the state vector, the posterior error covariance matrix, and the averaging kernel
464 matrix. Unlike in Zhang *et al.* (2021) and Qu *et al.* (2021), wetland fluxes are not treated as
465 separate elements in the state vector as we found that introduced uncertainties into the sectoral
466 attribution because the wetland flux areas used in Qu *et al.* (2021) could overlap the different
467 regions (Table 2) used in our approach to mitigate computational complexity.

468 The inverse problem is regularized by prior estimates for the state vector, which are compiled
469 from multiple bottom-up studies. The EDGAR v4.3.2 global emission inventory for 2012
470 (Janssens-Maenhout *et al.*, 2017) is used as default for anthropogenic emissions, superseded in
471 the U.S. by Maasakkers *et al.* (2016) and for the fossil fuel exploitation sector by Scarpelli *et al.*
472 (2020). Seasonalities of emissions from manure management and rice cultivation are specified

Deleted: We estimate top-down fluxes based on the approach described in Zhang *et al.* (2021) and Qu *et al.* (2021). We ...

476 following Maasakkers et al. (2016) and B. Zhang et al. (2016), respectively. Monthly wetland
477 emissions in 2019 are from the WetCHARTS v1.3.1 18-member ensemble mean (Bloom et al.,
478 2017). Note that in Zhang et al. (2021) and Qu et al. (2021), wetland fluxes are not included in
479 the gridded fluxes but instead estimated separately so as to better compare to bottom-up models
480 (Ma et al. 2021). In the top-down flux inversion used here, wetland fluxes are included with the
481 other emissions in each grid as we found that partitioning fluxes back to their sectoral
482 contribution (next section) was challenging due to gridding errors when wetland fluxes are
483 separately considered in the cost function. Daily global emissions from open fires are taken from
484 GFEDv4s (van der Werf et al., 2017). Global geological emissions for the flux inversion are set
485 to be 2 Tg a⁻¹ based on Hmiel et al. (2020) with the spatial distribution from Etiope et al. (2019).
486 Termite emissions are from Fung et al. (1991). The prior estimates for the hemispheric
487 tropospheric OH concentrations are based on a GEOS-Chem full chemistry simulation (Wecht et
488 al., 2014).

489 The GEOS-Chem CTM v12.5.0 (10.5281/zenodo.3403111) is used as forward model for
490 the inversion. The simulation is driven by MERRA-2 meteorological fields (Gelaro et al., 2017)
491 from the NASA Global Modeling and Assimilation Office (GMAO) with 2°×2.5°
492 horizontal resolution and 47 vertical layers (~ 30 layers in the troposphere). We excluded
493 observations poleward of 60°, where low Sun angles and extensive cloud cover make the
494 retrieval more difficult, and stratospheric CTM bias can affect the inversion (Turner et al., 2015).
495

496 The posterior estimate as defined by Bayesian inference assuming Gaussian error
497 statistics is obtained by minimizing the cost function $J(x)$:

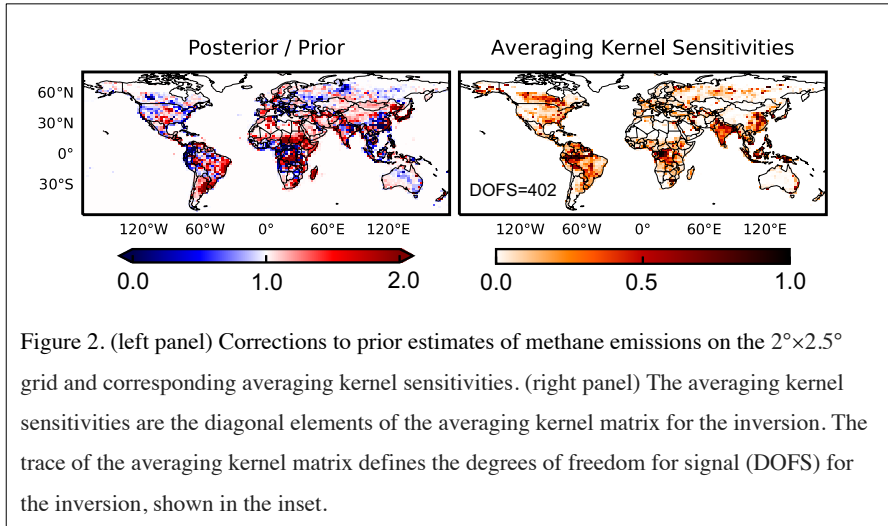
498

$$499 J(x) = (\mathbf{x} - \mathbf{x}_A)^T \mathbf{S}_A^{-1} (\mathbf{x} - \mathbf{x}_A) + \gamma (\mathbf{y} - \mathbf{Kx})^T \mathbf{S}_y^{-1} (\mathbf{y} - \mathbf{Kx}), \quad (1)$$

500

501

502 where \mathbf{K} is the Jacobian matrix describing the sensitivity of the observations to the state vector as
503 simulated by GEOS-Chem. The vector \mathbf{x}_A is the prior flux estimate. \mathbf{S}_A is the *a priori*
504 covariance matrix for this inversion and is a diagonal matrix that is constructed by assuming
505 50% prior error standard deviation for emissions on the 2°×2.5° grid and 10% prior error
506 standard deviation for hemispheric annual mean OH concentrations. \mathbf{S}_y is the observational error



507 covariance matrix. Diagonal elements of \mathbf{S}_y are calculated using the residual error method (Heald
 508 et al., 2004) as the variance of the residual difference between observations and the GEOS-Chem
 509 prior simulation on the $2^\circ \times 2.5^\circ$ grid after subtracting the mean difference. We use a
 510 regularization parameter γ (Hansen et al., 1999; Y. Zhang et al., 2018, 2020; Maasakkers et al.,
 511 2019; Lu et al., 2021) to account for the off-diagonal structure missing in \mathbf{S}_y . Based on the corner
 512 of the L-curve (Hansen et al., 1999) and the expected chi-square distribution of the cost function
 513 (Lu et al., 2021), we choose $\gamma = 0.5$ (Qu et al., 2021).

514 Assuming that the problem for quantifying methane fluxes from observed concentrations
 515 is linear, or only moderately non-linear, then the fluxes, \mathbf{x} , can be related to observed methane
 516 concentrations using the following equation: (Rodgers 2000):
 517

$$518 \quad \mathbf{x} = \mathbf{x}_A + \mathbf{SK}^T \mathbf{S}_y^{-1} (\mathbf{y} - \mathbf{Kx}_A) \quad (2)$$

519

520 The posterior error covariance matrix \mathbf{S} is given by:
 521

$$522 \quad \mathbf{S} = (\mathbf{K}^T \mathbf{S}_y^{-1} \mathbf{K} + \mathbf{S}_A^{-1})^{-1}. \quad (3)$$

523

524

525 This top-down flux inversion also provides the spatial resolution matrix or Averaging Kernel
526 Matrix \mathbf{A} , which defines the sensitivity of the solution to the true state:

527
528

$$529 \quad \mathbf{A} = \mathbf{I} - \mathbf{S}\mathbf{S}_\mathbf{A}^{-1}, \quad (4)$$

530

531 Summing the diagonal elements of the averaging kernel for a given region provides the
532 Degrees of Freedom for Signal (or DOFS), a useful metric for the sensitivity of the observing
533 system to the underlying fluxes as it describes the sensitivity of the estimated fluxes to the actual
534 distribution of fluxes (Rodgers 2000). Figure 2 (right panel) shows the averaging kernel
535 sensitivities (or diagonal elements of the averaging kernel matrix) of the inversions. The
536 averaging kernel sensitivities are highest over major anthropogenic source regions, where the
537 methane emissions are the largest and the observations have a good ability to determine the
538 posterior solution independently of the prior estimate. The inversion has ~402 DOFS for
539 methane emissions, meaning that it contains 402 independent pieces of information on the
540 distribution of methane emissions. Although our flux inversion is based on the top-down setup
541 described in Qu *et al.* (2021), this value is larger than the DOFS reported in Qu et al. (2021)
542 because that estimate separates wetlands from non-wetlands in the inversion scheme whereas the
543 flux estimate used here does not. The posterior / prior ratios for the 2019 inversion in Figure 2
544 (left panel) show consistent upward adjustments in the south-central US, Venezuela, and the
545 Middle East and downward adjustments in the western US and North China Plain, consistent
546 with Qu et al. (2021) and Zhang et al. (2021).

547 If the matrix $\mathbf{S}_\mathbf{A}$ in equations 1 and 3 represents the actual *a priori* uncertainty
548 corresponding to the *a priori* $\mathbf{x}_\mathbf{A}$, then the posterior error covariance describes the total error for
549 the estimate (Rodgers 2000). In practice, the matrix $\mathbf{S}_\mathbf{A}$ represents a “constraint matrix” that is
550 either a best guess for uncertainties of fluxes (e.g., assumed here to be 50%) within a grid and/or
551 it is constructed to ensure the inversion converges, typically because systematic errors in the data
552 and/or the model or numerical instabilities make it challenging to find a global minimum in the
553 cost function as shown in Equation 1 (Bowman *et al.* 2006). In the case where $\mathbf{S}_\mathbf{A}$ represents a
554 constraint matrix, the total posterior error becomes:

555

$$556 \quad \mathbf{S}_{\text{tot}} = (\mathbf{I} - \mathbf{A})\mathbf{S}_\mathbf{A}^{\text{true}}(\mathbf{I} - \mathbf{A})^\top + \mathbf{S}\mathbf{K}^\top\mathbf{S}_y^{-1}\mathbf{K}\mathbf{S} \quad (5)$$

557

558 Where the $\mathbf{S}_A^{\text{true}}$ is the *a priori* uncertainties for the estimate. In practice, $\mathbf{S}_A^{\text{true}}$ can be
 559 challenging to calculate due to lack of information about the emissions or fluxes and may not
 560 even be invertible because of correlations within the matrix. However, we use a set of informed
 561 inventories and models to generate a prior covariance for methane emissions as described in the
 562 next section. As discussed Worden *et al.* (2004), the smoothing error in the estimate is the first
 563 term on the right side, the error due to measurement uncertainty is the second/middle term, and
 564 the last term is that due to systematic errors in the model. While the variables in Equation 5 are
 565 representative here of the top-down flux estimate, the formulation can be generalized for any
 566 estimate to support interpretation of the results. For example, in a system with perfect resolution
 567 the averaging kernel matrix becomes the identity matrix and the smoothing error becomes zero,
 568 hence the reason that improving the spatial resolution reduces the smoothing error, an important
 569 goal which can be realized with the increased observation density of up-coming satellites such as
 570 CO2M, methane-sat, and Carbon Mapper. Equation 5 also demonstrates that poorly
 571 characterized prior uncertainties in one region affect an estimate in another regions because of
 572 cross-terms in the averaging kernel matrix \mathbf{A} . This aspect of top-down inversions must therefore
 573 be accounted for when interpreting the seasonality and magnitude of top-down fluxes (e.g. Ma *et*
 574 *al.* 2021).

575 Systematic errors can be included by adding the following term: $\mathbf{SK}_{\text{sys}}^T \mathbf{S}_{\text{sys}}^{-1} \mathbf{K}_{\text{sys}}^T \mathbf{S}$,
 576 where \mathbf{K}_{sys} is the Jacobian that describes the sensitivity of the modeled concentrations to different
 577 parameters in the model that relate emissions to concentrations and \mathbf{S}_{sys} is a matrix containing
 578 uncertainties for the model or data parameters. In this manuscript we do not explicitly calculate
 579 systematic errors for the fluxes. We are currently studying how to empirically evaluate
 580 systematic errors in the flux estimate, following the approach in Jiang *et al.* (2015) for use in
 581 quantifying uncertainties in methane fluxes and emissions.

582

583 **Evaluation of Top-Down Flux Estimates:** The combination of model (GEOS-chem)
 584 and data (GOSAT) used to quantify methane fluxes have been evaluated previously by
 585 comparing prior and posterior model concentrations to independent data. Maasakkers *et al*
 586 (2019) finds that posterior methane concentrations have correlations (R^2) of 0.76, 0.81, and 0.91
 587 with data from surface sites, aircraft, and total column data respectively. These correlations are

588 essentially the same as those for the GEOS-chem prior concentrations, likely because these
589 measurements are taken in background regions away from sources. These comparisons between
590 posterior concentrations with independent data sets demonstrate that the GEOS-Chem model
591 with GOSAT data has skill in quantifying atmospheric methane concentrations and that
592 assimilating GOSAT data into GEOS-Chem for the purpose of quantifying fluxes is at least as
593 skillful as using prior information when looking at background regions away from emissions
594 sources. Changes in fluxes based on GOSAT data are therefore driven entirely by differences in
595 satellite observed concentrations over source regions.

596

597

598 **2.2 Projecting Fluxes To Emissions And Their Uncertainties**

599

600 The derivation that describes how to project top-down fluxes back to emissions by sector
601 at arbitrary resolution is described in Cusworth *et al.* (2021) and summarized in this section.
602 For policy-relevance and CH₄ budget quantification, we wish to optimize emissions (**z**) using
603 atmospheric observations, i.e., we want to compute the explicit posterior representation without
604 re-simulation of an atmospheric transport model. The relationship we use between emissions **z** and
605 fluxes **x** is simple aggregation (the total flux within a grid box is the sum of emissions), and can
606 be represented by matrix **M**:

607

608 $\mathbf{x} = \mathbf{M}\mathbf{z}$. (6)

609

610 The solution for projecting fluxes back to emissions takes the form (Cusworth *et al.* 2021):

611

612 $\mathbf{z} = \mathbf{z}_A + \mathbf{Z}\mathbf{M}^T\mathbf{S}^{-1}[(\mathbf{I} - \mathbf{S}\mathbf{S}_A^{-1})(\mathbf{x}_A - \mathbf{M}\mathbf{z}_A) + (\mathbf{x} - \mathbf{x}_A)]$ (7)

613

614 where the (**z**) is the posterior emissions vector with error covariance (**Z**) and **I** is the identity matrix,
615 The posterior emission error covariance matrix **Z** is calculated explicitly given **M**, **S_A**, **S**, and prior
616 emissions error covariance matrix **Z_A**:

617

618 $\mathbf{Z} = (\mathbf{M}^T(\mathbf{S}^{-1} - \mathbf{S}_A^{-1})\mathbf{M} + \mathbf{Z}_A^{-1})^{-1} = (\mathbf{M}^T(\mathbf{K}^T\mathbf{S}_y^{-1}\mathbf{K})\mathbf{M} + \mathbf{Z}_A^{-1})^{-1}$ (8)

619

620 This solution depends on the top-down flux inversion providing the inversion characterization
 621 products (i.e., the flux prior \mathbf{x}_A and flux constraint matrix \mathbf{S}_A and the flux Hessian \mathbf{S}). Note that
 622 here we must use the Hessian as described in Equation 3, not the total posterior covariance as
 623 described by Equation 5 (Cusworth *et al.* 2021). To quantify the set of sectoral emissions \mathbf{z} , a
 624 corresponding prior emissions \mathbf{z}_A , and covariance matrix \mathbf{Z}_A , must be provided at the desired
 625 spatial grid; in this study we choose a 1 degree lon/lat grid. Note that the emissions and their
 626 prior uncertainties used to generate prior fluxes for the top-down flux inversion (\mathbf{x}_A) can be
 627 different from those used to project the top-down fluxes back to sectoral emissions for linear or
 628 moderately non-linear problems (e.g. Rodgers and Connor 2003; Bowman *et al.* 2006) as the
 629 information from the measurement is preserved in the $\mathbf{K}^T \mathbf{S}_y^{-1} \mathbf{K}$ term which is contained in
 630 $\mathbf{S}^{-1} - \mathbf{S}_A^{-1}$ as shown in Equation 8. This means that \mathbf{Mz}_A can be different from \mathbf{x}_A , and their
 631 corresponding covariances, as long as the inversion problem is linear or only moderately
 632 nonlinear (Bowman *et al.* 2006; Cusworth *et al.* 2021). However, the interpretation of fluxes will
 633 be different if these matrices (\mathbf{S}_A and \mathbf{Z}_A) are inconsistent (e.g. Shen *et al.* 2021), that is $\mathbf{S}_A \neq$
 634 $\mathbf{MZ}_A \mathbf{M}^T$.

635 The uncertainty for any given element of the state vector \mathbf{z} is generally given by the
 636 square root of the diagonal element of the total error covariance and includes the effects of the
 637 limited spatial resolution of the top-down flux and how this projects uncertainties from one grid
 638 box and sector into another grid box and sector as discussed in the previous section. For
 639 example, the estimate for the emissions for some emissions sector “*i*” at some lon/lat grid box “*j*”
 640 is given by (Rodgers and Connor 2003; Worden *et al.* 2004):

Deleted: For example,

641

$$642 z_{ij} = z_a^{ij} + A_{ij,ij}(z_{ij} - z_a^{ij}) + \mathbf{A}_{ij,xy}(\mathbf{z}_{xy} - \mathbf{z}_a^{xy}) + \delta_{ij} \quad (9)$$

643

644 Where the italicized variables in Equation 9 are scalar representations of the variables in
 645 Equations 7 and 8, the index “*x*” represents all sectors and the index “*y*” represents all other
 646 lat/lon elements and matrices and vectors are boldfaced. Note that the paired indices *x* and *y*
 647 exclude the paired indices *i* and *j*. The variable “ z_{xy} ” represents the “true” value corresponding
 648 to the estimate “ z_{ij} ” and the variable δ_{ij} represents the error due to random noise (we exclude

650 systematic error here to simplify the math but Equation 9 can be expanded to include this term).
651 Of course we do not actually know the true value and its errors but Equation 9 allows us to
652 represent them in a manner than allows us to calculate their statistics. The total error for z_{ij} ,
653 equivalent to an element of the total error in Equation 8, is:

654

655 $E \left\| z_{ij} - z_{xy} \right\| = (1 - A_{ij}) Z_a^{ij} (1 - A_{ij})^T + \mathbf{A}_{ij,xy} \mathbf{Z}_a^{xy} \mathbf{A}_{ij,xy}^T + S_{ij}^n \quad (10)$

656

657 Where the $E \left\| \cdot \right\|$ term describes the expectation operator for calculating the statistics of the
658 quantity of interest (Bowman *et al.* 2006). The diagonal elements of the total error covariance
659 therefore include the effect of the limited spatial resolution through the second term on the right
660 hand side of Equation 10, which projects prior uncertainties from one region and sector (x,y) into
661 the region and sector of interest (i,j). The last term is the covariance due to measurement noise.

662 As the spatial resolution increases, the averaging kernel matrix converges towards the identity
663 matrix; in this limit the first and second terms on the right side converge to zero such that the
664 total error is due to noise (last term in Equation 10) and any residual systematic errors (not
665 shown in Equation 10 but discussed in the previous section). Improving the spatial resolution of
666 the methane emissions estimate therefore improves the accuracy.

667

668 In order to calculate the uncertainty for an aggregation of the elements of the state vector
669 \mathbf{z} (e.g. the coal sector for a country), instead of an individual element, we must sum the desired
670 set of elements $[z_i]$ that represent this sector and region. The uncertainty for this sum (squared) is
671 then:

672

673 $\sigma_{ij}^2 = \mathbf{h} \mathbf{Z}_{ij} \mathbf{h}^T \quad (11)$

674

675 where \mathbf{h} is a vector that is the same length as $[z_i]$, with values of one in each element and \mathbf{Z}_{ij} is
676 the square sub-matrix of the covariance matrix \mathbf{Z} corresponding $[z_i]$ (e.g. the country and
677 emission sector of interest).

678

679 **2.3 Generation of Prior Emissions, Covariances, and Uncertainties**

680

Deleted: i

682 In order to project fluxes from a top-down inversion back to emissions using the
683 approach described in Section 2.2, sectoral emissions and their covariances, or \mathbf{z}_A and \mathbf{Z}_A , at the
684 desired spatial resolution are required. One challenge with the flux to emissions projection is that
685 the *a priori* covariance matrix \mathbf{Z}_A must be inverted (Equation 8), which can be computationally
686 expensive because this matrix can be quite large as the number of sectors and spatial resolution
687 of the emissions increases and because correlations within the matrix (next section) make it
688 challenging to invert. In order to reduce computational expense for our chosen spatial resolution
689 of 1 degree resolution (prior to calculating country wide emissions), we dis-aggregate global
690 emissions into ~~eight~~ regions (Table 2) chosen by regions with peaks in the inversion sensitivity
691 to the underlying fluxes as shown by the averaging kernel diagonals in Figure 2. The different
692 categories are shown in Table 2 for each region and by sector along with the provenance (or
693 manuscript reference) in the second column. Cross-terms in the averaging kernel (Equations 5,
694 9, and 10) matrix demonstrate that the change in emissions in one region affect the estimated
695 emissions in another. Subdividing the fluxes into these ~~eight~~ regions therefore introduces an
696 extra error term in the total error covariance for each region; however this extra error is
697 automatically included in the total error covariance for each region as demonstrated by Equation
698 10.

Deleted: seven

Deleted: 8

Formatted: Font color: Red

701 Table 2: *A priori* emissions by source and region used with sectoral attribution

Source Tg CH ₄ /yr	Ref	N. America (15%)	S. America (30%)	Africa (30%)	Europe W. Russia N. Africa Mid-East (15%)	E. Russia (30%)	India Eurasia (30%)	Asia (30%)	Indonesia Australia (20%)	Total
Lon / Lat		175W-40W 25N-80N	130W-30W 65S-25N	24W-60E 40S-20N	24W-60E 20N-80N	60E-179E 50N-90N	60E-90E 5N-50N	90E-179E 5N-50N	90E-179E 45S-5N	
Livestock	1,2	7.7 +/-1.2	21.6 +/-3.9	10.7 +/- 2.1	12.4 +/-1.8	0.6 +/-0.1	19.1 +/- 5.0	11.7 +/-2.4	3.9 +/- 0.8	87.6 +/- 7.4-17.2
Rice	2	0.4 +/-0.1	1.2 +/-0.3	1.8 +/-0.6	0.6 +/-0.1	0.04 +/- 0.01	8.7 +/-2.4	32.8 +/-8.5	4.4 +/- 0.9	36.9 +/- 8.9-12.9
Waste	2	7.4 +/-1.1	4.1 +/-1.3	7.1 +/-2.0	23.9 +/-3.6	0.9 +/-0.3	4.4 +/-1.3	6.8 +/-1.6	3.1 +/- 0.7	57.7 +/- 5.0 – 11.9
Oil	3	2.7 +/-0.4	4.5 +/-1.4	2.8 +/-0.8	17.7 +/- 2.9	10.6 +/-3.3	0.6 +/-0.2	2.0 +/-0.6	0.7 +/- 0.1	41.6 +/- 4.7-9.7
Coal	3	3.2 +/-0.5	0.4 +/-0.1	0.78 +/- 0.22	2.3 +/-0.3	2.8 +/-0.9	1.6 +/-0.5	19.2 +/-5.9	1.2 +/- 0.3	31.4 +/- 6.1-9.8
Gas	3	7.5 +/-1.1	0.4 +/-0.1	0.7 +/-0.2	8.9 +/-1.3	0.4 +/-0.1	3.7 +/-1.2	0.9 +/-0.3	1.1 +/- 0.2	24.5 +/- 2.1-4.7
Fires	4	1.4 +/-0.3	2.3 +/-0.4	4.9 +/-0.8	0.3 +/-0.03	1.5 +/-0.2	0.1 +/- 0.02	1.1 +/-0.2	3.6 +/- 0.6	15.1 +/- 1.1 – 2.5
Wetlands Aquatic	5,6	37.1 +/-7.2	72.8 +/-16.2	42.4 +/- 16.3	7.5 +/-1.5	8.6 +/-2.0	3.7 +/-1.1	8.6 +/-1.9	19.0 +/- 6.5	199.8 +/- 25.2 – 52.8
Seeps	7	7.8 +/-1.1	2.0 +/-0.6	0.4 +/-0.1	14.1 +/-2.5	2.8 +/-0.8	0.8 +/-0.2	2.7 +/-0.7	1.3 +/- 0.2	32.0 +/- 3.0 – 6.2
Total Tg CH ₄ /yr		75.2 +/- 7.6 – 12.9	109.3 +/- 16.8-24.4	71 +/- 16.6-23.1	87.8 +/- 5.9-14.1	28.9 +/- 4.0 – 7.8	42.7 +/- 5.9 – 11.9	85.8 +/- 11.0-22.1	38.3 +/- 6.7-10.4	526 +/- 29.5 – 127.7

702

703 Table 2: Prior emissions by source and regions. Single values for uncertainties are calculated by projecting the
 704 corresponding covariance to a single number for the indicated lon/lat region and taking the square root. Total values
 705 show a range of uncertainty with the lower bound being the sum (squared) of the individual region or sector
 706 (assumes errors are un-correlated) and the upper bound being the sum of the errors (assumes errors are completely
 707 correlated). The following references indicate the source for each emission type: 1) NASA CMS V1.0 (Wolf *et al.*
 708 2017), 2) EDGAR 6.0 (Crippa *et al.* 2020), 3) NASA GFEI V1 (Scarpelli *et al.* 2020), 4) GFED 4.1 (van der Werf *et*
 709 *al.* 2017), 5) WETCHARTS 1.3.1 (Bloom *et al.* 2017), 6) GCP (Poulter *et al.* 2017), 7) Etiope *et al.* (2019). The
 710 target uncertainty for each region and sector is given in brackets underneath each region.

711

712 Our prior emission distribution and magnitude represents, by necessity, a set of ad hoc
713 choices that are informed by the scientific literature and experience of the co-authors of this
714 paper with developing top-down flux estimates. For example, our chosen resolution for
715 reporting sectoral emissions is 1 degree, which represents a compromise between computational
716 expense while minimizing representation errors when quantifying emissions for each country,
717 which in turn is needed for these estimates to inform the global stock take. Future research will
718 evaluate if higher-resolution emissions estimates by sector can be quantified given the
719 computational expense of inverting Equation 8; our motivation for reporting top-down estimates
720 at a higher resolution are because many of the inventories are at these scales (e.g. 0.1 degree) and
721 also to better utilize high-resolution emissions estimates now available by aircraft data (e.g.
722 Duren *et al.* 2019) and from upcoming satellites such as Carbon Mapper (e.g. Cusworth *et al.*
723 2019; 2021).
724

Deleted: The prior emissions used in our analysis represent,

724 We make the following choices for which sectoral emission type is represented: wastewater
725 is not explicitly estimated as these emissions are spatially correlated with landfill emissions
726 based on inspection of EDGAR inventories when projected to 1 degree resolution. The waste
727 category should therefore be interpreted as a combination of landfill and wastewater. We also did
728 not consider biofuels or termites for this estimate as they represent a small component of the
729 budget. For these reasons, the biofuel and termite components of the methane budget will
730 slightly bias our other sectoral estimates by 15-30 Tg CH₄/yr based on bottom up estimates
731 reported in (Saunois *et al.* 2020). On the other hand, emissions for seeps are included as bottom-
732 up inventories suggest these could be as large as 30 Tg CH₄/yr; however given the co-location of
733 seep emissions with oil and coal (Figure 3), care must be taken in interpreting our results for
734 Seep emissions estimates. Our prior emissions for livestock are from a NASA Carbon
735 Monitoring System product (Wolf *et al.* 2017) and is found from post-processing to be too low
736 by ~25% due to not including a scaling factor in the overall emissions. Nonetheless we keep the
737 current set of (low) prior livestock emissions of ~89 Tg CH₄/yr as they demonstrate (along with
738 the analysis in Section 3.3, Figure 6) that our total results are largely independent of the choice
739 of priors because of the sensitivity of the fluxes to the underlying emissions as shown in the right
740 panel of Figure 2. A future version of these estimates will have an updated prior for livestock
741 emissions and will include termites, wastewater, and biofuels. Although there can be many

Deleted:

Deleted: For example,

Deleted: likely too low as this product ends in 2012.

746 emissions within a single grid box, uncertainty can still decrease for each emission type as shown
747 in Equation 8, which shows that these correlations are quantified in the posterior covariance.
748 Uncertainty reduction of a particular emission therefore depends on the magnitude of the
749 emission and its uncertainty, its correlations with nearby emissions of the same type (next
750 section) and the magnitude and uncertainty of emissions within the same grid box.

← Formatted: Indent: First line: 0"

751 Prior wetland emissions are based on an ensemble of process models from the
752 WETCHARTS system and the Global Carbon Project (Bloom *et al.* 2017; Poulter *et al.* 2017;
753 Ma *et al.* 2021) and include the effects of lakes and rivers. A future version of this system will
754 separately estimate these other sectors of the methane budget if further analysis using other
755 satellite data (e.g. TROPOMI) shows that they can be distinguished from these other sectors.

756 **Covariance Generation:** Generating representative prior covariances is challenging as there
757 are few global studies that allow for accurate representation of uncertainties for emissions across
758 the globe and their correlations that are based on data and/or well calibrated models. This
759 problem exists not just for methane emissions but with other inverse problems where there is
760 little data representative of the quantities of interest (e.g. with remote sensing; Worden *et al.*
761 2004). For this reason we need to make another set of ad-hoc choices that is based on prior
762 research in order to generate the covariances for each sector. We therefore use the following
763 approach: first we assume that the total anthropogenic emissions (by sector) in “Annex 1”
764 countries have an uncertainty of 15%. For example, we assume the total error for the N.
765 American Coal sector is ~15%, and so on for each anthropogenic sector. Similarly, the total error
766 for Annex 2 regions is 30%. These targeted uncertainties are listed underneath the label for each
767 region in Table 2. These uncertainties are reported in Janssens *et al.* (2019) and are based on
768 “expert opinion” as quantifying uncertainties over a country or region using bottom up-
769 approaches can be challenging. Total regional uncertainty for a specific sector is calculated using
770 Equation 11. In order for sectoral emissions at 1 degree resolution to project to a total regional
771 uncertainty of 15%, there must be significant uncertainty of any given emission within that 1
772 degree grid cell. However, even assuming very large uncertainties for an emission within a 1
773 degree grid cell (e.g. 100%), the regional total uncertainty can be much smaller than 15% once
774 projected over a large enough number of grid cells if the emission errors are assumed to be
775 uncorrelated. To address this issue we also add correlations between nearby emissions; we start
776 the diagonal values at 0.7 (squared) of the prior emissions, or 70% uncertainty, and with a

Commented [JDJ1]: You mean the errors are assumed to be uncorrelated. There's other places in the paper where you forgot to state 'error'

777 correlation of 0.7 between neighboring emissions of the same type that are within 400 km (or
778 four grid cells). The diagonal values and correlations are then adjusted until the projected
779 uncertainty reaches 15% (for Annex 1) or 30% (Annex 2). Final values typically range from 0.6
780 (squared) to 1.0 for the diagonal and 0.7 to 0.9 for the off-diagonal values with variations in
781 these numbers because of the different spatial distributions of the emissions. These numbers for
782 the correlation and length scale are based on regional studies for N. America which also indicate
783 that uncertainties for nearby emissions should be correlated (e.g. Maasakkers *et al.* 2016, 2019).

784 For wetlands, we use a slightly different approach for generating covariances. Here we
785 calculate the root mean square (RMS) of an ensemble of different wetland process models
786 (Bloom *et al.* 2017; Poulter *et al.* 2017; Ma *et al.* 2021) for a given region. We then follow a
787 similar covariance generation approach as used for the anthropogenic emissions, iterating with
788 different diagonal and off-diagonal values until the projected uncertainty for a region is
789 approximately the same as the corresponding variance of the models.

790 While generating representative prior covariances is challenging, Equations 7 and 8 from
791 the previous section allow us to swap in better priors and prior covariances as these become
792 available. For example, if a researcher finds that the uncertainties expressed in Z_A over a given
793 region for a given sector should be 10% instead of the value used (approximately 70%), then it is
794 straightforward to update the covariance matrix to reflect this improved knowledge so that the
795 attribution to each sector is improved. Of course this improved information could also be used to
796 improve the S_A constraint matrix in Equation 1 to improve convergence of the top-down flux
797 estimate. Furthermore the updated posterior covariances can be used for the next flux inversion
798 based on other independent data and at some point these covariances, because they are based on
799 observations, will best reflect our knowledge of the methane emission. Covariances and prior
800 emissions are all publicly available, as well as python code that demonstrates how to use these
801 files, so that a researcher can determine how other priors and changes to their uncertainty
802 structure affects this top-down result or to use them for their own top-down inversions. Links to
803 these data and codes are in the Data Repository section (Section 5).

804 **Uncertainty Calculation Approach:** The uncertainties shown in the Tables 1 and 2 are
805 calculated in the following manner. First the prior uncertainties for each sector and for each
806 region shown in Table 2 are calculated by projecting the regional (e.g. N. America, S. America)
807 posterior error covariance to a single number corresponding to the mean emissions for that

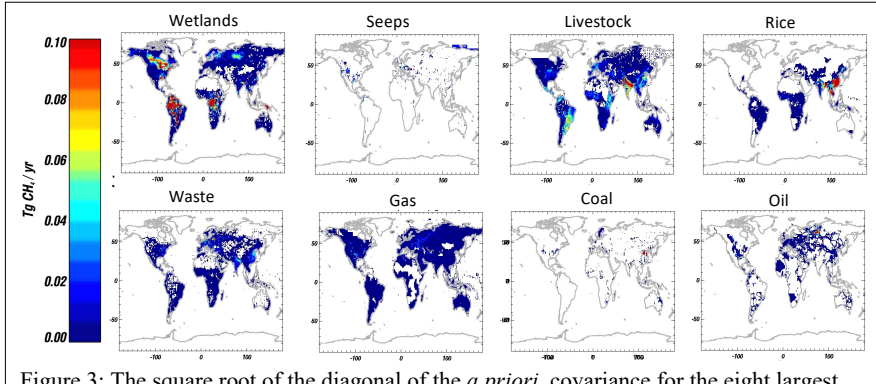


Figure 3: The square root of the diagonal of the *a priori* covariance for the eight largest sectors used in our analysis.

808 region using Equation 11. One approach is to then assume that these uncertainties are
 809 independent of each other in which case they are added in quadrature to get the total value; this is
 810 the smaller uncertainty shown in the **Total** column in Table 2. However, another method is to
 811 assume that the uncertainties are 100% correlated such that they should be added linearly; these
 812 are the values shown as the larger value in Table 2. We expect that the actual uncertainty is
 813 somewhere between these values. However, to be conservative we only report the larger value in
 814 Table 1 and for the remainder of the paper.

815 The prior uncertainties generated using the method described here are consistent with
 816 those reported in the literature even though the methodology differs. For example the values
 817 shown in the “prior” column of Table 1 are consistent (within reported ranges or uncertainties) of
 818 the equivalent sectors discussed in Saunois *et al.* (2020) and with the regional EDGAR v4.3.2
 819 inventories as discussed in Janssens-Maaenhouw *et al.* (2019). A caveat is that Janssens-
 820 Maaenhouw *et al.* (2019) also reports global totals for each sector, from a range of inventories and
 821 models, that are 2-3 times larger for each sector than those shown here. Another caveat is that
 822 Saunois *et al.* (2020) includes a freshwater category with a 120 ± 60 Tg CH₄/yr uncertainty
 823 whereas this category is subsumed into our Wetlands / Aquatic sector.

824 Figure 3 shows the (square root) diagonal of the covariance for each sector; as discussed
 825 previously, these are generally correlated with the magnitude of the emissions but also the
 826 chosen value for the regional total error (Table 2). Most of the sectors have enhancements and
 827 corresponding uncertainties that are spatially distinct. For example, the largest uncertainties for

828 oil are located in Eastern Europe and Russia; the largest uncertainties for coal are in China, and
829 the largest uncertainties for gas are in N. America and Central Asia. In turn, these fossil
830 emissions are spatially distinct from wetlands and livestock. However, the largest uncertainties
831 for rice and waste can spatially overlap those of livestock, especially in India and Asia, which
832 indicates that remote sensing will be challenged to distinguish these emissions.

833

834 **3.0 Results**

Deleted: : Total Emissions and Emissions by Country

835
836 In this next section we first present global estimates, followed by a discussion of the
837 sectoral emissions for the top-10 emitting countries, then emissions for all countries. Finally we
838 test if different assumptions about bottom-up emissions as discussed in recent literature, i.e.
839 larger wetland/aquatic emissions (Rosentreter *et al.* 2021), and larger fossil emissions
840 (Schweitzke *et al.* 2017) affect our conclusions about the top-down results presented here.

841

842

843

844

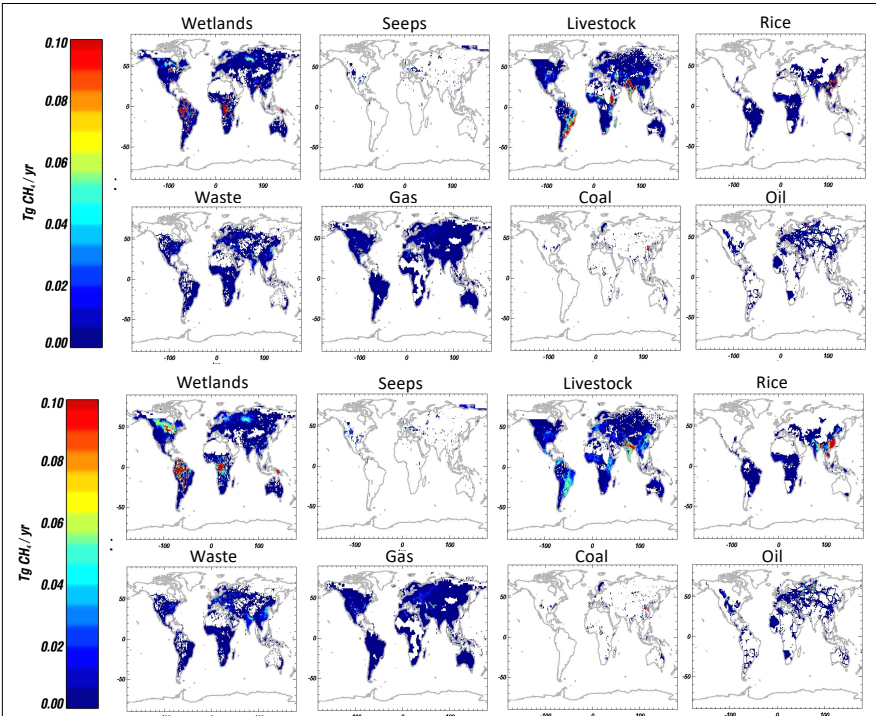


Figure 4: (top) Posterior methane emissions. (bottom) Poster emissions uncertainty as calculated by the square root of the diagonal of the posterior covariance matrix.

846 3.1 Global Methane Budget By Sector

847 Emissions by sector and their uncertainty at 1 degree resolution are shown in Figure 4
 848 with the top set of panels showing the posterior emissions and the bottom showing the
 849 uncertainty. As in Figure 3, the uncertainty at each longitude/latitude grid element is given by
 850 the square root of the diagonal of the total error covariance. [Uncertainty can decrease for](#)
 851 [emissions even when there is more than one type of emission in a grid box. As shown in](#)
 852 [Equation 8, this uncertainty reduction depends on the magnitude of the emission and its](#)
 853 [uncertainty, its correlations with nearby emissions of the same type \(Section 2.3\) and the](#)
 854 [magnitude and uncertainty of emissions within the same grid box.](#)

855 Inspection of Figure 4 (bottom panel) and Figure 3 shows reduction of uncertainty in
 856 many parts of the world relate to the prior such as the larger wetlands and agricultural regions in

← Formatted: Indent: First line: 0.5"

857 India and Asia. The right panel of Table 1 shows the global total posterior emissions by sector.
858 The increase in sectoral emissions relative to the prior for the agriculture sector and reduction in
859 fossil emissions reflect the top-down flux estimates (Figure 2) which show a lower posterior flux
860 relative to the prior in fossil emitting regions such as Russia and N. America (with the exception
861 of Southern USA) and increases in regions where livestock and rice emissions are expected to be
862 the largest source relative to other emissions such as in India, Brazil, Argentina, and East Africa.

863 **Comparisons to Previous Top-Down Inversions Using GOSAT and GEOS-Chem:** Our

864 results are consistent with previous top-down estimates based on the satellite GOSAT data. For
865 example, the results here are based on the inversion framework from Zhang *et al.* (2021) and Qu
866 *et al.* (2021), and are therefore generally consistent for the larger emissions such as wetlands, and
867 livestock, or the emissions which are spatially distinct from other sources and therefore easier to
868 resolve with remote sensing such as oil and coal. However, our estimates for rice, waste, seeps
869 are very different and this is likely because our choice of priors for these sectors are different and
870 because Qu *et al.* (2021) uses a uniform scaling approach to project fluxes to emissions whereas
871 we account for the prior uncertainties. Similarly, our results for wetlands, livestock, and fossil
872 emissions are consistent with previous GOSAT based inversions (e.g. Maasakkers *et al.* 2019;
873 Zhang *et al.*, 2021) with the caveat that these estimates are for earlier time periods and changes
874 in emissions can affect interpretation of any differences. Ma *et al.* (2021) uses GOSAT based
875 wetland estimates to show that wetland emissions for the years 2010-2018 are likely even lower
876 than our results. As with results presented here they take into account the spatial resolution and
877 prior of the top-down fluxes but use a different approach to quantify emissions; they select
878 “high” performing wetland models based on comparison of an ensemble of models with mean
879 wetland emissions and temporal variability. The total emissions for these highest performing
880 models 117 – 189 Tg CH₄/yr is lower, but within the uncertainty of the results here. These
881 difference in results, even when using similar models and data, highlight the importance of the
882 choice of priors as well as the methodology by which fluxes are projected back to emissions as
883 estimates for sectoral emissions can be very different from one estimate to the other depending
884 on these choices.

885 **Comparisons to Top-Down Inversions from GCP:** Emissions in Table 4 can be compared
886 to top-down inversions from the Global Carbon Project (GCP) when aggregated into combined
887 categories (Saunois *et al.* 2020). For example our agriculture and waste emissions are ~263 +/-

Deleted: 1

Deleted: 1

The distribution of total emissions from the top-down is substantively different from the bottom-up. For example, posterior emissions for livestock and rice are larger than the prior by more than 1-sigma of the reported uncertainties.

Deleted: Top-down fossil emissions are also much lower than expected from the prior although consistent within their uncertainties. These

Deleted: differences

Formatted: Font: Bold

Formatted: Indent: First line: 0.25"

Formatted: Font: Bold

Deleted: (

899 24 Tg CH₄/yr, anthropogenic fossil emissions are 82 +/- 12 Tg CH₄/yr, and natural
900 wetland/aquatic emissions are 180 +/- 10 Tg CH₄/yr. These are within the reported uncertainties
901 of top-down inversions in GCP which are [205-246 Tg CH₄/yr], [91-121 Tg CH₄/yr], and [155-
902 217 Tg CH₄/yr] respectively, but on the high side for agriculture and waste and on the low side
903 for fossil emissions. These differences between GCP and emissions reported here likely
904 represent the differences in information content and sampling from satellite versus ground-based
905 data as most of top-down ensembles reported in Saunois *et al.* (2020) are based on in situ
906 measurements which are typically in background regions and which are therefore not as sensitive
907 to the spatial distribution of emissions as the satellite based estimates (e.g. Figure 6 from Yin *et*
908 *al.* 2021). However, one set of results included with the top-down GCP results that is based on
909 GOSAT data (i.e. Tsuruta *et al.* 2017) is consistent with our results as they report biospheric
910 emissions of ~172 +/- 29 Tg CH₄/yr. Note the other paper citations in the GCP methane paper
911 that indicate use GOSAT data describe the model setup and results for CO emissions or for
912 regional results so we cannot explicitly compare to their results.

913 **Fossil Emissions:** Our posterior results for anthropogenic fossil emissions (82 +/- 12 Tg
914 CH₄/yr) and natural (22.5 +/- 3.8) are lower than our prior and in general do not reflect recent
915 papers that suggest much higher fossil emissions using measurements of δ¹³CH₄ (e.g.,
916 Schwietzke *et al.* 2016 indicates 211 +/- 33 Tg CH₄/yr for anthro + natural fossil emission) or
917 upscaled from aircraft measurements over USA basins (e.g. Alvarez *et al.* 2018). However, as
918 discussed in Turner *et al.* (2019), care must be taken in using isotope measurements to infer the
919 partitioning of methane sources because of large uncertainties in the emission factors of different
920 sources at different latitudes. Upscaling also can have large uncertainties as emission factors that
921 relate activity data to emissions can vary significantly from region to region. Our global
922 posterior fossil emissions are consistent with more recent reports of fossil emissions, ~84 Tg
923 CH₄/yr, to the UNFCCC (Scarpelli *et al.* 2022) for 2019, suggesting that our lower posterior
924 estimates of fossil emissions are not unreasonable.

925 Onshore geological seeps represent another largely uncertain source of fossil emissions
926 with values ranging from 2 to 30 Tg CH₄/yr. For example, the top-down flux estimate, used as a
927 basis for the sectoral emissions attribution, assumes a prior of ~2 Tg CH₄/yr. However, our
928 choice of prior (part of the \mathbf{z}_A vector, Equation 7) is based on Etiope *et al.* (2019) with a value of
929 32.0 +/- 6.2, resulting in a posterior of 22.5 +/- 3.8 Tg CH₄/yr. This reduction in uncertainty is

Deleted: . presents results from an ensemble of top-down estimates for emissions from wetlands (155-217 Tg CH₄/yr), agriculture/waste (205-246 Tg CH₄/yr), biomass and biofuel burning (25-32 Tg CH₄/yr), and fossil emissions (91-121 Tg CH₄/yr). Our global total results shown in Table 1 are consistent with theirs (within uncertainties) although our result for agriculture and waste (263 +/- 24 Tg CH₄/yr) is on the high side of theirs and our results for fossil emissions (82.1 +/- 12 Tg CH₄/yr) are on the low side of their estimates. But on the

Deleted:

Formatted: Font: Bold

Formatted: Indent: First line: 0.25"

Formatted: Font: Bold

Deleted: do not sample areas of strong livestock emissions such as Brazil, India, and Ethiopia.

943 substantial suggesting that remote sensing is providing good information about this source. A
 944 caveat is that seep emissions tend to overlap those from coal and oil (Figure 4) suggesting a
 945 potential equifinality between these emissions estimates. Combining fossil emissions from the
 946 seep category with anthropogenic fossil emissions increases the overall fossil total and would
 947 make the total fossil emissions (natural + anthropogenic) consistent with top-down results from
 948 GC. Based on these results, we suggest this category attention deserves measurements, especially
 949 from the up and coming high-resolution greenhouse gas measurements such as Carbon Mapper.
 950

Deleted: , likely because seeps have a geographically distinct distribution relative to other sources.

Deleted: it is possible that inventories are not specifying other emissions near seeps which would in turn misrepresent this attribution

Deleted: We therefore

3.2 Top 10 Emitting Countries

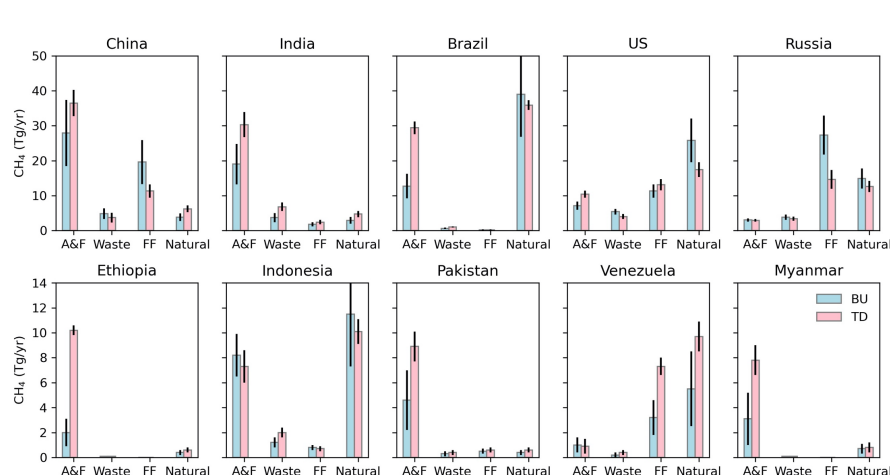


Figure 5: Emissions by sector for the top 10 emitters. AF represents agricultural and fires. FF represents fossil fuels or coal, oil, and gas. Natural represents wetlands, aquatic sources, and geological seeps. Bottom up (BU) inventory estimates are shown as blue bars and the remote sensing / top-down (TD) estimates are shown as pink bars. The uncertainties in both quantities are shown as black lines. Uncertainty calculations for bottom up and top-down estimates are discussed in Section 2.

954
 955
 956 Figure 5 lists the top 10 emitting Countries ranked by total anthropogenic emissions as
 957 calculated using this remote sensing system. Sectoral attribution is based on the nine categories

964 in Table 3; here we combine categories so that they are similar to what is being reported for the
965 CO₂ based carbon inventories. The different categories are AF, which includes the sectors for
966 agriculture (livestock and rice) and fires. This category is similar to the Agriculture, Forestry,
967 and Land Use category or “AFOLU” ~~a~~ used in CO₂ based carbon inventories. W is the waste
968 category, FF is the fossil category, which includes extraction, transport and use of coal, oil, and
969 natural gas (Scarpelli *et al.* 2020; 2021). The Natural category, includes wetlands and geological
970 seeps. The top five emitting countries are essentially the same from the bottom-up and top-down.
971 However, top emitting countries with most emissions from the agriculture sector, likely due to
972 livestock (see table in Section 4). While top-down and inventory emissions for China, USA, and
973 Indonesia are consistent; there are major differences between our top-down results and
974 inventories for the other countries. We next compare these results to those of previous studies;
975 however, as stated earlier, these results should be treated cautiously and as a starting point for
976 future research as differences can also be due to unquantified uncertainties in either the remote
977 sensing data or the transport model used to relate concentrations to fluxes.

978 Our results are consistent with those from Maasakkers *et al.* (2019), Zhang *et al.* (2021)
979 and Qu *et al.* (2021); however this is not too surprising as emissions that are reported here are
980 based on the flux inversion system from these studies. A notable difference in methodology is
981 that Qu *et al.* (2021) who also derives fluxes based on total column data from the Tropospheric
982 Monitoring Instrument (TROPOMI). However, Qu *et al.* (2021) finds that country totals for the
983 top-5 are essentially the same based on GOSAT and TROPOMI except for Brazil, but attributed
984 large differences between TROPOMI and GOSAT to systematic errors in the TROPOMI total
985 column data related to low surface albedo over Brazil; consequently, the TROPOMI based
986 estimates in this region should be treated more cautiously.

987 Comparisons of these results to other estimates discussed in the literature can show
988 substantial differences in either total emissions or attribution or both. For example Ganesan *et al.*
989 (2017), using in situ and satellite atmospheric methane data, finds much lower total Indian
990 emissions of 22 +/- 2.3 Tg CH₄/yr for the 2010-2015 time period as compared to 39.5 +/- 5.4 for
991 our study (and the Qu *et al.* 2021, Zhang *et al.* 2021 studies) and 36.5 +/- 5.3 from Janardanan *et*
992 *al.* (2020). Miller *et al.* (2019) provides similar total emissions for China of 61.5 +/- 2.7 Tg
993 CH₄/yr but different partitioning; for example they find that Coal is the largest source of
994 emissions based on comparison of top-down fluxes to EDGAR emissions and using a relative

Formatted: Font: Times New Roman

Deleted:

996 weighting attribution flux to emissions attribution approach, whereas we find that agriculture
997 (primarily Rice, Table 3 Section 4) is the largest sector. A major caveat is that attribution of
998 emissions from total fluxes is challenging for China because many of the strongest emissions
999 (e.g. coal, livestock, and rice as shown in Figures 3 and 4) overlap within the spatial resolution of
1000 the top-down estimate which is less than 2.5 degrees based on gridding used for the flux
1001 inversion and the variable sensitivity of the averaging kernel. While in principle these
1002 uncertainties due to limited spatial resolution are quantified based on our assumed prior
1003 covariance for each sector, it is quite possible that both our choice of the location of the
1004 emissions and corresponding prior covariance are incorrect due to less confidence in the
1005 emissions characterization in this region (Janssens-Maenhout *et al.* 2019). Our results are
1006 consistent (within uncertainties) for recent results by Deng *et al.* (2021); total anthropogenic
1007 emissions from Table 3 are within uncertainty of reported bottom-up and top-down total
1008 anthropogenic emissions shown in Figure 4 of Deng *et al.* (2021), even if the attribution of
1009 emissions may differ. Similarly, top-down based country level anthropogenic emissions from
1010 Stavert *et al.* (2022) are consistent, when we are able to directly compare emissions country to
1011 country, although many of their emissions only agree at the outer edge of the reported
1012 uncertainties.

1013 We find that Myanmar has anomalously large agricultural emissions (primarily from
1014 livestock, Table 3 Section 4) relative to prior assumptions. Given that the DOFS reported for
1015 Mynamar is 2.7, we expect that the fluxes here are well resolved such that, it is possible that
1016 poorly characterized prior emissions drive this difference between prior and posterior. For
1017 example, Janardanan *et al.* (2020) also reports similar top-down emissions of 6.1 +/- 0.8 Tg
1018 using a higher resolution satellite based flux inversion. However, an alternative explanation
1019 could be that errors in model transport could project to larger than expected fluxes (Equation 9)
1020 in this region as Jiang *et al.* (2013) finds that regions with substantial atmospheric convection
1021 can have large biases in top-down surface emission estimates.

1022 Ethiopia also has larger than expected agricultural (livestock emissions) as compared to
1023 the prior. As with Mynamar, the prior emissions could be too low. For example, the amount of
1024 cattle and other livestock, between 80 and 90 million in 2015 and growing (Bachewe *et al.* 2018,
1025 [statista.com](#)) is not that different in size than USA livestock, ~93 million in 2021 ([statista.com](#)),
1026 suggesting that they could also have comparable livestock emissions. An alternative explanation

Deleted:

Deleted: However,

Deleted: as

Deleted:

Deleted: Similarly

Deleted: However

Deleted: , which is supported by the results in Figure 5

1034 for this discrepancy are very low prior emissions in neighboring Sudan despite possible large
1035 numbers of cattle in this region as well (knoema.com) suggesting that livestock inventories in the
1036 E. African regions need to be re-examined.

1037 Russian posterior fossil emissions are substantially lower than those initially reported in
1038 Scarpelli *et al.* (2020), which are based on reports to the UNFCC in 2017. However, more recent
1039 reporting to the UNFCC also suggest a much smaller bottom-up fossil estimate of ~7 Tg CH₄/yr
1040 (Scarpelli *et al.* 2021). Table 3 (next section) indicates that remote sensing provides the best
1041 information about Russian oil and to some extent coal emissions as the reduction of uncertainty
1042 is largest for these sectors but has little change for gas emissions. Total emissions for oil and coal
1043 are 11.2 +/- 1.9 indicating that total fossil emissions are likely larger than expected for the latest
1044 reports to the UNFCC but smaller than previous. As discussed previously, these top-down
1045 estimates should be treated cautiously and only as a starting point for future studies due to the
1046 limited sensitivity and potential uncertainties in both top down and bottom up.

Deleted: However,

Deleted: a

Deleted: .

3.3 Results for all Countries

1047 This section presents the complete table (Table 3, Appendix 1) of emissions by sector and
1048 country. As discussed previously in Section 2.1, we project the sectoral emissions in each 1
1049 degree grid to each country using a country map to quantify the emissions and their uncertainties
1050 for each country. The table is ordered by Degrees of Freedom for Signal (DOFS), which is a
1051 metric of sensitivity for inversion problems. As discussed in Section 2.1, the DOFS is a metric
1052 for the sensitivity of the flux estimate. For example, a DOFS of 1 means that this remote sensing
1053 system (GOSAT plus GEOS-Chem) can generally resolve the countries total emissions,
1054 assuming the sensitivity is evenly distributed across the country. More DOFS means that more
1055 emissions can be spatially resolved. However, even a DOFS of 0.5 means that half of the
1056 estimate is weighted by the measurement, with the estimate increasingly weighted by the *a priori*
1057 as the DOFS approaches zero. For these reasons we report estimates for all countries, even if the
1058 DOFS are effectively zero as information about the *a priori* inventories from the measurement
1059 might be useful even if not well informed by the satellite data. To distinguish these different
1060 levels of sensitivity, we color countries with corresponding DOFS greater than 1.0 as green,
1061 between 0.5 and 1.0 as yellow, and below 0.5 as red.

1068 The DOFS are calculated from the Averaging Kernel matrix provided by the GEOS-
1069 Chem based inversion (Section 2.1). To calculate the DOFS for a given country we project the
1070 diagonal of the Averaging Kernel (Figure 2) to 1-degree resolution and then add up these values
1071 based on the 1-degree country map used in this study. Note that the total DOFS between the
1072 reduced resolution flux inversion and the 1-degree map is preserved. Table 3 indicates that the
1073 GOSAT based top-down estimate can quantify total emissions (i.e. reduce uncertainty) for
1074 approximately 57 countries as the DOFS for the 57th country is more than 1 and less than 1 for
1075 the 58th country. As discussed previously, As DOFS approaches zero there is less reduction in
1076 uncertainty using the top-down system discussed here. Furthermore, inspection of Table 3 shows
1077 that even countries where DOFS are between 1 and 2 show little reduction of uncertainty; this
1078 happens because of cross-terms in the sensitivity project uncertainty from one sector or region
1079 into another as shown in Equation 10.

Deleted: 8

Deleted: 8

Deleted: 9

1080 The astute reader will notice negative emissions in some countries in Table 3. Negative
1081 emissions are a possible solution for inverse problems using linear updates, such as used here,
1082 even if they are not physically possible. Typically negative emissions occur when there are
1083 limited constraints on emissions in one region with large values in the state vector in a
1084 neighboring region; this is also known as “jack-knifing” in the inverse community. For example,
1085 livestock emissions for Peru are shown to be negative in Table 3, likely because Peru is near the
1086 Amazon basin which has substantive wetland emissions and the cross-correlations between these
1087 regions result in negative values in Peru livestock. In this case we would assume there is no
1088 information from this remote sensing system on this category and ignore these results.

1089
1090 **3.4 What Happens to (Top Down) Methane Budget if Priors for Wetland/Aquatic and**
1091 **Fossil Emissions are Substantially Increased?**

1092 Equations 7 and 8 also allow us to test other prior emission inventories to determine if
1093 they are consistent with top-down fluxes. This approach is similar to the “prior swapping”
1094 approach described in Rodgers and Connor (2003) but can also include “prior covariance
1095 swapping” as discussed in Cusworth *et al.* (2021). This approach involves replacing the \mathbf{z}_A and
1096 \mathbf{Z}_A shown in Section 2.2 with different formulations. In this section we test what happens if we
1097 inflate the prior emissions for the wetland or fossil fuel categories such that they are consistent
1098 with other studies indicating much higher values than expected from top-down estimates, e.g.
1099

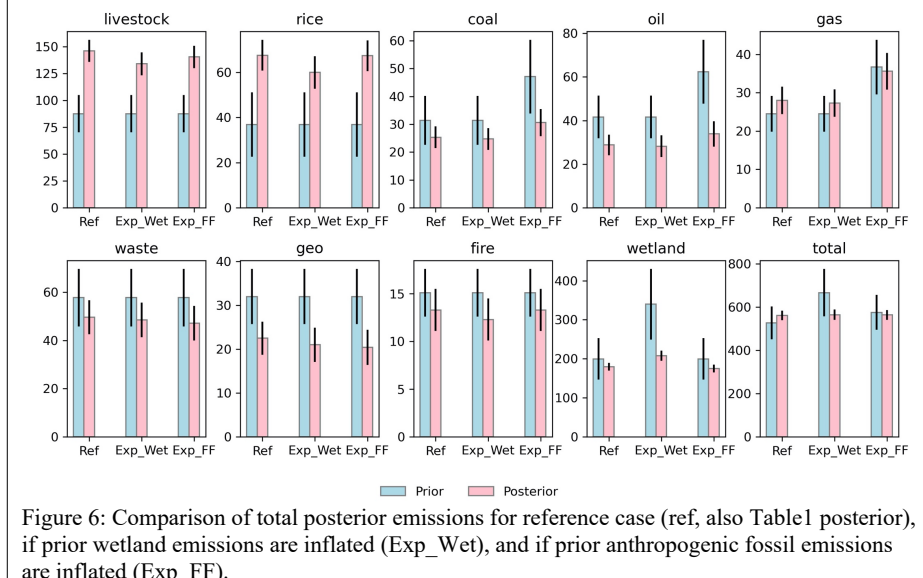


Figure 6: Comparison of total posterior emissions for reference case (ref, also Table1 posterior), if prior wetland emissions are inflated (Exp_Wet), and if prior anthropogenic fossil emissions are inflated (Exp_FF).

Rosentreter *et al.* (2021) for wetland/aquatic emissions and Schwietzke *et al.* (2017) for fossil emissions. Figure 6 shows the results of these two studies. The bars labeled “Ref” indicate the prior used for the results reported in this manuscript. The bars labeled “Wet” indicated the increased wetland study (which also includes increases to lake and river emissions as the wetland models include these categories, Bloom *et al.* 2017) and the bars labeled “FF” indicate the study where anthropogenic fossil fuels are increased by 50%. We find that even with a very large prior emissions for wetland/aquatic sources, the posterior gives an estimate of 208 ± 12.8 Tg CH₄/yr as compared to 179.8 ± 10 for the reference values. This decrease from the inflated prior of ~340 Tg CH₄/ yr to 208 Tg CH₄/yr happens because the global total is constrained to ~560 Tg CH₄/yr through knowledge of the methane sink and because wetland emissions tend to be spatially distinct from other sources. For the same reasons, fossil emissions, especially coal, oil, and geological seeps show a substantial decrease in uncertainty. Consequently, the posterior emissions difference between the reference and inflated fossil studies are consistent within uncertainty and generally these emissions are much less than either the reference or inflated priors. For these reasons, it is challenging to reconcile these inflated aquatic emissions or inflated fossil emissions with top-down results. As noted previously, these comparisons should still be

1119 treated cautiously and as a starting point for further research because of poorly characterized
1120 systematic errors in the chemistry transport model used to relate observed concentrations to
1121 fluxes and because sources that are not included in the prior state vector but co-located with
1122 other sectors cannot be distinguished. For example, if there are significant (unspecified) aquatic
1123 emissions that are co-located with livestock emissions then the corresponding livestock
1124 emissions estimate would be biased high.

1125

1126 **4.0 Summary and Future Directions**

1127 In this paper we demonstrate, using a new Bayesian algorithm, estimates of emissions by
1128 sector at 1 degree resolution and by country, by using a combination of prior information of the
1129 emissions, satellite data, and a global chemistry transport model. Uncertainties are provided for
1130 representation (or smoothing) error and data precision but not for systematic errors in the
1131 transport model or data. Using a metric called the degrees-of-freedom for signal (DOFS), we
1132 show that the combination of GOSAT based satellite data with the GEOS-Chem model and prior
1133 uncertainties can estimate total emissions for about 57% of the 242 countries, with only partial
1134 information for the remaining countries. Our results can be used for comparison to country
1135 level, bottom-up inventories by sector that might be, for example, provided by the global stock
1136 take. However, any discrepancies between these top-down and inventory based estimates should
1137 be considered as a starting point for future investigations given the potential for systematic errors
1138 affecting the top-down results such as from accuracy limitations in the data or in the chemistry
1139 transport model used to estimate fluxes from the data (e.g. Buchwitz *et al.* 2015; Jiang *et al.*
1140 2015; McNorton *et al.* 2020; Schuh *et al.* 2019). Alternatively, countries with little capability for
1141 quantifying bottom-up emissions could use these results, along with other published top-down
1142 estimates (e.g. Deng *et al.* 2021; Stavert *et al.* 2022) for their contribution to the global stock
1143 take.

1144 In the absence of systematic errors, we find robust estimates for livestock, coal, oil, seeps,
1145 fires, and wetlands as these can (on average) be distinguished from other sources using remote
1146 sensing given their distinct locations. Our results are consistent (within uncertainty) with
1147 previous top-down estimates such as the 2017 Global Carbon Project that are primarily based on
1148 in situ data. However, these remote sensing estimates are on the high side for agricultural and
1149 waste emissions and the low side for fossil and wetland emissions. On the other hand, total fossil

Deleted: 8

Deleted: .

Deleted: W

Deleted: , natural gas

1154 emissions reported here are consistent with recent reports of fossil emissions to the UNFCCC
1155 (Scarpelli *et al.* 2022).

1156 The new Bayesian algorithm we demonstrate can be used to test if different prior emissions
1157 are consistent with our posterior emissions estimates. For example, we find that inflating the
1158 priors for wetland/aquatic fluxes, or alternatively fossil emissions do not fundamentally alter our
1159 estimates for these sectors. Consequently, the remote sensing estimates reported here show much
1160 lower wetland and fossil emissions than these studies based on bottom-up models and isotope
1161 data, and much larger agricultural and waste emissions. The largest differences between remote
1162 sensing and these other estimates occur in Brazil and India (primarily related to livestock),
1163 Russia (fossil emissions), and Central and E. Africa (livestock). These contrasting differences
1164 between the remote sensing based results and bottom-up models suggest that additional research
1165 is needed in these geographical areas to reconcile global methane budget estimates.

1166 **Future Directions:** We are evaluating how to characterize systematic errors related to the
1167 atmospheric chemistry transport model (e.g. Schuh *et al.* 2019) and in the satellite data to our
1168 error analysis and we expect the next version of these estimates to contain these uncertainties. We
1169 also expect to add isotopic information through new flux estimates based on the surface network
1170 and the GEOS-Chem model; these independent data can be used to test the partitioning of
1171 biogenic, fossil, and pyrogenic emissions (e.g. Worden *et al.* 2017). We are also examining how
1172 to combine high-resolution emissions estimates based on aircraft data and imaging spectrometers
1173 such as GHG-Sat or Carbon Mapper to the top-down fluxes to improve inventory estimates at
1174 finer spatial scales than reported here. Finally, the posterior emissions and covariances
1175 demonstrated in this manuscript can be used as priors in subsequent emissions estimates using
1176 data from other measurements such as from the upcoming CO2M, Methane-Sat, and Carbon
1177 Mapper instruments.

1178

1179

1180 5.0 Data Repositories

1181 The prior and posterior emissions and covariances are stored on <https://cmsflux.jpl.nasa.gov/>.

1182

1183 Please refer to Qu *et al.* (2021) for data related to the top-down flux inversion.

1184

1185

Moved (insertion) [1]

Deleted: We did not consider biofuels and termites in these initial estimates as they are thought to be small contributors to the methane; future estimates will add these other sources, especially in conjunction with more high resolution estimates that might be provided by regional TROPOMI inversions or future satellites such as CO2M, MethaneSAT or Carbon Mapper.

Deleted: also

Deleted: result in similar (within the calculated uncertainties)

Formatted: Font: Bold

Deleted: also

Deleted: add

Deleted: .

Deleted: ¶

Our results can be used for comparison to country level, bottom-up inventories by sector that might be, for example, provided by the global stock take. However, any discrepancies between these top-down and inventory based estimates should be considered as a starting point for future investigations given the potential for systematic errors affecting the top-down results.

Moved up [1]: The new Bayesian algorithm we demonstrate can be also used to test if different prior emissions result in similar (within the calculated uncertainties) posterior emissions estimates.

1211 The provenance of individual inventories that are used to generate the emissions and inventories
1212 are shown in Table 2.

1213

1214 **6.0 Author Contributions**

1215

1216 JW led the integration of results and writing and developed the prior covariances. DC provided
1217 the emissions attribution with JW and AB and co-wrote Section 2.2. ZQ and YZ provided the
1218 flux estimates and co-wrote section 2.1. YY SM and AB supported the attribution derivation and
1219 analysis. BB and DC helped link results to the global stock take. TS and JM supported the
1220 inventory description and analysis. RD and DJ helped design the overall flux inversion and
1221 emissions attribution system described in the paper. All co-authors have read the paper and
1222 provided feedback.

1223

1224 **7.0 Acknowledgements**

1225

1226 **Acknowledgments.** Part of this work research was carried out at the Jet Propulsion Laboratory,
1227 California Institute of Technology, under a contract with the National Aeronautics and Space
1228 Administration (80NM0018D0004). This research was motivated by CEOS (Committee on Earth
1229 Observing Satellites) activities related to quantifying greenhouse gas emissions. This research was
1230 supported by funding from NASA's Carbon Monitoring System (CMS) and AIST programs.
1231 Yuzhong Zhang acknowledges funding by NSFC (42007198).

1232

1233

1234

1235 **8.0 Appendix table of emissions for each country ordered by DOFS**
1236

1237 Table 3: Table of Emissions for Each Country.

1238 This table provides the top-down and bottom up estimates for each sector based on the
 1239 methodology described in this paper. The table is ordered by DOFS which is the metric for
 1240 sensitivity for the remote sensing system described in this paper. The first row for each country
 1241 provides the top-down result and the second row is the bottom-up. [Prior inventories are shown in](#)
 1242 [Table 2. Green are for results where DOFS > 1. Yellow corresponds to 0.5 < DOFS < 1. Red](#)
 1243 [corresponds to DOFS < 0.5](#)

Sector	Livestock Tg CH ₄ /yr	Rice Tg CH ₄ /yr	Waste Tg CH ₄ /yr	Fire Tg CH ₄ /yr	Oil Tg CH ₄ /yr	Coal Tg CH ₄ /yr	Gas Tg CH ₄ /yr	Seeps Tg CH ₄ /yr	Wetland/ Aquatic Tg CH ₄ /yr	DOFS	Total Anthro
1) Brazil	27.5+/- 1.3	0.20+/- 0.10	1.0+/- 0.2	1.7+/- 0.4	0.18+/- 0.05	0.05+/- 0.02	0.00+/- 0.00	0.05+/- 0.02	35.9+/- 1.4	46	30.6+/- (1.4- 2.0)
Inventory	11.0+/- 3.0	0.26+/- 0.09	0.55+/- 0.20	1.5+/- 0.4	0.16+/- 0.05	0.05+/- 0.02	0.00+/- 0.00	0.06+/- 0.02	39.0+/- 12.2		13.5+/- (3.0- 3.7)
2) Russian Federation	1.3+/-0.2 0.02	0.07+/- 0.02	3.4+/- 0.6	1.5+/- 0.2	7.6+/- 1.4	3.6+/- 0.5	3.3+/- 0.7	1.4+/- 0.4	11.3+/- 1.2	35.8	20.9+/- (1.8- 3.7)
Inventory	1.3+/-0.3 0.02	0.09+/- 0.02	3.8+/- 0.8	1.6+/- 0.2	20.4+/- 3.9	2.5+/- 0.9	4.4+/- 0.8	2.6+/- 0.6	12.3+/- 2.3		34.1+/- (4.2- 6.8)
3) United States of America	9.9+/-0.9 0.07	0.27+/- 0.07	4.0+/- 0.7	0.22+/- 0.04	2.4+/- 0.3	2.8+/- 0.4	7.9+/- 0.9	2.7+/- 0.8	14.6+/- 1.3	32.2	27.6+/- (1.5- 3.3)
Inventory	6.4+/-1.1 0.06	0.38+/- 0.06	5.4+/- 0.8	0.26+/- 0.06	1.7+/- 0.3	3.0+/- 0.5	6.5+/- 1.1	6.7+/- 1.1	19.0+/- 5.3		23.8+/- (1.9- 3.9)
4) Canada	0.90+/- 0.15	0.00+/- 0.00	0.43+/- 0.37	0.76+/- 0.20	0.74+/- 0.26	0.05+/- 0.01	0.82+/- 0.17	1.1+/- 0.2	9.2+/- 0.7	31.5	3.7+/- (0.5- 1.2)
Inventory	0.91+/- 0.15	0.00+/- 0.00	1.2+/- 0.4	1.1+/- 0.3	0.88+/- 0.27	0.05+/- 0.01	0.80+/- 0.18	1.1+/- 0.2	18.0+/- 4.6		5.0+/- (0.6- 1.3)
5) China	6.6+/-1.7 2.1	29.6+/- 1.4	3.7+/- 0.6	0.23+/- 0.03	1.1+/- 0.3	10.1+/- 1.6	0.11+/- 0.03	1.2+/- 0.3	5.0+/- 0.8	26.5	51.5+/- (3.4- 7.1)
Inventory	8.6+/-2.1 7.4	19.1+/- 4.5	4.8+/- 1.5	0.23+/- 0.03	0.99+/- 0.28	18.5+/- 5.9	0.12+/- 0.03	1.0+/- 0.3	2.8+/- 0.8		52.3+/- (9.8- 17.3)
6) India	23.9+/- 2.0	6.3+/- 1.6	6.8+/- 1.2	0.09+/- 0.02	0.03+/- 0.01	0.91+/- 0.37	1.5+/- 0.2	0.12+/- 0.06	4.6+/- 0.8	20.8	39.5+/- (2.8- 5.4)
Inventory	13.0+/- 4.1	5.9+/- 1.7	3.7+/- 1.3	0.09+/- 0.02	0.03+/- 0.01	0.84+/- 0.38	0.90+/- 0.24	0.13+/- 0.06	2.8+/- 0.9		24.5+/- (4.6- 7.7)

7) Democratic Republic of the Congo	0.05+/- 0.02	0.06+/- 0.03	0.22+/- 0.05	1.5+/- 0.3	0.07+/- 0.04	0.00+/- 0.00	0.00+/- 0.00	0.04+/- 0.01	17.6+/- 1.0	16.9	1.8+/- (0.4- 0.5)	Formatted: Font color: Accent 6
Inventory	0.06+/- 0.02	0.07+/- 0.03	0.24+/- 0.05	1.1+/- 0.4	0.07+/- 0.05	0.00+/- 0.00	0.01+/- 0.00	0.04+/- 0.01	21.2+/- 11.1		1.6+/- (0.4- 0.5)	Formatted: Font color: Accent 6
8) Indonesia	0.95+/- 0.23	4.2+/- 0.6	2.0+/- 0.4	2.1+/- 0.5	0.48+/- 0.14	0.13+/- 0.05	0.08+/- 0.01	0.65+/- 0.17	9.4+/- 0.8	16.1	10.0+/- (0.9- 1.9)	Formatted: Font color: Accent 6
Inventory	0.83+/- 0.23	4.3+/- 0.9	1.2+/- 0.4	3.0+/- 0.6	0.54+/- 0.14	0.14+/- 0.05	0.09+/- 0.01	0.62+/- 0.17	10.9+/- 4.0		10.1+/- (1.2- 2.4)	Formatted: Font color: Accent 6
9) Peru	-0.52+/- 0.20	- 0.11+/- 0.10	0.04+/- 0.07	0.02+/- 0.01	0.07+/- 0.05	0.00+/- 0.00	0.02+/- 0.01	0.05+/- 0.02	7.8+/- 0.5	6.9	0.48+/- (0.24- 0.43)	Formatted: Font color: Accent 6
Inventory	0.48+/- 0.26	0.15+/- 0.09	0.14+/- 0.08	0.02+/- 0.01	0.07+/- 0.05	0.00+/- 0.00	0.02+/- 0.01	0.06+/- 0.02	10.9+/- 8.1		0.88+/- (0.29- 0.49)	Formatted: Font color: Accent 6
10) Australia	1.3+/- 0.3	0.02+/- 0.00	3.0+/- 0.3	0.48+/- 0.05	0.02+/- 0.00	1.7+/- 0.2	0.38+/- 0.06	0.22+/- 0.07	1.0+/- 0.2	6.9	6.9+/- (0.5- 0.9)	Formatted: Font color: Accent 6
Inventory	2.2+/- 0.5	0.03+/- 0.00	1.4+/- 0.5	0.48+/- 0.05	0.02+/- 0.00	1.0+/- 0.3	0.37+/- 0.06	0.27+/- 0.08	1.1+/- 0.2		5.5+/- (0.8- 1.4)	Formatted: Font color: Accent 6
11) Venezuela (Bolivarian Republic of)	0.77+/- 0.52	0.02+/- 0.03	0.41+/- 0.17	0.08+/- 0.03	7.3+/- 0.7	0.00+/- 0.00	0.01+/- 0.00	1.3+/- 0.4	8.4+/- 0.9	5	8.6+/- (0.9- 1.5)	Formatted: Font color: Accent 6
Inventory	0.85+/- 0.55	0.03+/- 0.02	0.25+/- 0.18	0.08+/- 0.03	3.2+/- 1.4	0.00+/- 0.00	0.00+/- 0.00	0.66+/- 0.37	4.8+/- 2.6		4.4+/- (1.5- 2.1)	Formatted: Font color: Accent 6
12) Colombia	-1.97+/- 0.64	0.05+/- 0.14	0.18+/- 0.31	0.03+/- 0.01	0.33+/- 0.10	0.32+/- 0.14	0.01+/- 0.00	0.37+/- 0.23	-0.79+/- 0.73	5	1.05+/- (0.74- 1.34)	Formatted: Font color: Accent 6
Inventory	1.3+/- 0.8	0.16+/- 0.12	0.46+/- 0.33	0.03+/- 0.01	0.26+/- 0.11	0.37+/- 0.14	0.01+/- 0.00	0.40+/- 0.24	3.7+/- 2.0		2.6+/- (0.9- 1.5)	Formatted: Font color: Accent 6
13) Argentina	6.6+/- 0.6	0.03+/- 0.04	0.22+/- 0.07	0.09+/- 0.03	0.29+/- 0.10	0.00+/- 0.00	0.06+/- 0.02	0.26+/- 0.08	5.2+/- 0.6	4.6	7.3+/- (0.6- 0.9)	Formatted: Font color: Accent 6
Inventory	2.6+/- 1.2	0.04+/- 0.03	0.15+/- 0.07	0.08+/- 0.03	0.31+/- 0.10	0.00+/- 0.00	0.06+/- 0.02	0.18+/- 0.09	2.4+/- 1.3		3.2+/- (1.2- 1.4)	Formatted: Font color: Accent 6
14) Papua New Guinea	0.04+/- 0.02	0.00+/- 0.00	0.02+/- 0.00	0.08+/- 0.02	0.03+/- 0.02	0.01+/- 0.00	0.01+/- 0.00	0.13+/- 0.05	2.8+/- 0.4	4.4	0.19+/- (0.03- 0.06)	Formatted: Font color: Accent 6
Inventory	0.04+/- 0.02	0.00+/- 0.00	0.02+/- 0.00	0.08+/- 0.02	0.04+/- 0.02	0.01+/- 0.00	0.01+/- 0.00	0.15+/- 0.05	6.0+/- 4.4		0.19+/- (0.03- 0.06)	Formatted: Font color: Accent 6
15) Iran (Islamic Republic of)	2.2+/- 0.2	0.18+/- 0.06	0.69+/- 0.12	0.00+/- 0.00	3.0+/- 0.4	0.02+/- 0.00	0.73+/- 0.16	0.26+/- 0.07	0.46+/- 0.13	4.3	8.8+/- (0.5- 1.0)	Formatted: Font color: Accent 6
Inventory	0.74+/- 0.36	0.15+/- 0.05	0.41+/- 0.12	0.00+/- 0.00	3.4+/- 1.6	0.02+/- 0.00	0.47+/- 0.17	0.26+/- 0.07	0.19+/- 0.14		5.2+/- (1.7- 2.3)	Formatted: Font color: Accent 6
16) Bolivia (Plurinational State of)	0.60+/- 0.28	0.02+/- 0.02	0.03+/- 0.02	0.31+/- 0.16	0.05+/- 0.02	0.00+/- 0.00	0.02+/- 0.01	0.18+/- 0.08	2.2+/- 0.5	4.3	1.0+/- (0.3- 0.5)	Formatted: Font color: Accent 6

Inventory	0.61+/- 0.32	0.03+/- 0.02	0.03+/- 0.02	0.34+/- 0.16	0.05+/- 0.02	0.00+/- 0.00	0.02+/- 0.01	0.19+/- 0.08	3.4+/- 2.4	1.1+/- (0.4- 0.5)	Formatted: Font color: Accent 6
17) Mexico	4.1+/-0.5 -0.00	0.00+/- -0.5	1.2+/- -0.04	0.12+/- -0.03	0.07+/- -0.03	0.12+/- -0.04	0.55+/- -0.12	0.19+/- -0.07	1.1+/- -0.3	3.7 6.1+/- (0.7- 1.2)	Formatted: Font color: Accent 6
Inventory	2.0+/-0.9 -0.00	0.01+/- -1.3	2.4+/- -0.04	0.12+/- -0.03	0.07+/- -0.03	0.09+/- -0.04	0.34+/- -0.12	0.19+/- -0.07	0.81+/- -0.32	5.0+/- (1.5- 2.3)	Formatted: Font color: Accent 6
18) Pakistan	6.7+/-0.6 -0.5	2.2+/- -0.16	0.39+/- -0.00	0.01+/- -0.09	0.26+/- -0.04	0.06+/- -0.11	0.29+/- -0.11	0.53+/- -0.16	0.08+/- -0.03	3.6 9.9+/- (0.9- 1.6)	Formatted: Font color: Accent 6
Inventory	3.4+/-1.9 -0.5	1.2+/- -0.16	0.28+/- -0.00	0.01+/- -0.09	0.19+/- -0.04	0.06+/- -0.11	0.25+/- -0.18	0.35+/- -0.03	0.08+/- -0.03	5.4+/- (2.0- 2.8)	Formatted: Font color: Accent 6
19) Congo	0.01+/- -0.00	0.00+/- -0.00	0.01+/- -0.00	0.06+/- -0.04	- 0.26+/- -0.11	0.00+/- -0.00	0.00+/- -0.00	0.04+/- -0.01	7.5+/- -0.9	3.4 - 0.18+/- (0.12- 0.16)	Formatted: Font color: Accent 6
Inventory	0.01+/- -0.00	0.00+/- -0.00	0.01+/- -0.00	0.07+/- -0.04	0.21+/- -0.14	0.00+/- -0.00	0.00+/- -0.00	0.04+/- -0.01	8.0+/- -6.4	0.30+/- (0.15- 0.19)	Formatted: Font color: Accent 6
20) United Republic of Tanzania	2.8+/-0.4 -0.13	0.18+/- -0.04	0.13+/- -0.10	0.34+/- -0.10	0.00+/- -0.00	0.00+/- -0.00	0.05+/- -0.03	0.06+/- -0.02	1.9+/- -0.4	3.5+/- (0.4- 0.7)	Formatted: Font color: Accent 6
Inventory	0.96+/- -0.59	0.20+/- -0.14	0.12+/- -0.04	0.23+/- -0.10	0.00+/- -0.00	0.00+/- -0.00	0.05+/- -0.03	0.06+/- -0.02	1.5+/- -0.8	1.6+/- (0.6- 0.9)	Formatted: Font color: Accent 6
21) South Africa	1.9+/-0.2 -0.00	0.00+/- -0.15	0.72+/- -0.01	0.05+/- -0.01	0.00+/- -0.00	0.71+/- -0.13	0.00+/- -0.00	0.04+/- -0.01	0.21+/- -0.07	3.4+/- (0.3- 0.5)	Formatted: Font color: Accent 6
Inventory	0.52+/- -0.30	0.00+/- -0.00	0.65+/- -0.25	0.05+/- -0.01	0.00+/- -0.00	0.43+/- -0.19	0.00+/- -0.00	0.04+/- -0.01	0.16+/- -0.07	1.6+/- (0.4- 0.7)	Formatted: Font color: Accent 6
22) Ethiopia	10.1+/- -0.4	0.01+/- -0.00	0.12+/- -0.04	0.09+/- -0.05	0.00+/- -0.00	0.00+/- -0.00	0.00+/- -0.00	0.14+/- -0.04	0.43+/- -0.11	10.3+/- (0.4- 0.5)	Formatted: Font color: Accent 6
Inventory	1.9+/-1.1 -0.00	0.01+/- -0.04	0.10+/- -0.05	0.08+/- -0.05	0.00+/- -0.00	0.00+/- -0.00	0.00+/- -0.00	0.12+/- -0.05	0.27+/- -0.12	2.1+/- (1.1- 1.2)	Formatted: Font color: Accent 6
23) Angola	0.13+/- -0.03	0.00+/- -0.00	0.08+/- -0.05	0.75+/- -0.22	- 1.38+/- -0.21	0.00+/- -0.00	0.00+/- -0.00	0.04+/- -0.01	1.4+/- -0.1	2.8 - 0.41+/- (0.34- 0.51)	Formatted: Font color: Accent 6
Inventory	0.15+/- -0.03	0.01+/- -0.00	0.14+/- -0.05	0.74+/- -0.31	0.63+/- -0.36	0.00+/- -0.00	0.00+/- -0.00	0.04+/- -0.01	0.41+/- -0.16	1.7+/- (0.5- 0.8)	Formatted: Font color: Accent 6
24) Myanmar	0.67+/- -0.47	6.9+/- -0.6	0.05+/- -0.01	0.23+/- -0.06	0.00+/- -0.00	0.01+/- -0.00	0.01+/- -0.00	0.08+/- -0.04	0.72+/- -0.31	7.8+/- (0.8- 1.2)	Formatted: Font color: Accent 6
Inventory	0.83+/- -0.56	2.0+/- -1.4	0.05+/- -0.01	0.24+/- -0.06	0.00+/- -0.00	0.01+/- -0.00	0.01+/- -0.00	0.09+/- -0.04	0.64+/- -0.33	3.2+/- (1.5- 2.1)	Formatted: Font color: Accent 6
25) Thailand	0.21+/- -0.18	2.7+/- -0.8	0.27+/- -0.16	0.10+/- -0.03	0.10+/- -0.16	0.02+/- -0.01	0.07+/- -0.06	0.06+/- -0.02	0.18+/- -0.35	2.4 3.5+/- (0.8- 1.4)	Formatted: Font color: Accent 6
Inventory	0.31+/- -0.18	2.9+/- -2.2	0.26+/- -0.16	0.10+/- -0.03	0.21+/- -0.16	0.02+/- -0.01	0.09+/- -0.06	0.06+/- -0.02	0.62+/- -0.39	3.8+/- (2.2- 2.8)	Formatted: Font color: Accent 6
26) Nigeria	1.4+/-0.4 -0.3	1.2+/- -0.15	0.53+/- -0.05	0.12+/- -0.08	0.13+/- -0.12	0.38+/- -0.12	0.25+/- -0.13	0.04+/- -0.01	1.6+/- -0.3	2.3 4.0+/- (0.6- 1.2)	Formatted: Font color: Accent 6

Inventory	0.87+/- 0.52	0.49+/- 0.40	0.47+/- 0.15	0.12+/- 0.05	0.15+/- 0.08	0.25+/- 0.12	0.20+/- 0.13	0.04+/- 0.01	0.84+/- 0.49	2.5+/- (0.7- 1.5)	Formatted: Font color: Accent 6
27) Malaysia	0.04+/- 0.02	0.10+/- 0.07	0.26+/- 0.20	0.04+/- 0.01	0.11+/- 0.03	0.00+/- 0.00	0.11+/- 0.08	0.27+/- 0.13	0.68+/- 0.27	2.2 0.66+/- (0.23- 0.41)	Formatted: Font color: Accent 6
Inventory	0.05+/- 0.02	0.19+/- 0.06	0.47+/- 0.22	0.04+/- 0.01	0.11+/- 0.03	0.00+/- 0.00	0.30+/- 0.08	0.27+/- 0.13	1.1+/- 0.5	1.2+/- (0.2- 0.4)	Formatted: Font color: Accent 6
28) Sudan	0.32+/- 0.03	0.00+/- 0.00	0.08+/- 0.02	0.02+/- 0.02	0.14+/- 0.03	0.00+/- 0.00	0.00+/- 0.00	0.04+/- 0.01	0.17+/- 0.03	2.1 0.57+/- (0.05- 0.10)	Formatted: Font color: Accent 6
Inventory	0.04+/- 0.04	0.00+/- 0.00	0.07+/- 0.02	0.03+/- 0.02	0.06+/- 0.03	0.00+/- 0.00	0.00+/- 0.00	0.04+/- 0.01	0.11+/- 0.03	0.21+/- (0.06- 0.11)	Formatted: Font color: Accent 6
29) Zambia	0.13+/- 0.05	0.00+/- 0.00	0.07+/- 0.03	0.81+/- 0.16	0.00+/- 0.00	0.00+/- 0.00	0.00+/- 0.00	0.04+/- 0.01	0.91+/- 0.24	2.1 1.0+/- (0.2- 0.2)	Formatted: Font color: Accent 6
Inventory	0.13+/- 0.05	0.00+/- 0.00	0.08+/- 0.04	0.42+/- 0.19	0.00+/- 0.00	0.00+/- 0.00	0.00+/- 0.00	0.04+/- 0.01	0.87+/- 0.43	0.64+/- (0.20- 0.27)	Formatted: Font color: Accent 6
30) South Sudan	0.05+/- 0.03	0.00+/- 0.00	0.02+/- 0.00	- 0.07+/- 0.16	0.26+/- 0.06	0.00+/- 0.00	0.00+/- 0.00	0.04+/- 0.01	3.1+/- 0.4	0.25+/- (0.17- 0.25)	Formatted: Font color: Accent 6
Inventory	0.03+/- 0.03	0.00+/- 0.00	0.02+/- 0.00	0.34+/- 0.16	0.11+/- 0.06	0.00+/- 0.00	0.00+/- 0.00	0.04+/- 0.01	1.8+/- 1.3	0.50+/- (0.18- 0.26)	Formatted: Font color: Accent 6
31) Turkey	0.89+/- 0.28	0.04+/- 0.02	1.8+/- 0.5	0.01+/- 0.00	0.02+/- 0.01	0.23+/- 0.04	0.10+/- 0.03	0.33+/- 0.15	0.10+/- 0.05	3.1+/- (0.6- 0.9)	Formatted: Font color: Accent 6
Inventory	0.70+/- 0.33	0.05+/- 0.02	2.0+/- 0.8	0.01+/- 0.00	0.02+/- 0.01	0.22+/- 0.04	0.10+/- 0.03	0.47+/- 0.17	0.10+/- 0.05	3.1+/- (0.9- 1.2)	Formatted: Font color: Accent 6
32) Saudi Arabia	0.16+/- 0.05	0.00+/- 0.00	0.29+/- 0.07	0.00+/- 0.00	0.12+/- 0.09	0.00+/- 0.00	0.65+/- 0.21	0.09+/- 0.03	0.00+/- 0.00	1.2+/- (0.2- 0.4)	Formatted: Font color: Accent 6
Inventory	0.10+/- 0.06	0.00+/- 0.00	0.23+/- 0.07	0.00+/- 0.00	0.29+/- 0.11	0.00+/- 0.00	0.53+/- 0.26	0.10+/- 0.03	0.00+/- 0.00	1.2+/- (0.3- 0.5)	Formatted: Font color: Accent 6
33) Kazakhstan	0.58+/- 0.08	0.02+/- 0.01	0.15+/- 0.03	0.05+/- 0.01	0.12+/- 0.06	1.2+/- 0.3	0.15+/- 0.05	0.25+/- 0.07	0.39+/- 0.09	2.3+/- (0.4- 0.6)	Formatted: Font color: Accent 6
Inventory	0.54+/- 0.08	0.03+/- 0.01	0.13+/- 0.04	0.05+/- 0.01	0.20+/- 0.07	0.90+/- 0.38	0.17+/- 0.06	0.21+/- 0.07	0.36+/- 0.10	2.0+/- (0.4- 0.6)	Formatted: Font color: Accent 6
34) Central African Republic	0.04+/- 0.07	0.00+/- 0.00	0.02+/- 0.00	- 0.79+/- 0.17	0.00+/- 0.00	0.00+/- 0.00	0.01+/- 0.00	0.04+/- 0.01	-1.00+/- 0.19	1.8 -0.73+/- (0.18- 0.25)	Formatted: Font color: Accent 6
Inventory	0.13+/- 0.07	0.00+/- 0.00	0.02+/- 0.00	0.40+/- 0.19	0.00+/- 0.00	0.00+/- 0.00	0.01+/- 0.00	0.04+/- 0.01	0.52+/- 0.32	0.55+/- (0.20- 0.27)	Formatted: Font color: Accent 6
35) Viet Nam	0.58+/- 0.21	3.6+/- 0.9	0.20+/- 0.10	0.08+/- 0.02	0.02+/- 0.04	0.09+/- 0.03	0.04+/- 0.03	0.08+/- 0.02	0.61+/- 0.50	1.7 4.6+/- (0.9- 1.3)	Formatted: Font color: Accent 6
Inventory	0.35+/- 0.22	2.7+/- 1.6	0.19+/- 0.10	0.07+/- 0.02	0.12+/- 0.10	0.09+/- 0.03	0.04+/- 0.03	0.08+/- 0.02	1.0+/- 0.6	3.6+/- (1.7- 2.1)	Formatted: Font color: Accent 6
36) France	2.2+/-0.4	0.00+/- 0.00	0.86+/- 0.28	0.00+/- 0.00	0.00+/- 0.00	0.00+/- 0.00	0.05+/- 0.01	0.20+/- 0.06	0.09+/- 0.05	1.7 3.1+/- (0.5- 0.7)	Formatted: Font color: Accent 6
Inventory	1.2+/-0.6	0.00+/- 0.00	0.70+/- 0.33	0.00+/- 0.00	0.00+/- 0.00	0.00+/- 0.00	0.05+/- 0.01	0.19+/- 0.06	0.08+/- 0.05	2.0+/- (0.7- 1.0)	Formatted: Font color: Accent 6

37) Uzbekistan	0.79+/- 0.23	0.02+/- 0.01	0.10+/- 0.04	0.00+/- 0.00	0.04+/- 0.02	0.01+/- 0.00	2.9+/- 0.4	0.04+/- 0.01	0.04+/- 0.02	1.6	3.9+/- (0.5- 0.8)	Formatted: Font color: Accent 6
Inventory	0.56+/- 0.26	0.03+/- 0.01	0.08+/- 0.04	0.00+/- 0.00	0.03+/- 0.02	0.01+/- 0.00	2.3+/- 1.0	0.04+/- 0.01	0.04+/- 0.02		3.0+/- (1.1- 1.4)	Formatted: Font color: Accent 6
38) Turkmenistan	0.35+/- 0.11	0.04+/- 0.01	0.02+/- 0.01	0.00+/- 0.00	1.5+/- 0.3	0.00+/- 0.00	1.1+/- 0.2	1.2+/- 0.2	0.01+/- 0.00	1.6	3.0+/- (0.4- 0.6)	Formatted: Font color: Accent 6
Inventory	0.22+/- 0.11	0.05+/- 0.01	0.02+/- 0.01	0.00+/- 0.00	0.85+/- 0.33	0.00+/- 0.00	0.58+/- 0.26	0.58+/- 0.30	0.01+/- 0.00		1.7+/- (0.4- 0.7)	Formatted: Font color: Accent 6
39) Philippines	0.25+/- 0.14	0.20+/- 0.52	0.84+/- 0.31	0.01+/- 0.00	0.01+/- 0.01	0.04+/- 0.01	0.01+/- 0.00	0.29+/- 0.15	0.45+/- 0.15	1.5	0.96+/- (0.62- 0.99)	Formatted: Font color: Accent 6
Inventory	0.26+/- 0.14	1.6+/- 0.9	0.52+/- 0.33	0.01+/- 0.00	0.01+/- 0.01	0.04+/- 0.01	0.01+/- 0.00	0.32+/- 0.15	0.25+/- 0.16		2.4+/- (1.0- 1.4)	Formatted: Font color: Accent 6
40) Paraguay	0.64+/- 0.40	0.01+/- 0.02	0.03+/- 0.03	0.05+/- 0.03	0.00+/- 0.00	0.00+/- 0.00	0.00+/- 0.00	0.04+/- 0.01	1.4+/- 0.6	1.5	0.74+/- (0.40- 0.47)	Formatted: Font color: Accent 6
Inventory	0.59+/- 0.48	0.02+/- 0.02	0.03+/- 0.03	0.05+/- 0.03	0.00+/- 0.00	0.00+/- 0.00	0.00+/- 0.00	0.04+/- 0.01	1.5+/- 1.1		0.69+/- (0.49- 0.56)	Formatted: Font color: Accent 6
41) Guyana	0.01+/- 0.01	0.07+/- 0.07	0.00+/- 0.00	0.01+/- 0.00	0.00+/- 0.00	0.00+/- 0.00	0.00+/- 0.00	0.04+/- 0.01	1.5+/- 0.3	1.5	0.09+/- (0.08- 0.09)	Formatted: Font color: Accent 6
Inventory	0.01+/- 0.01	0.08+/- 0.07	0.00+/- 0.00	0.01+/- 0.00	0.00+/- 0.00	0.00+/- 0.00	0.00+/- 0.00	0.04+/- 0.01	1.4+/- 1.3		0.10+/- (0.07- 0.08)	Formatted: Font color: Accent 6
42) Mozambique	0.09+/- 0.02	0.04+/- 0.03	0.08+/- 0.02	0.64+/- 0.14	0.00+/- 0.00	0.02+/- 0.01	0.01+/- 0.01	0.04+/- 0.01	1.2+/- 0.2	1.4	0.87+/- (0.15- 0.22)	Formatted: Font color: Accent 6
Inventory	0.10+/- 0.03	0.04+/- 0.03	0.08+/- 0.02	0.35+/- 0.15	0.00+/- 0.00	0.02+/- 0.01	0.01+/- 0.01	0.04+/- 0.01	0.62+/- 0.25		0.60+/- (0.16- 0.24)	Formatted: Font color: Accent 6
43) Egypt	1.1+/-0.3	0.23+/- 0.13	2.0+/- 0.3	0.00+/- 0.00	0.43+/- 0.11	0.00+/- 0.00	0.09+/- 0.04	0.04+/- 0.01	0.06+/- 0.02	1.4	3.9+/- (0.4- 0.8)	Formatted: Font color: Accent 6
Inventory	0.44+/- 0.29	0.22+/- 0.12	0.66+/- 0.41	0.00+/- 0.00	0.33+/- 0.12	0.00+/- 0.00	0.07+/- 0.04	0.04+/- 0.01	0.04+/- 0.02		1.7+/- (0.5- 1.0)	Formatted: Font color: Accent 6
44) Cameroon	0.42+/- 0.15	0.05+/- 0.04	0.13+/- 0.10	0.08+/- 0.05	0.01+/- 0.02	0.00+/- 0.00	0.04+/- 0.03	0.04+/- 0.01	-0.69+/- 0.30	1.3	0.71+/- (0.20- 0.39)	Formatted: Font color: Accent 6
Inventory	0.23+/- 0.18	0.04+/- 0.04	0.24+/- 0.10	0.09+/- 0.05	0.03+/- 0.02	0.00+/- 0.00	0.03+/- 0.03	0.04+/- 0.01	0.72+/- 0.47		0.67+/- (0.22- 0.42)	Formatted: Font color: Accent 6
45) Algeria	0.25+/- 0.11	0.00+/- 0.00	0.16+/- 0.08	0.00+/- 0.00	0.05+/- 0.01	0.00+/- 0.00	3.2+/- 0.3	0.12+/- 0.02	0.04+/- 0.03	1.3	3.7+/- (0.3- 0.5)	Formatted: Font color: Accent 6
Inventory	0.22+/- 0.12	0.00+/- 0.00	0.19+/- 0.09	0.00+/- 0.00	0.05+/- 0.01	0.00+/- 0.00	1.2+/- 0.6	0.11+/- 0.02	0.05+/- 0.03		1.6+/- (0.6- 0.8)	Formatted: Font color: Accent 6
46) Bangladesh	1.0+/-0.5	1.2+/- 1.3	0.15+/- 0.08	0.01+/- 0.00	0.00+/- 0.00	0.01+/- 0.01	0.04+/- 0.03	0.04+/- 0.01	1.4+/- 0.6	1.3	2.4+/- (1.4- 2.0)	Formatted: Font color: Accent 6
Inventory	0.92+/- 0.60	2.6+/- 1.5	0.12+/- 0.08	0.01+/- 0.00	0.00+/- 0.00	0.01+/- 0.01	0.04+/- 0.03	0.04+/- 0.01	0.98+/- 0.60		3.7+/- (1.6- 2.2)	Formatted: Font color: Accent 6
47) Ukraine	0.44+/- 0.16	0.00+/- 0.00	0.48+/- 0.16	0.05+/- 0.01	0.07+/- 0.02	0.57+/- 0.19	0.99+/- 0.39	-0.05+/- 0.24	0.33+/- 0.17	1.3	2.6+/- (0.5- 0.9)	Formatted: Font color: Accent 6

Inventory	0.36+/- 0.16	0.01+/- 0.00	0.50+/- 0.17	0.05+/- 0.01	0.07+/- 0.02	0.66+/- 0.20	1.0+/- 0.5	0.67+/- 0.31	0.31+/- 0.18		2.7+/- (0.6- 1.0)	Formatted: Font color: Accent 6
48) Germany	1.7+/-0.5 -0.00	0.00+/- -0.6	2.0+/- -0.6	0.00+/- -0.00	0.01+/- -0.00	0.10+/- -0.03	0.18+/- -0.10	0.22+/- -0.09	0.09+/- -0.06	1.3	4.0+/- (0.8- 1.2)	Formatted: Font color: Accent 6
Inventory	1.0+/-0.6 -0.00	0.00+/- -0.8	1.6+/- -0.00	0.00+/- -0.00	0.01+/- -0.00	0.10+/- -0.03	0.18+/- -0.10	0.21+/- -0.09	0.08+/- -0.06		2.9+/- (1.0- 1.5)	Formatted: Font color: Accent 6
49) Madagascar	1.3+/-0.2 0.13	0.56+/- 0.00	0.02+/- 0.04	0.12+/- 0.00	0.01+/- 0.00	0.00+/- 0.00	0.05+/- 0.02	0.04+/- 0.01	1.1+/- 0.2	1.3	2.1+/- (0.2- 0.4)	Formatted: Font color: Accent 6
Inventory	0.32+/- 0.21	0.18+/- 0.15	0.02+/- -0.00	0.09+/- 0.04	0.01+/- 0.00	0.00+/- 0.00	0.04+/- 0.02	0.04+/- 0.01	0.34+/- 0.20		0.66+/- (0.26- 0.42)	Formatted: Font color: Accent 6
50) Spain	1.1+/-0.2 -0.01	0.02+/- -0.27	0.94+/- -0.00	0.00+/- -0.00	0.00+/- -0.00	0.01+/- -0.00	0.03+/- -0.01	0.09+/- -0.02	0.09+/- -0.05	1.2	2.1+/- (0.4- 0.5)	Formatted: Font color: Accent 6
Inventory	0.57+/- 0.31	0.03+/- -0.01	0.81+/- -0.37	0.00+/- -0.00	0.00+/- -0.00	0.01+/- -0.00	0.03+/- -0.01	0.09+/- -0.02	0.08+/- -0.05		1.4+/- (0.5- 0.7)	Formatted: Font color: Accent 6
51) Gabon	0.00+/- -0.00	0.00+/- -0.00	0.01+/- -0.00	0.00+/- -0.00	0.01+/- -0.00	0.00+/- -0.00	0.00+/- -0.00	0.04+/- -0.01	0.55+/- -0.21	1.2	0.02+/- (0.01- 0.01)	Formatted: Font color: Accent 6
Inventory	0.00+/- -0.00	0.00+/- -0.00	0.01+/- -0.00	0.01+/- -0.00	0.01+/- -0.00	0.00+/- -0.00	0.00+/- -0.00	0.04+/- -0.01	0.69+/- -0.60		0.03+/- (0.01- 0.01)	Formatted: Font color: Accent 6
52) Kenya	1.5+/-0.4 -0.01	0.01+/- -0.03	0.08+/- -0.00	0.01+/- -0.00	0.00+/- -0.00	0.00+/- -0.00	0.00+/- -0.00	0.10+/- -0.04	0.48+/- -0.15	1.2	1.6+/- (0.4- 0.4)	Formatted: Font color: Accent 6
Inventory	0.92+/- -0.67	0.01+/- -0.01	0.07+/- -0.03	0.01+/- -0.00	0.00+/- -0.00	0.00+/- -0.00	0.00+/- -0.00	0.10+/- -0.04	0.34+/- -0.17		1.0+/- (0.7- 0.7)	Formatted: Font color: Accent 6
53) Suriname	0.01+/- -0.00	0.02+/- -0.02	0.00+/- -0.00	0.00+/- -0.00	0.01+/- -0.01	0.00+/- -0.00	0.00+/- -0.00	0.04+/- -0.01	2.3+/- -0.3	1.1	0.04+/- (0.02- 0.03)	Formatted: Font color: Accent 6
Inventory	0.01+/- -0.00	0.02+/- -0.02	0.00+/- -0.00	0.00+/- -0.00	0.01+/- -0.01	0.00+/- -0.00	0.00+/- -0.00	0.04+/- -0.01	1.7+/- -1.5		0.04+/- (0.02- 0.03)	Formatted: Font color: Accent 6
54) Chad	1.9+/-0.2 -0.03	0.00+/- -0.01	0.03+/- -0.05	-0.02+/- -0.04	0.02+/- -0.00	0.00+/- -0.00	0.00+/- -0.00	0.04+/- -0.01	1.7+/- -0.3	1.1	2.0+/- (0.2- 0.3)	Formatted: Font color: Accent 6
Inventory	0.32+/- -0.22	0.03+/- -0.03	0.03+/- -0.01	0.09+/- -0.05	0.07+/- -0.04	0.00+/- -0.00	0.00+/- -0.00	0.04+/- -0.01	0.67+/- -0.40		0.55+/- (0.23- 0.36)	Formatted: Font color: Accent 6
55) Ecuador	-0.31+/- -0.21	0.01+/- -0.12	0.01+/- -0.01	0.00+/- -0.00	0.03+/- -0.02	0.00+/- -0.00	0.00+/- -0.00	0.04+/- -0.02	-0.32+/- -0.34	1	-0.26+/- (0.24- 0.36)	Formatted: Font color: Accent 6
Inventory	0.30+/- -0.24	0.13+/- -0.11	0.01+/- -0.01	0.00+/- -0.00	0.04+/- -0.02	0.00+/- -0.00	0.00+/- -0.00	0.06+/- -0.02	0.72+/- -0.79		0.48+/- (0.27- 0.38)	Formatted: Font color: Accent 6
56) Uganda	0.17+/- -0.34	0.01+/- -0.01	0.01+/- -0.00	0.05+/- -0.04	0.01+/- -0.00	0.00+/- -0.00	0.05+/- -0.05	0.04+/- -0.01	0.23+/- -0.37	1	0.31+/- (0.35- 0.45)	Formatted: Font color: Accent 6
Inventory	0.47+/- -0.41	0.01+/- -0.01	0.01+/- -0.00	0.07+/- -0.04	0.01+/- -0.00	0.00+/- -0.00	0.06+/- -0.05	0.04+/- -0.01	0.82+/- -0.68		0.63+/- (0.41- 0.51)	Formatted: Font color: Accent 6
57) Japan	0.42+/- -0.10	3.0+/- -0.4	0.51+/- -0.17	0.01+/- -0.00	0.00+/- -0.00	0.02+/- -0.00	0.01+/- -0.01	5.7+/- -0.4	1.2+/- -0.2	1	4.0+/- (0.4- 0.7)	Formatted: Font color: Accent 6
Inventory	0.22+/- -0.10	0.89+/- -0.46	0.28+/- -0.18	0.01+/- -0.00	0.00+/- -0.00	0.02+/- -0.00	0.01+/- -0.01	0.96+/- -0.58	0.44+/- -0.21		1.4+/- (0.5- 0.8)	Formatted: Font color: Accent 6

58) Cambodia	0.13+/- 0.11	1.4+/- 0.4	0.02+/- 0.01	0.21+/- 0.08	0.00+/- 0.00	0.00+/- 0.00	0.02+/- 0.02	0.05+/- 0.02	0.86+/- 0.57	0.95	1.8+/- (0.4- 0.7)	Formatted: Font color: Accent 4
Inventory	0.12+/- 0.11	0.66+/- 0.66	0.02+/- 0.01	0.21+/- 0.08	0.00+/- 0.00	0.00+/- 0.00	0.02+/- 0.02	0.05+/- 0.02	0.87+/- 0.72		1.0+/- (0.7- 0.9)	Formatted: Font color: Accent 4
59) Poland	0.31+/- 0.23	0.00+/- 0.00	0.19+/- 0.40	0.00+/- 0.00	0.05+/- 0.01	0.42+/- 0.16	0.07+/- 0.04	0.22+/- 0.12	0.08+/- 0.06	0.95	1.0+/- (0.5- 0.8)	Formatted: Font color: Accent 4
Inventory	0.42+/- 0.24	0.00+/- 0.00	0.95+/- 0.48	0.00+/- 0.00	0.05+/- 0.01	0.52+/- 0.17	0.08+/- 0.04	0.28+/- 0.12	0.10+/- 0.06		2.0+/- (0.6- 0.9)	Formatted: Font color: Accent 4
60) Italy	0.30+/- 0.22	0.06+/- 0.04	0.66+/- 0.41	0.01+/- 0.00	0.01+/- 0.00	0.00+/- 0.00	0.16+/- 0.09	0.61+/- 0.55	0.13+/- 0.08	0.93	1.2+/- (0.5- 0.8)	Formatted: Font color: Accent 4
Inventory	0.55+/- 0.24	0.07+/- 0.03	0.88+/- 0.45	0.01+/- 0.00	0.01+/- 0.00	0.00+/- 0.00	0.17+/- 0.09	2.9+/- 1.1	0.13+/- 0.08		1.7+/- (0.5- 0.8)	Formatted: Font color: Accent 4
61) Uruguay	1.8+/-0.3	0.05+/- 0.07	0.04+/- 0.02	0.00+/- 0.00	0.00+/- 0.00	0.00+/- 0.00	0.00+/- 0.00	0.04+/- 0.01	0.18+/- 0.09	0.89	1.9+/- (0.3- 0.4)	Formatted: Font color: Accent 4
Inventory	0.62+/- 0.55	0.08+/- 0.07	0.03+/- 0.02	0.00+/- 0.00	0.00+/- 0.00	0.00+/- 0.00	0.00+/- 0.00	0.04+/- 0.01	0.17+/- 0.09		0.73+/- (0.56- 0.64)	Formatted: Font color: Accent 4
62) Iraq	0.27+/- 0.08	0.01+/- 0.00	0.23+/- 0.08	0.00+/- 0.00	0.13+/- 0.05	0.00+/- 0.00	0.01+/- 0.00	0.16+/- 0.06	0.02+/- 0.01	0.88	0.65+/- (0.12- 0.22)	Formatted: Font color: Accent 4
Inventory	0.13+/- 0.09	0.01+/- 0.00	0.15+/- 0.09	0.00+/- 0.00	0.13+/- 0.06	0.00+/- 0.00	0.01+/- 0.00	0.13+/- 0.07	0.02+/- 0.01		0.43+/- (0.14- 0.24)	Formatted: Font color: Accent 4
63) Mali	1.2+/-0.2	0.19+/- 0.10	0.04+/- 0.01	0.05+/- 0.03	0.00+/- 0.00	0.00+/- 0.00	0.00+/- 0.00	0.04+/- 0.01	0.22+/- 0.07	0.86	1.5+/- (0.2- 0.3)	Formatted: Font color: Accent 4
Inventory	0.52+/- 0.33	0.13+/- 0.12	0.04+/- 0.01	0.05+/- 0.03	0.00+/- 0.00	0.00+/- 0.00	0.00+/- 0.00	0.04+/- 0.01	0.18+/- 0.07		0.75+/- (0.35- 0.49)	Formatted: Font color: Accent 4
64) Chile	0.43+/- 0.12	0.00+/- 0.00	0.49+/- 0.11	0.01+/- 0.01	0.01+/- 0.01	0.01+/- 0.00	0.02+/- 0.01	0.15+/- 0.05	0.28+/- 0.07	0.85	0.97+/- (0.16- 0.26)	Formatted: Font color: Accent 4
Inventory	0.24+/- 0.14	0.00+/- 0.00	0.18+/- 0.12	0.01+/- 0.01	0.01+/- 0.01	0.01+/- 0.00	0.02+/- 0.01	0.13+/- 0.05	0.27+/- 0.08		0.48+/- (0.18- 0.29)	Formatted: Font color: Accent 4
65) United Kingdom of Great Britain and Northern Ireland											1.3+/- (0.8- 1.3)	Formatted: Font color: Accent 4
Inventory	0.75+/- 0.44	0.00+/- 0.00	3.8+/- 2.3	0.00+/- 0.00	0.01+/- 0.00	0.02+/- 0.01	0.16+/- 0.10	0.55+/- 0.22	0.12+/- 0.08		4.8+/- (2.3- 2.8)	Formatted: Font color: Accent 4
66) Republic of Korea	0.30+/- 0.12	1.5+/- 0.2	0.08+/- 0.05	0.00+/- 0.00	0.14+/- 0.09	0.02+/- 0.01	0.12+/- 0.08	0.04+/- 0.01	0.06+/- 0.04	0.78	2.2+/- (0.3- 0.6)	Formatted: Font color: Accent 4
Inventory	0.15+/- 0.13	0.35+/- 0.29	0.06+/- 0.05	0.00+/- 0.00	0.10+/- 0.09	0.02+/- 0.01	0.08+/- 0.08	0.04+/- 0.01	0.05+/- 0.04		0.77+/- (0.34- 0.64)	Formatted: Font color: Accent 4
67) New Zealand	1.5+/-0.2	0.00+/- 0.00	0.26+/- 0.11	0.00+/- 0.00	0.00+/- 0.00	0.01+/- 0.00	0.01+/- 0.00	0.18+/- 0.07	0.43+/- 0.12	0.77	1.8+/- (0.3- 0.4)	Formatted: Font color: Accent 4
Inventory	0.70+/- 0.41	0.00+/- 0.00	0.21+/- 0.12	0.00+/- 0.00	0.00+/- 0.00	0.01+/- 0.00	0.01+/- 0.00	0.17+/- 0.07	0.27+/- 0.12		0.93+/- (0.43- 0.53)	Formatted: Font color: Accent 4

68) Afghanistan	0.70+/- 0.19	0.04+/- 0.01	0.03+/- 0.01	0.00+/- 0.00	0.01+/- 0.01	0.13+/- 0.05	0.01+/- 0.00	0.04+/- 0.01	0.00+/- 0.00	0.74	0.92+/- (0.20- 0.28)	Formatted: Font color: Accent 4
Inventory	0.40+/- 0.27	0.05+/- 0.01	0.03+/- 0.01	0.00+/- 0.00	0.01+/- 0.01	0.11+/- 0.05	0.01+/- 0.00	0.04+/- 0.01	0.00+/- 0.00		0.60+/- (0.28- 0.35)	Formatted: Font color: Accent 4
69) Niger	1.5+/-0.2 0.01	0.01+/- 0.05	0.13+/- 0.00	0.00+/- 0.00	0.01+/- 0.00	0.00+/- 0.00	0.00+/- 0.00	0.04+/- 0.01	0.08+/- 0.02	0.72	1.6+/- (0.2- 0.3)	Formatted: Font color: Accent 4
Inventory	0.50+/- 0.34	0.01+/- 0.01	0.12+/- 0.05	0.00+/- 0.00	0.01+/- 0.00	0.00+/- 0.00	0.00+/- 0.00	0.04+/- 0.01	0.04+/- 0.02		0.65+/- (0.35- 0.41)	Formatted: Font color: Accent 4
70) Cote d'Ivoire	0.04+/- 0.05	0.02+/- 0.04	0.03+/- 0.02	0.05+/- 0.03	0.78+/- 0.31	0.00+/- 0.00	0.11+/- 0.09	0.04+/- 0.01	-0.03+/- 0.29	0.72	1.0+/- (0.3- 0.5)	Formatted: Font color: Accent 4
Inventory	0.06+/- 0.05	0.04+/- 0.04	0.04+/- 0.02	0.05+/- 0.03	0.65+/- 0.41	0.00+/- 0.00	0.11+/- 0.09	0.04+/- 0.01	0.46+/- 0.35		0.94+/- (0.43- 0.64)	Formatted: Font color: Accent 4
71) Sweden	0.12+/- 0.04	0.00+/- 0.00	0.12+/- 0.05	0.00+/- 0.00	0.00+/- 0.00	0.00+/- 0.00	0.00+/- 0.00	0.04+/- 0.01	1.8+/- 0.4	0.71	0.25+/- (0.07- 0.09)	Formatted: Font color: Accent 4
Inventory	0.11+/- 0.04	0.00+/- 0.00	0.11+/- 0.05	0.00+/- 0.00	0.00+/- 0.00	0.00+/- 0.00	0.00+/- 0.00	0.04+/- 0.01	0.86+/- 0.56		0.22+/- (0.07- 0.10)	Formatted: Font color: Accent 4
72) Zimbabwe	0.01+/- 0.11	0.00+/- 0.00	0.01+/- 0.05	0.04+/- 0.01	0.00+/- 0.00	0.00+/- 0.00	0.00+/- 0.00	0.04+/- 0.01	0.03+/- 0.03	0.71	0.05+/- (0.12- 0.18)	Formatted: Font color: Accent 4
Inventory	0.16+/- 0.13	0.00+/- 0.00	0.14+/- 0.07	0.03+/- 0.01	0.00+/- 0.00	0.00+/- 0.00	0.00+/- 0.00	0.04+/- 0.01	0.06+/- 0.04		0.33+/- (0.15- 0.22)	Formatted: Font color: Accent 4
73) United Arab Emirates	0.04+/- 0.02	0.00+/- 0.00	0.37+/- 0.18	0.00+/- 0.00	0.72+/- 0.21	0.00+/- 0.00	0.05+/- 0.05	0.04+/- 0.01	0.01+/- 0.01	0.71	1.2+/- (0.3- 0.5)	Formatted: Font color: Accent 4
Inventory	0.03+/- 0.02	0.00+/- 0.00	0.27+/- 0.20	0.00+/- 0.00	1.3+/- 0.7	0.00+/- 0.00	0.07+/- 0.05	0.04+/- 0.01	0.01+/- 0.01		1.6+/- (0.7- 1.0)	Formatted: Font color: Accent 4
74) Romania	0.14+/- 0.15	0.00+/- 0.00	0.09+/- 0.18	0.01+/- 0.00	0.14+/- 0.04	0.19+/- 0.10	0.18+/- 0.15	0.79+/- 0.45	0.02+/- 0.05	0.7	0.75+/- (0.29- 0.62)	Formatted: Font color: Accent 4
Inventory	0.22+/- 0.16	0.00+/- 0.00	0.30+/- 0.19	0.01+/- 0.00	0.13+/- 0.05	0.24+/- 0.10	0.22+/- 0.15	2.1+/- 1.0	0.06+/- 0.05		1.1+/- (0.3- 0.6)	Formatted: Font color: Accent 4
75) Nepal	-1.08+/- -0.29	-0.04+/- 0.24	0.09+/- 0.05	0.01+/- 0.00	0.00+/- 0.00	0.00+/- 0.00	0.04+/- 0.02	0.06+/- 0.03	0.19+/- 0.08	0.69	-0.98+/- (0.38- 0.60)	Formatted: Font color: Accent 4
Inventory	0.54+/- 0.45	0.40+/- 0.25	0.06+/- 0.05	0.01+/- 0.00	0.00+/- 0.00	0.00+/- 0.00	0.04+/- 0.02	0.07+/- 0.03	0.10+/- 0.09		1.0+/- (0.5- 0.8)	Formatted: Font color: Accent 4
76) Botswana	0.08+/- 0.04	0.00+/- 0.00	0.40+/- 0.24	0.03+/- 0.01	0.00+/- 0.00	0.01+/- 0.01	0.00+/- 0.00	0.04+/- 0.01	0.16+/- 0.11	0.66	0.52+/- (0.24- 0.29)	Formatted: Font color: Accent 4
Inventory	0.09+/- 0.04	0.00+/- 0.00	3.9+/- 1.8	0.03+/- 0.01	0.00+/- 0.00	0.01+/- 0.01	0.00+/- 0.00	0.04+/- 0.01	0.20+/- 0.13		4.0+/- (1.8- 3.9)	Formatted: Font color: Accent 4
77) Finland	0.07+/- 0.03	0.00+/- 0.00	0.11+/- 0.29	0.00+/- 0.00	0.00+/- 0.00	0.00+/- 0.00	0.00+/- 0.00	0.04+/- 0.01	0.17+/- 0.32	0.63	0.18+/- (0.29- 0.32)	Formatted: Font color: Accent 4
Inventory	0.07+/- 0.03	0.00+/- 0.00	0.60+/- 0.36	0.00+/- 0.00	0.00+/- 0.00	0.00+/- 0.00	0.00+/- 0.00	0.04+/- 0.01	0.68+/- 0.49		0.67+/- (0.36- 0.38)	Formatted: Font color: Accent 4
78) Ghana	0.02+/- 0.08	0.01+/- 0.04	0.08+/- 0.04	0.06+/- 0.05	0.04+/- 0.03	0.00+/- 0.00	0.00+/- 0.00	0.04+/- 0.01	-0.10+/- 0.29	0.63	0.21+/- (0.12- 0.25)	Formatted: Font color: Accent 4

Inventory	0.10+/- 0.09	0.05+/- 0.05	0.09+/- 0.04	0.09+/- 0.05	0.05+/- 0.03	0.00+/- 0.00	0.00+/- 0.00	0.04+/- 0.01	0.49+/- 0.39		0.37+/- (0.12- 0.26)
79) Lao People's Democratic Republic	0.09+/- 0.10	0.27+/- 0.18	0.01+/- 0.01	0.10+/- 0.03	0.00+/- 0.00	0.00+/- 0.00	0.01+/- 0.01	0.05+/- 0.01	0.07+/- 0.14	0.59	- 0.06+/- (0.21- 0.32)
Inventory	0.12+/- 0.10	0.25+/- 0.21	0.01+/- 0.01	0.10+/- 0.03	0.00+/- 0.00	0.00+/- 0.00	0.01+/- 0.01	0.05+/- 0.01	0.21+/- 0.15		0.49+/- (0.23- 0.35)
80) Democratic People's Republic of Korea	0.06+/- 0.03	0.34+/- 0.09	0.15+/- 0.08	0.00+/- 0.00	0.00+/- 0.00	0.63+/- 0.22	0.00+/- 0.00	0.05+/- 0.01	0.10+/- 0.04	0.55	1.2+/- (0.3- 0.4)
Inventory	0.05+/- 0.03	0.15+/- 0.08	0.10+/- 0.08	0.00+/- 0.00	0.00+/- 0.00	0.48+/- 0.27	0.00+/- 0.00	0.05+/- 0.01	0.07+/- 0.05		0.78+/- (0.29- 0.47)
81) French Guiana	0.00+/- 0.00	0.00+/- 0.00	0.00+/- 0.00	0.00+/- 0.00	0.00+/- 0.00	0.00+/- 0.00	0.04+/- 0.01	0.37+/- 0.17	0.48	0.00+/- (0.00- 0.00)	
Inventory	0.00+/- 0.00	0.00+/- 0.00	0.00+/- 0.00	0.00+/- 0.00	0.00+/- 0.00	0.00+/- 0.00	0.04+/- 0.01	0.30+/- 0.36		0.00+/- (0.00- 0.00)	
82) Tajikistan	0.27+/- 0.13	0.00+/- 0.00	0.06+/- 0.03	0.00+/- 0.00	0.00+/- 0.00	0.01+/- 0.00	0.16+/- 0.08	0.05+/- 0.01	0.01+/- 0.01	0.47	0.50+/- (0.16- 0.26)
Inventory	0.18+/- 0.16	0.01+/- 0.00	0.04+/- 0.04	0.00+/- 0.00	0.00+/- 0.00	0.01+/- 0.00	0.13+/- 0.10	0.05+/- 0.01	0.01+/- 0.01		0.37+/- (0.19- 0.30)
83) Honduras	0.54+/- 0.11	0.00+/- 0.00	0.08+/- 0.04	0.01+/- 0.01	0.00+/- 0.00	0.00+/- 0.00	0.01+/- 0.01	0.08+/- 0.03	0.80+/- 0.24	0.46	0.65+/- (0.12- 0.17)
Inventory	0.15+/- 0.14	0.00+/- 0.00	0.05+/- 0.04	0.01+/- 0.01	0.00+/- 0.00	0.00+/- 0.00	0.01+/- 0.01	0.07+/- 0.03	0.55+/- 0.48		0.22+/- (0.15- 0.20)
84) Burkina Faso	0.36+/- 0.17	0.02+/- 0.02	0.02+/- 0.01	0.01+/- 0.01	0.00+/- 0.00	0.00+/- 0.00	0.03+/- 0.02	0.04+/- 0.01	0.02+/- 0.01	0.45	0.44+/- (0.17- 0.23)
Inventory	0.32+/- 0.26	0.02+/- 0.02	0.02+/- 0.01	0.02+/- 0.01	0.00+/- 0.00	0.00+/- 0.00	0.03+/- 0.02	0.04+/- 0.01	0.02+/- 0.01		0.41+/- (0.26- 0.32)
85) Syrian Arab Republic	0.15+/- 0.08	0.00+/- 0.00	0.15+/- 0.06	0.00+/- 0.00	0.01+/- 0.00	0.00+/- 0.00	0.02+/- 0.01	0.09+/- 0.02	0.00+/- 0.00	0.41	0.33+/- (0.10- 0.15)
Inventory	0.12+/- 0.09	0.00+/- 0.00	0.13+/- 0.08	0.00+/- 0.00	0.01+/- 0.00	0.00+/- 0.00	0.02+/- 0.01	0.09+/- 0.02	0.00+/- 0.00		0.28+/- (0.12- 0.18)
86) Azerbaijan	0.46+/- 0.14	0.00+/- 0.00	0.06+/- 0.03	0.00+/- 0.00	0.36+/- 0.25	0.00+/- 0.00	0.03+/- 0.02	- 0.35+/- 0.51	0.03+/- 0.02	0.41	0.92+/- (0.29- 0.44)
Inventory	0.20+/- 0.16	0.00+/- 0.00	0.05+/- 0.03	0.00+/- 0.00	0.48+/- 0.25	0.00+/- 0.00	0.03+/- 0.02	2.8+/- 1.7	0.02+/- 0.02		0.76+/- (0.30- 0.46)
87) Morocco	0.31+/- 0.12	0.00+/- 0.00	0.11+/- 0.09	0.00+/- 0.00	0.00+/- 0.00	0.00+/- 0.00	0.04+/- 0.02	0.08+/- 0.02	0.00+/- 0.00	0.4	0.48+/- (0.16- 0.24)
Inventory	0.25+/- 0.15	0.00+/- 0.00	0.21+/- 0.10	0.00+/- 0.00	0.00+/- 0.00	0.00+/- 0.00	0.05+/- 0.02	0.09+/- 0.02	0.00+/- 0.00		0.51+/- (0.18- 0.28)
88) Somalia	1.4+/-0.2	0.00+/- 0.00	0.04+/- 0.01	0.00+/- 0.00	0.00+/- 0.00	0.00+/- 0.00	0.02+/- 0.01	0.04+/- 0.01	0.21+/- 0.06	0.39	1.4+/- (0.2- 0.3)

Inventory	0.52+/- 0.41	0.00+/- 0.00	0.04+/- 0.01	0.00+/- 0.00	0.00+/- 0.00	0.00+/- 0.00	0.02+/- 0.01	0.04+/- 0.01	0.13+/- 0.06		0.58+/- (0.41- 0.43)
89) Kyrgyzstan	0.15+/- 0.03	0.00+/- 0.00	0.12+/- 0.05	0.00+/- 0.00	0.02+/- 0.01	0.00+/- 0.00	0.15+/- 0.06	0.05+/- 0.01	0.07+/- 0.06	0.39	0.44+/- (0.08- 0.15)
Inventory	0.14+/- 0.04	0.00+/- 0.00	0.07+/- 0.05	0.00+/- 0.00	0.02+/- 0.01	0.00+/- 0.00	0.09+/- 0.06	0.04+/- 0.01	0.08+/- 0.06		0.32+/- (0.09- 0.16)
90) Libya	0.04+/- 0.02	0.00+/- 0.00	0.04+/- 0.02	0.00+/- 0.00	0.43+/- 0.10	0.00+/- 0.00	0.01+/- 0.00	0.17+/- 0.05	0.01+/- 0.01	0.38	0.53+/- (0.11- 0.15)
Inventory	0.05+/- 0.02	0.00+/- 0.00	0.05+/- 0.02	0.00+/- 0.00	0.32+/- 0.12	0.00+/- 0.00	0.01+/- 0.00	0.15+/- 0.05	0.02+/- 0.01		0.44+/- (0.12- 0.17)
91) Oman	0.04+/- 0.02	0.00+/- 0.00	0.03+/- 0.01	0.00+/- 0.00	0.12+/- 0.03	0.00+/- 0.00	0.01+/- 0.00	0.04+/- 0.01	0.03+/- 0.02	0.38	0.19+/- (0.04- 0.07)
Inventory	0.03+/- 0.02	0.00+/- 0.00	0.02+/- 0.01	0.00+/- 0.00	0.12+/- 0.04	0.00+/- 0.00	0.01+/- 0.00	0.04+/- 0.01	0.03+/- 0.02		0.18+/- (0.04- 0.07)
92) Bulgaria	0.01+/- 0.05	0.00+/- 0.00	- 0.21+/- 0.16	0.01+/- 0.00	0.00+/- 0.00	0.03+/- 0.01	0.01+/- 0.00	- 0.04+/- 0.16	0.02+/- 0.05	0.38	- 0.14+/- (0.17- 0.23)
Inventory	0.07+/- 0.05	0.00+/- 0.00	0.31+/- 0.20	0.01+/- 0.00	0.00+/- 0.00	0.03+/- 0.01	0.01+/- 0.00	0.31+/- 0.17	0.06+/- 0.05		0.43+/- (0.21- 0.27)
93) Nicaragua	0.56+/- 0.17	0.01+/- 0.01	0.03+/- 0.03	0.01+/- 0.00	0.00+/- 0.00	0.00+/- 0.00	0.16+/- 0.08	0.52+/- 0.16		0.61+/- (0.17- 0.21)	
Inventory	0.23+/- 0.21	0.01+/- 0.01	0.03+/- 0.03	0.01+/- 0.00	0.00+/- 0.00	0.00+/- 0.00	0.14+/- 0.09	0.23+/- 0.22		0.28+/- (0.21- 0.25)	
94) Namibia	0.04+/- 0.04	0.00+/- 0.00	0.01+/- 0.00	0.02+/- 0.01	0.00+/- 0.00	0.00+/- 0.00	0.00+/- 0.00	0.04+/- 0.01	- 0.01+/- 0.03	0.34	0.07+/- (0.04- 0.06)
Inventory	0.08+/- 0.04	0.00+/- 0.00	0.01+/- 0.00	0.02+/- 0.01	0.00+/- 0.00	0.00+/- 0.00	0.00+/- 0.00	0.04+/- 0.01	0.05+/- 0.04		0.11+/- (0.04- 0.06)
95) Austria	0.06+/- 0.11	0.00+/- 0.00	0.02+/- 0.08	0.00+/- 0.00	0.00+/- 0.00	0.00+/- 0.00	0.02+/- 0.01	0.19+/- 0.10	0.03+/- 0.02	0.33	0.10+/- (0.14- 0.21)
Inventory	0.18+/- 0.14	0.00+/- 0.00	0.13+/- 0.09	0.00+/- 0.00	0.00+/- 0.00	0.00+/- 0.00	0.02+/- 0.01	0.25+/- 0.11	0.03+/- 0.02		0.33+/- (0.17- 0.25)
96) Guinea	0.06+/- 0.11	0.37+/- 0.14	0.02+/- 0.01	0.09+/- 0.05	0.00+/- 0.00	0.00+/- 0.00	0.02+/- 0.01	0.04+/- 0.01	0.03+/- 0.01	0.32	0.56+/- (0.18- 0.32)
Inventory	0.15+/- 0.13	0.19+/- 0.18	0.02+/- 0.01	0.08+/- 0.05	0.00+/- 0.00	0.00+/- 0.00	0.02+/- 0.01	0.04+/- 0.01	0.03+/- 0.01		0.46+/- (0.22- 0.37)
97) Sri Lanka	0.07+/- 0.04	0.41+/- 0.23	0.01+/- 0.00	0.00+/- 0.00	0.00+/- 0.00	0.00+/- 0.00	0.00+/- 0.00	0.04+/- 0.01	0.72+/- 0.18	0.3	0.49+/- (0.23- 0.27)
Inventory	0.06+/- 0.04	0.37+/- 0.25	0.01+/- 0.00	0.00+/- 0.00	0.00+/- 0.00	0.00+/- 0.00	0.00+/- 0.00	0.04+/- 0.01	0.25+/- 0.23		0.44+/- (0.25- 0.30)
98) Greece	0.04+/- 0.06	0.00+/- 0.00	- 0.04+/- 0.15	0.00+/- 0.00	0.00+/- 0.00	0.03+/- 0.01	0.00+/- 0.00	0.17+/- 0.06	0.03+/- 0.06	0.3	0.04+/- (0.16- 0.23)
Inventory	0.10+/- 0.07	0.01+/- 0.00	0.24+/- 0.17	0.00+/- 0.00	0.00+/- 0.00	0.03+/- 0.01	0.00+/- 0.00	0.18+/- 0.06	0.06+/- 0.06		0.39+/- (0.19- 0.25)

^{109) Malawi}	0.15+/- 0.05	0.01+/- 0.01	0.02+/- 0.01	0.07+/- 0.02	0.00+/- 0.00	0.00+/- 0.00	0.00+/- 0.00	0.04+/- 0.01	0.58+/- 0.12	0.29	0.25+/- (0.05- 0.08)	Formatted: Font color: Dark Red
^{Inventory}	0.06+/- 0.05	0.01+/- 0.01	0.02+/- 0.01	0.03+/- 0.02	0.00+/- 0.00	0.00+/- 0.00	0.00+/- 0.00	0.04+/- 0.01	0.21+/- 0.15		0.12+/- (0.05- 0.09)	Formatted: Font color: Dark Red
^{100) Guatemala}	0.60+/- 0.17	0.00+/- 0.00	0.11+/- 0.06	0.02+/- 0.01	0.01+/- 0.00	0.00+/- 0.00	0.00+/- 0.00	0.08+/- 0.04	0.13+/- 0.05	0.29	0.73+/- (0.18- 0.25)	Formatted: Font color: Dark Red
^{Inventory}	0.23+/- 0.21	0.00+/- 0.00	0.07+/- 0.06	0.02+/- 0.01	0.01+/- 0.00	0.00+/- 0.00	0.00+/- 0.00	0.08+/- 0.04	0.10+/- 0.06		0.33+/- (0.22- 0.30)	Formatted: Font color: Dark Red
^{101) Mongolia}	0.55+/- 0.08	0.00+/- 0.00	0.01+/- 0.01	0.04+/- 0.01	0.02+/- 0.01	0.01+/- 0.00	0.00+/- 0.00	0.11+/- 0.04	0.14+/- 0.03	0.28	0.64+/- (0.09- 0.12)	Formatted: Font color: Dark Red
^{Inventory}	0.37+/- 0.09	0.00+/- 0.00	0.01+/- 0.01	0.04+/- 0.01	0.02+/- 0.01	0.01+/- 0.00	0.00+/- 0.00	0.09+/- 0.04	0.13+/- 0.03		0.45+/- (0.09- 0.12)	Formatted: Font color: Dark Red
^{102) Czech Republic}	0.01+/- 0.07	0.00+/- 0.00	0.00+/- 0.13	0.00+/- 0.00	0.00+/- 0.00	0.23+/- 0.11	0.02+/- 0.02	0.09+/- 0.05	0.01+/- 0.01	0.27	0.26+/- (0.19- 0.33)	Formatted: Font color: Dark Red
^{Inventory}	0.09+/- 0.08	0.00+/- 0.00	0.23+/- 0.16	0.00+/- 0.00	0.00+/- 0.00	0.29+/- 0.12	0.02+/- 0.02	0.11+/- 0.05	0.01+/- 0.01		0.63+/- (0.21- 0.37)	Formatted: Font color: Dark Red
^{103) Eritrea}	0.67+/- 0.06	0.00+/- 0.00	0.01+/- 0.00	0.00+/- 0.00	0.00+/- 0.00	0.00+/- 0.00	0.01+/- 0.00	0.10+/- 0.03	0.02+/- 0.01	0.27	0.68+/- (0.06- 0.07)	Formatted: Font color: Dark Red
^{Inventory}	0.08+/- 0.08	0.00+/- 0.00	0.01+/- 0.00	0.00+/- 0.00	0.00+/- 0.00	0.00+/- 0.00	0.01+/- 0.00	0.08+/- 0.03	0.02+/- 0.01		0.10+/- (0.08- 0.08)	Formatted: Font color: Dark Red
^{104) Norway}	0.07+/- 0.01	0.00+/- 0.00	0.02+/- 0.01	0.00+/- 0.00	0.01+/- 0.00	0.00+/- 0.00	0.01+/- 0.01	0.04+/- 0.01	0.41+/- 0.15	0.26	0.11+/- (0.02- 0.04)	Formatted: Font color: Dark Red
^{Inventory}	0.06+/- 0.01	0.00+/- 0.00	0.02+/- 0.01	0.00+/- 0.00	0.01+/- 0.00	0.00+/- 0.00	0.01+/- 0.01	0.04+/- 0.01	0.26+/- 0.17		0.11+/- (0.02- 0.04)	Formatted: Font color: Dark Red
^{105) Belarus}	0.28+/- 0.17	0.00+/- 0.00	1.2+/- 0.5	0.00+/- 0.00	0.00+/- 0.00	0.00+/- 0.00	0.03+/- 0.01	0.04+/- 0.01	0.07+/- 0.10	0.26	1.6+/- (0.5- 0.7)	Formatted: Font color: Dark Red
^{Inventory}	0.24+/- 0.17	0.00+/- 0.00	2.3+/- 1.5	0.00+/- 0.00	0.00+/- 0.00	0.00+/- 0.00	0.03+/- 0.01	0.04+/- 0.01	0.11+/- 0.10		2.6+/- (1.5- 1.7)	Formatted: Font color: Dark Red
^{106) Switzerland}	0.25+/- 0.13	0.00+/- 0.00	0.04+/- 0.05	0.00+/- 0.00	0.00+/- 0.00	0.00+/- 0.00	0.01+/- 0.01	0.16+/- 0.06	0.06+/- 0.05	0.24	0.30+/- (0.13- 0.18)	Formatted: Font color: Dark Red
^{Inventory}	0.17+/- 0.15	0.00+/- 0.00	0.05+/- 0.05	0.00+/- 0.00	0.00+/- 0.00	0.00+/- 0.00	0.01+/- 0.01	0.15+/- 0.07	0.05+/- 0.05		0.23+/- (0.16- 0.21)	Formatted: Font color: Dark Red
^{107) Hungary}	0.03+/- 0.05	0.00+/- 0.00	0.17+/- 0.16	0.00+/- 0.00	0.01+/- 0.00	0.00+/- 0.00	0.02+/- 0.02	0.05+/- 0.02	0.03+/- 0.02	0.24	0.23+/- (0.16- 0.23)	Formatted: Font color: Dark Red
^{Inventory}	0.05+/- 0.05	0.00+/- 0.00	0.28+/- 0.20	0.00+/- 0.00	0.01+/- 0.00	0.00+/- 0.00	0.02+/- 0.02	0.06+/- 0.02	0.03+/- 0.02		0.36+/- (0.20- 0.27)	Formatted: Font color: Dark Red
^{108) Senegal}	0.03+/- 0.12	0.05+/- 0.05	0.04+/- 0.02	0.02+/- 0.02	0.00+/- 0.00	0.00+/- 0.00	0.00+/- 0.00	0.04+/- 0.01	0.02+/- 0.02	0.23	0.15+/- (0.14- 0.21)	Formatted: Font color: Dark Red
^{Inventory}	0.18+/- 0.15	0.05+/- 0.06	0.04+/- 0.02	0.03+/- 0.02	0.00+/- 0.00	0.00+/- 0.00	0.00+/- 0.00	0.04+/- 0.01	0.03+/- 0.02		0.30+/- (0.17- 0.25)	Formatted: Font color: Dark Red
^{109) Netherlands}	1.2+/-0.3	0.00+/- 0.00	0.36+/- 0.13	0.00+/- 0.00	0.01+/- 0.00	0.00+/- 0.00	0.03+/- 0.02	0.05+/- 0.01	0.03+/- 0.03	0.23	1.6+/- (0.3- 0.4)	Formatted: Font color: Dark Red

Inventory	0.37+/- 0.30	0.00+/- 0.00	0.20+/- 0.15	0.00+/- 0.00	0.01+/- 0.00	0.00+/- 0.00	0.02+/- 0.02	0.05+/- 0.01	0.03+/- 0.03	0.60+/- (0.33- 0.47)	Formatted: Font color: Dark Red
110) Serbia	-0.02+/- -0.05	0.00+/- -0.00	0.01+/- -0.07	0.00+/- -0.00	0.02+/- -0.01	0.03+/- -0.01	0.01+/- -0.01	0.04+/- -0.02	0.01+/- -0.02	0.23	Formatted: Font color: Dark Red
Inventory	0.06+/- -0.06	0.00+/- -0.00	0.11+/- -0.08	0.00+/- -0.00	0.02+/- -0.01	0.03+/- -0.01	0.01+/- -0.01	0.05+/- -0.02	0.01+/- -0.02	0.23	Formatted: Font color: Dark Red
111) Panama	0.09+/- -0.07	0.01+/- -0.01	0.03+/- -0.03	0.00+/- -0.00	0.00+/- -0.00	0.00+/- -0.00	0.00+/- -0.00	0.05+/- -0.02	0.85+/- -0.18	0.23	Formatted: Font color: Dark Red
Inventory	0.09+/- -0.07	0.01+/- -0.01	0.04+/- -0.03	0.00+/- -0.00	0.00+/- -0.00	0.00+/- -0.00	0.00+/- -0.00	0.05+/- -0.02	0.30+/- -0.25	0.15+/- (0.08- 0.11)	Formatted: Font color: Dark Red
112) Georgia	0.10+/- -0.06	0.00+/- -0.00	0.07+/- -0.05	0.00+/- -0.00	0.01+/- -0.00	0.00+/- -0.00	0.07+/- -0.05	0.47+/- -0.17	0.01+/- -0.01	0.23	Formatted: Font color: Dark Red
Inventory	0.07+/- -0.07	0.00+/- -0.00	0.07+/- -0.05	0.00+/- -0.00	0.01+/- -0.00	0.00+/- -0.00	0.07+/- -0.06	0.41+/- -0.19	0.01+/- -0.01	0.22+/- (0.10- 0.18)	Formatted: Font color: Dark Red
113) Tunisia	-0.01+/- -0.06	0.00+/- -0.00	0.03+/- -0.03	0.00+/- -0.00	0.02+/- -0.01	0.00+/- -0.00	0.02+/- -0.01	0.05+/- -0.02	0.01+/- -0.02	0.23	Formatted: Font color: Dark Red
Inventory	0.09+/- -0.06	0.00+/- -0.00	0.07+/- -0.04	0.00+/- -0.00	0.03+/- -0.01	0.00+/- -0.00	0.02+/- -0.01	0.07+/- -0.02	0.02+/- -0.02	0.20+/- (0.08- 0.12)	Formatted: Font color: Dark Red
114) Mauritania	0.49+/- 0.10	0.01+/- 0.01	0.01+/- 0.00	0.00+/- 0.00	0.00+/- 0.00	0.00+/- 0.00	0.00+/- 0.00	0.04+/- 0.01	0.01+/- 0.00	0.22	Formatted: Font color: Dark Red
Inventory	0.19+/- -0.15	0.01+/- -0.01	0.01+/- -0.00	0.00+/- -0.00	0.00+/- -0.00	0.00+/- -0.00	0.00+/- -0.00	0.04+/- -0.01	0.01+/- -0.00	0.22+/- (0.15- 0.17)	Formatted: Font color: Dark Red
115) Yemen	0.16+/- -0.10	0.00+/- -0.00	0.07+/- -0.03	0.00+/- -0.00	0.01+/- -0.00	0.00+/- -0.00	0.00+/- -0.00	0.09+/- -0.02	0.02+/- -0.01	0.22	Formatted: Font color: Dark Red
Inventory	0.14+/- -0.11	0.00+/- -0.00	0.06+/- -0.03	0.00+/- -0.00	0.01+/- -0.00	0.00+/- -0.00	0.00+/- -0.00	0.08+/- -0.02	0.01+/- -0.01	0.22+/- (0.12- 0.15)	Formatted: Font color: Dark Red
116) Cuba	0.12+/- -0.15	0.03+/- -0.04	0.13+/- -0.15	0.02+/- -0.01	0.10+/- -0.06	0.00+/- -0.00	0.01+/- -0.00	0.08+/- -0.04	0.07+/- -0.17	0.22	Formatted: Font color: Dark Red
Inventory	0.24+/- -0.16	0.05+/- -0.04	0.24+/- -0.16	0.02+/- -0.01	0.11+/- -0.06	0.00+/- -0.00	0.01+/- -0.00	0.08+/- -0.04	0.26+/- -0.19	0.66+/- (0.24- 0.44)	Formatted: Font color: Dark Red
117) Portugal	0.12+/- -0.08	0.01+/- -0.01	- 0.29+/- -0.22	0.00+/- -0.00	0.00+/- -0.00	0.00+/- -0.00	0.00+/- -0.00	0.04+/- -0.01	0.01+/- -0.01	0.2	Formatted: Font color: Dark Red
Inventory	0.11+/- -0.09	0.01+/- -0.00	0.42+/- -0.28	0.00+/- -0.00	0.00+/- -0.00	0.00+/- -0.00	0.00+/- -0.00	0.04+/- -0.01	0.01+/- -0.01	0.55+/- (0.30- 0.38)	Formatted: Font color: Dark Red
118) Jordan	0.03+/- -0.02	0.00+/- -0.00	0.14+/- -0.08	0.00+/- -0.00	0.00+/- -0.00	0.00+/- -0.00	0.04+/- -0.02	0.04+/- -0.01	0.00+/- -0.00	0.2	Formatted: Font color: Dark Red
Inventory	0.02+/- -0.02	0.00+/- -0.00	0.14+/- -0.12	0.00+/- -0.00	0.00+/- -0.00	0.00+/- -0.00	0.03+/- -0.02	0.04+/- -0.01	0.00+/- -0.00	0.20+/- (0.12- 0.16)	Formatted: Font color: Dark Red
119) Bahamas	0.00+/- 0.00	0.00+/- 0.00	0.00+/- 0.00	0.00+/- 0.00	0.00+/- 0.00	0.00+/- 0.00	0.00+/- 0.00	0.04+/- 0.01	0.00+/- 0.00	-0.2	Formatted: Font color: Dark Red
Inventory	0.00+/- -0.00	0.00+/- -0.00	0.00+/- -0.00	0.00+/- -0.00	0.00+/- -0.00	0.00+/- -0.00	0.00+/- -0.00	0.04+/- -0.01	0.00+/- -0.00	0.00+/- (0.00- 0.00)	Formatted: Font color: Dark Red

120) Benin	-0.08+/- -0.08	0.00+/- 0.01	0.03+/- 0.01	0.02+/- 0.02	0.00+/- 0.00	0.00+/- 0.00	0.02+/- 0.01	0.04+/- 0.01	0.02+/- 0.03	0.19	0.01+/- (0.09 0.14)	Formatted: Font color: Dark Red
Inventory	0.09+/- -0.10	0.01+/- -0.01	0.03+/- -0.01	0.02+/- -0.02	0.00+/- -0.00	0.00+/- -0.00	0.01+/- -0.01	0.04+/- -0.01	0.03+/- -0.03		0.17+/- (0.10 0.16)	Formatted: Font color: Dark Red
121) Rwanda	-0.02+/- -0.05	0.00+/- -0.01	0.02+/- -0.01	0.00+/- -0.00	0.00+/- -0.00	0.02+/- -0.02	0.04+/- -0.01	0.19+/- -0.09		0.17	0.03+/- (0.06 0.10)	Formatted: Font color: Dark Red
Inventory	0.05+/- -0.06	0.01+/- -0.01	0.02+/- -0.01	0.00+/- -0.00	0.00+/- -0.00	0.02+/- -0.02	0.04+/- -0.01	0.10+/- -0.12			0.10+/- (0.06 0.10)	Formatted: Font color: Dark Red
122) Slovakia	0.02+/- -0.02	0.00+/- -0.00	0.05+/- -0.06	0.00+/- -0.00	0.00+/- -0.00	0.01+/- -0.04	0.04+/- -0.04	0.07+/- -0.02	0.00+/- -0.00	0.17	0.12+/- (0.07 0.12)	Formatted: Font color: Dark Red
Inventory	0.02+/- -0.02	0.00+/- -0.00	0.09+/- -0.07	0.00+/- -0.00	0.00+/- -0.00	0.01+/- -0.00	0.05+/- -0.04	0.08+/- -0.02	0.00+/- -0.00		0.17+/- (0.08 0.13)	Formatted: Font color: Dark Red
123) Croatia	0.00+/- -0.04	0.00+/- -0.00	0.02+/- -0.04	0.00+/- -0.00	0.00+/- -0.00	0.03+/- -0.01	0.01+/- -0.00	0.06+/- -0.05	0.01+/- -0.01	0.16	0.06+/- (0.06 0.10)	Formatted: Font color: Dark Red
Inventory	0.05+/- -0.04	0.00+/- -0.00	0.06+/- -0.04	0.00+/- -0.00	0.00+/- -0.00	0.03+/- -0.01	0.01+/- -0.00	0.11+/- -0.05	0.01+/- -0.01		0.15+/- (0.06 0.10)	Formatted: Font color: Dark Red
124) Israel	0.03+/- -0.02	0.00+/- -0.00	0.33+/- -0.11	0.00+/- -0.00	0.00+/- -0.00	0.00+/- -0.00	0.04+/- -0.02	0.04+/- -0.01	0.00+/- -0.00	0.16	0.40+/- (0.12 0.16)	Formatted: Font color: Dark Red
Inventory	0.02+/- -0.02	0.00+/- -0.00	0.23+/- -0.18	0.00+/- -0.00	0.00+/- -0.00	0.03+/- -0.02	0.04+/- -0.01	0.00+/- -0.00			0.29+/- (0.18 0.23)	Formatted: Font color: Dark Red
125) Belize	0.00+/- -0.00	0.00+/- -0.00	0.00+/- -0.01	0.01+/- -0.00	0.00+/- -0.00	0.00+/- -0.00	0.00+/- -0.00	0.04+/- -0.01	0.22+/- -0.09	0.16	0.02+/- (0.01 0.01)	Formatted: Font color: Dark Red
Inventory	0.00+/- -0.00	0.00+/- -0.00	0.00+/- -0.00	0.01+/- -0.01	0.00+/- -0.00	0.00+/- -0.00	0.00+/- -0.00	0.04+/- -0.01	0.14+/- -0.14		0.02+/- (0.01 0.01)	Formatted: Font color: Dark Red
126) Bhutan	0.01+/- -0.02	0.00+/- -0.00	0.00+/- -0.00	0.00+/- -0.00	0.00+/- -0.00	0.00+/- -0.00	0.00+/- -0.00	0.04+/- -0.01	0.00+/- -0.00	0.14	0.02+/- (0.02 0.02)	Formatted: Font color: Dark Red
Inventory	0.01+/- -0.02	0.00+/- -0.00	0.00+/- -0.00	0.00+/- -0.00	0.00+/- -0.00	0.00+/- -0.00	0.00+/- -0.00	0.04+/- -0.01	0.00+/- -0.00		0.02+/- (0.02 0.02)	Formatted: Font color: Dark Red
127) Dominican Republic	-0.09+/- -0.15	-0.02+/- -0.07	-0.02+/- -0.05	-0.00+/- -0.00	-0.00+/- -0.00	-0.00+/- -0.00	-0.00+/- -0.00	-0.05+/- -0.01	-0.02+/- -0.06	0.14	-0.05+/- (0.17 0.26)	Formatted: Font color: Dark Red
Inventory	0.19+/- -0.17	0.07+/- -0.06	0.05+/- -0.05	0.00+/- -0.00	0.00+/- -0.00	0.00+/- -0.00	0.00+/- -0.00	0.05+/- -0.01	0.09+/- -0.07		0.31+/- (0.19 0.28)	Formatted: Font color: Dark Red
128) Burundi	0.01+/- -0.03	0.00+/- -0.01	0.01+/- -0.00	0.00+/- -0.00	0.00+/- -0.00	0.00+/- -0.00	0.01+/- -0.01	0.04+/- -0.01	0.13+/- -0.04	0.14	0.04+/- (0.04 0.06)	Formatted: Font color: Dark Red
Inventory	0.03+/- -0.04	0.00+/- -0.01	0.01+/- -0.00	0.00+/- -0.00	0.00+/- -0.00	0.00+/- -0.00	0.01+/- -0.01	0.04+/- -0.01	0.03+/- -0.05		0.05+/- (0.04 0.06)	Formatted: Font color: Dark Red
129) Sierra Leone	0.02+/- -0.03	0.16+/- -0.07	0.02+/- -0.01	0.04+/- -0.02	0.00+/- -0.00	0.00+/- -0.00	0.01+/- -0.01	0.04+/- -0.01	0.10+/- -0.09	0.14	0.25+/- (0.08 0.14)	Formatted: Font color: Dark Red
Inventory	0.03+/- -0.03	0.07+/- -0.09	0.02+/- -0.01	0.03+/- -0.02	0.00+/- -0.00	0.00+/- -0.00	0.01+/- -0.01	0.04+/- -0.01	0.11+/- -0.09		0.16+/- (0.10 0.16)	Formatted: Font color: Dark Red

130) Costa Rica	0.17+/- 0.08	0.01+/- 0.01	0.01+/- 0.01	0.00+/- 0.00	0.00+/- 0.00	0.00+/- 0.00	0.00+/- 0.05	0.11+/- 0.12	0.64+/- 0.13	0.18+/- (0.08- 0.10)	Formatted: Font color: Dark Red
Inventory	0.09+/- 0.09	0.01+/- -0.01	0.01+/- -0.01	0.00+/- -0.00	0.00+/- -0.00	0.00+/- -0.00	0.00+/- -0.06	0.10+/- -0.16	0.16+/- -0.16	0.11+/- (0.09- 0.11)	Formatted: Font color: Dark Red
131) Liberia	0.00+/- -0.00	0.01+/- -0.01	0.01+/- -0.00	0.00+/- -0.00	0.00+/- -0.00	0.00+/- -0.01	0.01+/- -0.01	0.04+/- -0.06	0.05+/- -0.06	0.04+/- (0.01- 0.03)	Formatted: Font color: Dark Red
Inventory	0.00+/- -0.00	0.01+/- -0.01	0.01+/- -0.00	0.00+/- -0.00	0.00+/- -0.00	0.00+/- -0.00	0.01+/- -0.01	0.04+/- -0.01	0.08+/- -0.06	0.04+/- (0.01- 0.03)	Formatted: Font color: Dark Red
132) Belgium	0.29+/- -0.10	0.00+/- -0.00	0.15+/- -0.07	0.00+/- -0.00	0.00+/- -0.00	0.00+/- -0.01	0.01+/- -0.01	0.04+/- -0.01	0.00+/- -0.00	0.45+/- (0.12- 0.18)	Formatted: Font color: Dark Red
Inventory	0.12+/- -0.11	0.00+/- -0.00	0.10+/- -0.09	0.00+/- -0.00	0.00+/- -0.00	0.00+/- -0.01	0.01+/- -0.01	0.04+/- -0.01	0.00+/- -0.00	0.24+/- (0.14- 0.21)	Formatted: Font color: Dark Red
133) Togo	-0.02+/- -0.04	0.00+/- -0.01	0.02+/- -0.01	0.01+/- -0.01	0.00+/- -0.00	0.00+/- -0.00	0.01+/- -0.01	0.04+/- -0.01	0.03+/- -0.04	0.03+/- (0.05- 0.09)	Formatted: Font color: Dark Red
Inventory	0.03+/- -0.04	0.01+/- -0.01	0.02+/- -0.01	0.02+/- -0.01	0.00+/- -0.00	0.00+/- -0.00	0.01+/- -0.01	0.04+/- -0.01	0.05+/- -0.04	0.09+/- (0.05- 0.09)	Formatted: Font color: Dark Red
134) Taiwan	0.00+/- -0.00	0.01+/- -0.08	- 0.11+/- 0.12	0.00+/- -0.00	0.01+/- -0.02	0.00+/- -0.00	0.02+/- -0.02	- 0.21+/- 0.15	0.02+/- -0.03	- 0.07+/- (0.15- 0.25)	Formatted: Font color: Dark Red
Inventory	0.00+/- -0.00	0.08+/- -0.08	0.14+/- -0.13	0.00+/- -0.00	0.02+/- -0.02	0.00+/- -0.00	0.03+/- -0.02	0.20+/- -0.16	0.03+/- -0.03	0.27+/- (0.15- 0.25)	Formatted: Font color: Dark Red
135) Equatorial Guinea	0.00+/- -0.00	0.00+/- -0.00	0.00+/- -0.00	0.00+/- -0.00	- 0.12+/- 0.09	0.01+/- -0.00	0.01+/- -0.01	0.05+/- -0.02	- 0.15+/- 0.06	- 0.11+/- (0.09- 0.10)	Formatted: Font color: Dark Red
Inventory	0.00+/- -0.00	0.00+/- -0.00	0.00+/- -0.00	0.00+/- -0.00	0.09+/- -0.09	0.01+/- -0.00	0.01+/- -0.01	0.05+/- -0.02	0.05+/- -0.07	0.16+/- (0.09- 0.10)	Formatted: Font color: Dark Red
136) Cyprus	0.01+/- -0.01	0.00+/- -0.00	0.02+/- -0.02	0.00+/- -0.00	0.00+/- -0.00	0.00+/- -0.00	0.00+/- -0.00	0.04+/- -0.01	0.00+/- -0.00	0.03+/- (0.02- 0.03)	Formatted: Font color: Dark Red
Inventory	0.01+/- -0.01	0.00+/- -0.00	0.02+/- -0.02	0.00+/- -0.00	0.00+/- -0.00	0.00+/- -0.00	0.00+/- -0.00	0.04+/- -0.01	0.00+/- -0.00	0.03+/- (0.02- 0.03)	Formatted: Font color: Dark Red
137) Kuwait	0.00+/- -0.00	0.00+/- -0.00	0.35+/- -0.30	0.00+/- -0.00	0.05+/- -0.03	0.00+/- -0.00	0.00+/- -0.00	0.09+/- -0.04	0.00+/- -0.00	0.40+/- (0.30- 0.33)	Formatted: Font color: Dark Red
Inventory	0.00+/- -0.00	0.00+/- -0.00	0.53+/- -0.41	0.00+/- -0.00	0.06+/- -0.03	0.00+/- -0.00	0.00+/- -0.00	0.09+/- -0.04	0.00+/- -0.00	0.59+/- (0.41- 0.45)	Formatted: Font color: Dark Red
138) Trinidad and Tobago	0.00+/- -0.00	0.00+/- -0.00	0.00+/- -0.00	0.00+/- -0.04	0.11+/- -0.04	0.00+/- -0.00	0.07+/- -0.04	0.22+/- -0.06	0.00+/- -0.00	0.19+/- (0.05- 0.09)	Formatted: Font color: Dark Red
Inventory	0.00+/- -0.00	0.00+/- -0.00	0.00+/- -0.00	0.00+/- -0.04	0.06+/- -0.04	0.00+/- -0.00	0.05+/- -0.04	0.10+/- -0.07	0.00+/- -0.00	0.12+/- (0.06- 0.09)	Formatted: Font color: Dark Red
139) Ireland	0.19+/- -0.28	0.00+/- -0.00	0.06+/- -0.05	0.00+/- -0.00	0.00+/- -0.00	0.00+/- -0.00	0.00+/- -0.00	0.04+/- -0.01	0.05+/- -0.06	0.26+/- (0.28- 0.33)	Formatted: Font color: Dark Red
Inventory	0.39+/- -0.30	0.00+/- -0.00	0.07+/- -0.05	0.00+/- -0.00	0.00+/- -0.00	0.00+/- -0.00	0.00+/- -0.00	0.04+/- -0.01	0.06+/- -0.06	0.47+/- (0.31- 0.36)	Formatted: Font color: Dark Red

<u>140) Haiti</u>	-0.03+/- -0.07	0.00+/- -0.01	0.03+/- -0.04	0.00+/- -0.00	0.00+/- -0.00	0.00+/- -0.00	0.02+/- -0.01	0.04+/- -0.01	0.00+/- -0.00	0.09	0.02+/- (0.08- 0.13)	Formatted: Font color: Dark Red
<u>Inventory</u>	0.09+/- -0.08	0.01+/- -0.01	0.04+/- -0.04	0.00+/- -0.00	0.00+/- -0.00	0.00+/- -0.00	0.02+/- -0.01	0.04+/- -0.01	0.00+/- -0.00		0.15+/- (0.09- 0.14)	Formatted: Font color: Dark Red
<u>141) Denmark</u>	0.57+/- 0.14	0.00+/- 0.00	0.25+/- 0.09	0.00+/- 0.00	0.00+/- 0.00	0.00+/- 0.00	0.00+/- 0.00	0.04+/- 0.01	0.03+/- 0.02	0.09	0.82+/- (0.16- 0.23)	Formatted: Font color: Dark Red
<u>Inventory</u>	0.18+/- -0.14	0.00+/- -0.00	0.13+/- -0.10	0.00+/- -0.00	0.00+/- -0.00	0.00+/- -0.00	0.00+/- -0.00	0.04+/- -0.01	0.02+/- -0.02		0.32+/- (0.17- 0.24)	Formatted: Font color: Dark Red
<u>142) Lesotho</u>	0.14+/- -0.02	0.00+/- -0.00	0.01+/- -0.00	0.00+/- -0.00	0.00+/- -0.00	0.00+/- -0.00	0.00+/- -0.00	0.04+/- -0.01	0.00+/- -0.00	0.09	0.15+/- (0.02- 0.03)	Formatted: Font color: Dark Red
<u>Inventory</u>	0.02+/- -0.03	0.00+/- -0.00	0.00+/- -0.00	0.00+/- -0.00	0.00+/- -0.00	0.00+/- -0.00	0.00+/- -0.00	0.04+/- -0.01	0.00+/- -0.00		0.03+/- (0.03- 0.03)	Formatted: Font color: Dark Red
<u>143) Estonia</u>	0.01+/- -0.01	0.00+/- -0.00	-0.01+/- -0.07	0.00+/- -0.00	0.00+/- -0.00	0.00+/- -0.00	0.00+/- -0.00	0.04+/- -0.01	-0.06+/- -0.07	0.08	0.01+/- (0.07- 0.08)	Formatted: Font color: Dark Red
<u>Inventory</u>	0.02+/- -0.01	0.00+/- -0.00	0.11+/- -0.08	0.00+/- -0.00	0.00+/- -0.00	0.00+/- -0.00	0.00+/- -0.00	0.04+/- -0.01	0.07+/- -0.08		0.13+/- (0.08- 0.09)	Formatted: Font color: Dark Red
<u>144) Qatar</u>	0.00+/- -0.00	0.00+/- -0.00	0.02+/- -0.02	0.00+/- -0.00	0.00+/- -0.00	0.00+/- -0.00	0.00+/- -0.01	0.04+/- -0.01	0.00+/- -0.00	0.08	0.03+/- (0.02- 0.03)	Formatted: Font color: Dark Red
<u>Inventory</u>	0.00+/- -0.00	0.00+/- -0.00	0.02+/- -0.02	0.00+/- -0.00	0.00+/- -0.00	0.00+/- -0.00	0.01+/- -0.01	0.04+/- -0.01	0.00+/- -0.00		0.03+/- (0.02- 0.03)	Formatted: Font color: Dark Red
<u>145) Latvia</u>	0.03+/- -0.03	0.00+/- -0.00	0.01+/- -0.03	0.00+/- -0.00	0.00+/- -0.00	0.00+/- -0.00	0.01+/- -0.00	0.04+/- -0.01	0.00+/- -0.05	0.08	0.05+/- (0.04- 0.06)	Formatted: Font color: Dark Red
<u>Inventory</u>	0.03+/- -0.03	0.00+/- -0.00	0.05+/- -0.04	0.00+/- -0.00	0.00+/- -0.00	0.00+/- -0.00	0.01+/- -0.00	0.04+/- -0.01	0.05+/- -0.05		0.09+/- (0.04- 0.07)	Formatted: Font color: Dark Red
<u>146) Guinea-Bissau</u>	0.00+/- 0.03	0.05+/- 0.04	0.01+/- 0.00	0.01+/- 0.01	0.00+/- 0.00	0.00+/- 0.00	0.00+/- 0.00	0.04+/- 0.01	0.02+/- 0.06	0.08	0.07+/- (0.05- 0.09)	Formatted: Font color: Dark Red
<u>Inventory</u>	0.03+/- -0.03	0.04+/- -0.05	0.01+/- -0.00	0.01+/- -0.01	0.00+/- -0.00	0.00+/- -0.00	0.00+/- -0.00	0.04+/- -0.01	0.08+/- -0.07		0.09+/- (0.06- 0.10)	Formatted: Font color: Dark Red
<u>147) Bosnia and Herzegovina</u>	-0.02+/- -0.04	0.00+/- 0.00	0.00+/- 0.03	0.00+/- 0.00	0.00+/- 0.00	0.00+/- 0.00	0.00+/- 0.00	0.03+/- 0.02	0.00+/- 0.00	0.07	-0.02+/- (0.05- 0.07)	Formatted: Font color: Dark Red
<u>Inventory</u>	0.04+/- -0.04	0.00+/- -0.00	0.04+/- -0.03	0.00+/- -0.00	0.00+/- -0.00	0.00+/- -0.00	0.00+/- -0.00	0.05+/- -0.02	0.00+/- -0.00		0.08+/- (0.05- 0.08)	Formatted: Font color: Dark Red
<u>148) Albania</u>	-0.03+/- -0.05	0.00+/- -0.00	-0.01+/- -0.03	0.00+/- -0.00	0.00+/- -0.00	0.00+/- -0.00	0.00+/- -0.00	0.07+/- -0.04	0.00+/- -0.01	0.06	-0.04+/- (0.06- 0.08)	Formatted: Font color: Dark Red
<u>Inventory</u>	0.05+/- -0.05	0.00+/- -0.00	0.04+/- -0.04	0.00+/- -0.00	0.00+/- -0.00	0.00+/- -0.00	0.00+/- -0.00	0.10+/- -0.04	0.01+/- -0.01		0.10+/- (0.06- 0.09)	Formatted: Font color: Dark Red
<u>149) Lithuania</u>	0.05+/- 0.04	0.00+/- 0.00	-0.02+/- 0.06	0.00+/- 0.00	0.01+/- 0.00	0.00+/- 0.00	0.01+/- 0.01	0.04+/- 0.01	0.01+/- 0.03	0.06	0.04+/- (0.08- 0.12)	Formatted: Font color: Dark Red
<u>Inventory</u>	0.06+/- -0.04	0.00+/- -0.00	0.09+/- -0.08	0.00+/- -0.00	0.01+/- -0.00	0.00+/- -0.00	0.01+/- -0.01	0.04+/- -0.01	0.02+/- -0.03		0.17+/- (0.09- 0.13)	Formatted: Font color: Dark Red

<u>150) Armenia</u>	0.06+/- -0.03	0.00+/- -0.00	0.02+/- -0.01	0.00+/- -0.00	0.00+/- -0.00	0.00+/- -0.00	0.03+/- -0.02	0.08+/- -0.03	0.01+/- -0.02	0.06	0.10+/- (0.04- -0.07)
<u>Inventory</u>	0.03+/- -0.03	0.00+/- -0.00	0.02+/- -0.01	0.00+/- -0.00	0.00+/- -0.00	0.00+/- -0.00	0.03+/- -0.03	0.08+/- -0.04	0.01+/- -0.02		0.07+/- (0.04- -0.07)
<u>151) Lebanon</u>	0.01+/- -0.01	0.00+/- -0.00	0.07+/- -0.06	0.00+/- -0.00	0.00+/- -0.00	0.00+/- -0.00	0.04+/- -0.01	0.00+/- -0.00		0.06	0.09+/- (0.06- -0.08)
<u>Inventory</u>	0.01+/- -0.01	0.00+/- -0.00	0.10+/- -0.09	0.00+/- -0.00	0.00+/- -0.00	0.00+/- -0.00	0.00+/- -0.00	0.04+/- -0.01	0.00+/- -0.00		0.11+/- (0.09- -0.10)
<u>152) El Salvador</u>	0.16+/- -0.05	0.00+/- -0.00	0.02+/- -0.01	0.00+/- -0.00	0.00+/- -0.00	0.00+/- -0.00	0.04+/- -0.01	0.16+/- -0.07		0.05	0.18+/- (0.05- -0.06)
<u>Inventory</u>	0.04+/- -0.05	0.00+/- -0.00	0.01+/- -0.01	0.00+/- -0.00	0.00+/- -0.00	0.00+/- -0.00	0.04+/- -0.01	0.06+/- -0.08			0.05+/- (0.05- -0.07)
<u>153) Kosovo</u>	-0.01+/- -0.03	0.00+/- -0.00	-0.02+/- -0.04	0.00+/- -0.00	0.00+/- -0.00	0.00+/- -0.00	0.04+/- -0.01	0.00+/- -0.00		0.05	-0.03+/- (-0.05- -0.07)
<u>Inventory</u>	0.03+/- -0.03	0.00+/- -0.00	0.04+/- -0.04	0.00+/- -0.00	0.00+/- -0.00	0.00+/- -0.00	0.04+/- -0.01	0.00+/- -0.00			0.08+/- (0.05- -0.07)
<u>154) Swaziland</u>	0.04+/- -0.02	0.00+/- -0.00	0.00+/- -0.00	0.00+/- -0.00	0.00+/- -0.00	0.00+/- -0.00	0.04+/- -0.01	0.00+/- -0.00		0.05	0.05+/- (0.02- -0.02)
<u>Inventory</u>	0.01+/- -0.02	0.00+/- -0.00	0.00+/- -0.00	0.00+/- -0.00	0.00+/- -0.00	0.00+/- -0.00	0.04+/- -0.01	0.00+/- -0.00			0.02+/- (0.02- -0.02)
<u>155) The former Yugoslav Republic of Macedonia</u>	0.00+/- -0.02	0.00+/- -0.00	-0.01+/- -0.02	0.00+/- -0.00	0.00+/- -0.00	0.01+/- -0.00	0.00+/- -0.00	0.04+/- -0.01	0.00+/- -0.00	0.05	0.00+/- (0.03- -0.04)
<u>Inventory</u>	0.02+/- -0.02	0.00+/- -0.00	0.02+/- -0.02	0.00+/- -0.00	0.00+/- -0.00	0.01+/- -0.00	0.00+/- -0.00	0.04+/- -0.01	0.00+/- -0.00		0.05+/- (0.03- -0.04)
<u>156) Brunei Darussalam</u>	0.00+/- -0.00	0.00+/- -0.00	0.00+/- -0.00	0.02+/- -0.03	0.00+/- -0.00	-0.01+/- -0.04	0.04+/- -0.01	0.00+/- -0.00		0.04	0.01+/- (-0.05- -0.07)
<u>Inventory</u>	0.00+/- -0.00	0.00+/- -0.00	0.00+/- -0.00	0.00+/- -0.03	0.00+/- -0.00	0.03+/- -0.04	0.04+/- -0.04	0.04+/- -0.01	0.00+/- -0.00		0.07+/- (0.05- -0.07)
<u>157) Grenada</u>	0.00+/- -0.00	0.00+/- -0.00	0.00+/- -0.00	0.00+/- -0.00	0.00+/- -0.00	0.00+/- -0.00	0.04+/- -0.01	0.00+/- -0.00		0.04	0.00+/- (0.00- -0.00)
<u>Inventory</u>	0.00+/- -0.00	0.00+/- -0.00	0.00+/- -0.00	0.00+/- -0.00	0.00+/- -0.00	0.00+/- -0.00	0.04+/- -0.01	0.00+/- -0.00			0.00+/- (0.00- -0.00)
<u>158) Slovenia</u>	0.01+/- -0.02	0.00+/- -0.00	0.00+/- -0.01	0.00+/- -0.00	0.00+/- -0.00	0.01+/- -0.00	0.00+/- -0.00	0.04+/- -0.01	0.02+/- -0.02	0.03	0.02+/- (0.03- -0.04)
<u>Inventory</u>	0.02+/- -0.02	0.00+/- -0.00	0.01+/- -0.02	0.00+/- -0.00	0.00+/- -0.00	0.01+/- -0.00	0.00+/- -0.00	0.04+/- -0.01	0.02+/- -0.02		0.04+/- (0.03- -0.04)
<u>159) Montenegro</u>	-0.01+/- -0.02	0.00+/- -0.00	0.00+/- -0.01	0.00+/- -0.00	0.00+/- -0.00	0.00+/- -0.00	0.00+/- -0.00	0.04+/- -0.01	0.01+/- -0.01	0.03	-0.01+/- (-0.02- -0.03)
<u>Inventory</u>	0.02+/- -0.02	0.00+/- -0.00	0.01+/- -0.01	0.00+/- -0.00	0.00+/- -0.00	0.00+/- -0.00	0.00+/- -0.00	0.04+/- -0.01	0.01+/- -0.01		0.03+/- (0.02- -0.03)

^{160) Svalbard and Jan Mayen Islands}	0.00+/- 0.00	0.00+/- 0.00	0.00+/- 0.00	0.00+/- 0.00	0.01+/- 0.00	0.00+/- 0.00	0.04+/- 0.01	0.00+/- 0.00	0.03	0.02+/- (0.00- 0.01)	Formatted: Font color: Dark Red	
^{Inventory}	0.01+/- 0.00	0.00+/- 0.00	0.00+/- 0.00	0.00+/- 0.00	0.01+/- 0.00	0.00+/- 0.00	0.04+/- 0.01	0.00+/- 0.00		0.02+/- (0.00- 0.01)	Formatted: Font color: Dark Red	
^{161) Western Sahara}	0.00+/- 0.00	0.00+/- 0.00	0.00+/- 0.00	0.00+/- 0.00	0.00+/- 0.00	0.00+/- 0.00	0.04+/- 0.01	0.00+/- 0.00	0.03	0.01+/- (0.00- 0.00)	Formatted: Font color: Dark Red	
^{Inventory}	0.00+/- 0.00	0.00+/- 0.00	0.00+/- 0.00	0.00+/- 0.00	0.00+/- 0.00	0.00+/- 0.00	0.04+/- 0.01	0.00+/- 0.00		0.01+/- (0.00- 0.00)	Formatted: Font color: Dark Red	
^{162) Puerto Rico}	0.00+/- 0.00	0.00+/- 0.06	0.05+/- 0.00	0.00+/- 0.00	0.00+/- 0.00	0.00+/- 0.00	0.04+/- 0.01	0.00+/- 0.00	0.02	0.06+/- (0.06- 0.06)	Formatted: Font color: Dark Red	
^{Inventory}	0.00+/- 0.00	0.00+/- 0.06	0.06+/- 0.00	0.00+/- 0.00	0.00+/- 0.00	0.00+/- 0.00	0.04+/- 0.01	0.00+/- 0.00		0.06+/- (0.06- 0.06)	Formatted: Font color: Dark Red	
^{163) Djibouti}	0.02+/- 0.02	0.00+/- 0.00	0.00+/- 0.00	0.00+/- 0.01	0.01+/- 0.00	0.00+/- 0.00	0.05+/- 0.01	0.01+/- 0.01	0.02	0.04+/- (0.02- 0.03)	Formatted: Font color: Dark Red	
^{Inventory}	0.01+/- 0.02	0.00+/- 0.00	0.00+/- 0.00	0.00+/- 0.01	0.01+/- 0.00	0.00+/- 0.00	0.04+/- 0.01	0.01+/- 0.01		0.02+/- (0.02- 0.03)	Formatted: Font color: Dark Red	
^{164) Republic of Moldova}	0.01+/- 0.01	0.00+/- 0.00	0.05+/- 0.06	0.00+/- 0.00	0.00+/- 0.00	0.01+/- 0.01	0.13+/- 0.09	0.00+/- 0.00	0.02	0.07+/- (0.06- 0.08)	Formatted: Font color: Dark Red	
^{Inventory}	0.01+/- 0.01	0.00+/- 0.00	0.07+/- 0.06	0.00+/- 0.00	0.00+/- 0.00	0.01+/- 0.01	0.17+/- 0.10	0.00+/- 0.00		0.09+/- (0.06- 0.08)	Formatted: Font color: Dark Red	
^{165) Jamaica}	0.01+/- 0.01	0.00+/- 0.00	0.07+/- 0.06	0.00+/- 0.00	0.00+/- 0.00	0.00+/- 0.00	0.07+/- 0.03	0.00+/- 0.00	0.02	0.08+/- (0.06- 0.07)	Formatted: Font color: Dark Red	
^{Inventory}	0.01+/- 0.01	0.00+/- 0.00	0.07+/- 0.06	0.00+/- 0.00	0.00+/- 0.00	0.00+/- 0.00	0.06+/- 0.03	0.00+/- 0.00		0.08+/- (0.07- 0.08)	Formatted: Font color: Dark Red	
^{166) Sao Tome and Principe}	0.00+/- 0.00	0.00+/- 0.00	0.00+/- 0.00	0.00+/- 0.00	0.00+/- 0.00	0.00+/- 0.00	0.04+/- 0.01	0.00+/- 0.00	0.02	0.00+/- (0.00- 0.00)	Formatted: Font color: Dark Red	
^{Inventory}	0.00+/- 0.00	0.00+/- 0.00	0.00+/- 0.00	0.00+/- 0.00	0.00+/- 0.00	0.00+/- 0.00	0.04+/- 0.01	0.00+/- 0.00		0.00+/- (0.00- 0.00)	Formatted: Font color: Dark Red	
^{167) Turks and Caicos Islands}	0.00+/- 0.00	0.00+/- 0.00	0.00+/- 0.00	0.00+/- 0.00	0.00+/- 0.00	0.00+/- 0.00	0.04+/- 0.01	0.00+/- 0.00	0.02	0.00+/- (0.00- 0.00)	Formatted: Font color: Dark Red	
^{Inventory}	0.00+/- 0.00	0.00+/- 0.00	0.00+/- 0.00	0.00+/- 0.00	0.00+/- 0.00	0.00+/- 0.00	0.04+/- 0.01	0.00+/- 0.00		0.00+/- (0.00- 0.00)	Formatted: Font color: Dark Red	
^{168) Jersey}	0.00+/- 0.00	0.00+/- 0.00	0.00+/- 0.00	0.00+/- 0.00	0.00+/- 0.00	0.00+/- 0.00	0.04+/- 0.01	0.00+/- 0.00	0.01	0.00+/- (0.00- 0.00)	Formatted: Font color: Dark Red	
^{Inventory}	0.00+/- 0.00	0.00+/- 0.00	0.00+/- 0.00	0.00+/- 0.00	0.00+/- 0.00	0.00+/- 0.00	0.04+/- 0.01	0.00+/- 0.00		0.00+/- (0.00- 0.00)	Formatted: Font color: Dark Red	
^{169) Timor- Leste}	0.02+/- 0.01	0.01+/- 0.00	0.01+/- 0.01	0.00+/- 0.01	0.03+/- 0.01	0.01+/- 0.00	0.00+/- 0.00	0.09+/- 0.04	0.00+/- 0.00	0.01	0.08+/- (0.02- 0.04)	Formatted: Font color: Dark Red
^{Inventory}	0.01+/- 0.01	0.01+/- 0.00	0.01+/- 0.01	0.00+/- 0.01	0.03+/- 0.01	0.01+/- 0.00	0.00+/- 0.00	0.08+/- 0.04	0.00+/- 0.00		0.08+/- (0.02- 0.04)	Formatted: Font color: Dark Red

170) Bonaire Saint Eustatius and Saba	0.00+/- 0.00	0.00+/- 0.00	0.00+/- 0.00	0.00+/- 0.00	0.00+/- 0.00	0.00+/- 0.00	0.04+/- 0.01	0.00+/- 0.00	0.01	0.01+/- (0.00- 0.01)	Formatted: Font color: Dark Red
Inventory	0.00+/- 0.00	0.00+/- 0.00	0.00+/- 0.00	0.00+/- 0.00	0.00+/- 0.00	0.00+/- 0.00	0.04+/- 0.01	0.00+/- 0.00		0.01+/- (0.00- 0.01)	Formatted: Font color: Dark Red
171) Cayman Islands	0.00+/- 0.00	0.00+/- 0.00	0.00+/- 0.00	0.00+/- 0.00	0.00+/- 0.00	0.00+/- 0.00	0.04+/- 0.01	0.00+/- 0.00	0.01	0.00+/- (0.00- 0.00)	Formatted: Font color: Dark Red
Inventory	0.00+/- 0.00	0.00+/- 0.00	0.00+/- 0.00	0.00+/- 0.00	0.00+/- 0.00	0.00+/- 0.00	0.04+/- 0.01	0.00+/- 0.00		0.00+/- (0.00- 0.00)	Formatted: Font color: Dark Red
172) Fiji	0.01+/- 0.01	0.00+/- 0.01	0.01+/- 0.00	0.00+/- 0.00	0.00+/- 0.00	0.00+/- 0.00	0.04+/- 0.01	0.00+/- 0.00	0.01	0.01+/- (0.02- 0.02)	Formatted: Font color: Dark Red
Inventory	0.02+/- 0.01	0.00+/- 0.00	0.01+/- 0.01	0.00+/- 0.00	0.00+/- 0.00	0.00+/- 0.00	0.04+/- 0.01	0.00+/- 0.00		0.03+/- (0.02- 0.02)	Formatted: Font color: Dark Red
173) Saint Vincent and the Grenadines	0.00+/- 0.00	0.00+/- 0.00	0.00+/- 0.00	0.00+/- 0.00	0.00+/- 0.00	0.00+/- 0.00	0.04+/- 0.01	0.00+/- 0.00	0.01	0.00+/- (0.00- 0.00)	Formatted: Font color: Dark Red
Inventory	0.00+/- 0.00	0.00+/- 0.00	0.00+/- 0.00	0.00+/- 0.00	0.00+/- 0.00	0.00+/- 0.00	0.04+/- 0.01	0.00+/- 0.00		0.00+/- (0.00- 0.00)	Formatted: Font color: Dark Red
174) Saint Pierre and Miquelon	0.00+/- 0.00	0.00+/- 0.00	0.00+/- 0.00	0.00+/- 0.00	0.00+/- 0.00	0.00+/- 0.00	0.04+/- 0.01	0.00+/- 0.00	0.01	0.00+/- (0.00- 0.00)	Formatted: Font color: Dark Red
Inventory	0.00+/- 0.00	0.00+/- 0.00	0.00+/- 0.00	0.00+/- 0.00	0.00+/- 0.00	0.00+/- 0.00	0.04+/- 0.01	0.00+/- 0.00		0.00+/- (0.00- 0.00)	Formatted: Font color: Dark Red
175) United States Minor Outlying Islands	0.00+/- 0.00	0.00+/- 0.00	0.00+/- 0.00	0.00+/- 0.00	0.00+/- 0.00	0.00+/- 0.00	0.04+/- 0.01	0.00+/- 0.00	0.01	0.00+/- (0.00- 0.00)	Formatted: Font color: Dark Red
Inventory	0.00+/- 0.00	0.00+/- 0.00	0.00+/- 0.00	0.00+/- 0.00	0.00+/- 0.00	0.00+/- 0.00	0.04+/- 0.01	0.00+/- 0.00		0.00+/- (0.00- 0.00)	Formatted: Font color: Dark Red
176) Iceland	0.01+/- 0.00	0.00+/- 0.01	0.01+/- 0.00	0.00+/- 0.00	0.00+/- 0.00	0.00+/- 0.00	0.04+/- 0.01	0.02+/- 0.02	0.01	0.02+/- (0.01- 0.01)	Formatted: Font color: Dark Red
Inventory	0.01+/- 0.00	0.00+/- 0.00	0.01+/- 0.01	0.00+/- 0.00	0.00+/- 0.00	0.00+/- 0.00	0.04+/- 0.01	0.02+/- 0.02		0.02+/- (0.01- 0.01)	Formatted: Font color: Dark Red
177) Aland Islands	0.00+/- 0.00	0.00+/- 0.00	0.00+/- 0.00	0.00+/- 0.00	0.00+/- 0.00	0.00+/- 0.00	0.04+/- 0.01	0.00+/- 0.00	0	0.00+/- (0.00- 0.00)	Formatted: Font color: Dark Red
Inventory	0.00+/- 0.00	0.00+/- 0.00	0.00+/- 0.00	0.00+/- 0.00	0.00+/- 0.00	0.00+/- 0.00	0.04+/- 0.01	0.00+/- 0.00		0.00+/- (0.00- 0.00)	Formatted: Font color: Dark Red
178) Mayotte	0.00+/- 0.00	0.00+/- 0.00	0.00+/- 0.00	0.00+/- 0.00	0.00+/- 0.00	0.00+/- 0.00	0.04+/- 0.01	0.00+/- 0.00	0	0.00+/- (0.00- 0.00)	Formatted: Font color: Dark Red
Inventory	0.00+/- 0.00	0.00+/- 0.00	0.00+/- 0.00	0.00+/- 0.00	0.00+/- 0.00	0.00+/- 0.00	0.04+/- 0.01	0.00+/- 0.00		0.00+/- (0.00- 0.00)	Formatted: Font color: Dark Red
179) Solomon Islands	0.00+/- 0.00	0.00+/- 0.00	0.00+/- 0.00	0.00+/- 0.00	0.00+/- 0.00	0.00+/- 0.00	0.04+/- 0.01	0.00+/- 0.00	0	0.01+/- (0.00- 0.00)	Formatted: Font color: Dark Red
Inventory	0.00+/- 0.00	0.00+/- 0.00	0.00+/- 0.00	0.00+/- 0.00	0.00+/- 0.00	0.00+/- 0.00	0.04+/- 0.01	0.00+/- 0.00		0.01+/- (0.00- 0.00)	Formatted: Font color: Dark Red

180) French Southern Territories	-0.00+/- 0.00	0.04+/- 0.01	0.00+/- 0.00	0	0.00+/- (0.00- 0.00)						
Inventory	0.00+/- -0.00	0.00+/- -0.00	0.00+/- -0.00	0.00+/- -0.00	0.00+/- -0.00	0.00+/- -0.00	0.04+/- -0.01	0.00+/- -0.00			0.00+/- (0.00- 0.00)
181) Comoros	0.00+/- 0.00	0.00+/- 0.00	0.00+/- 0.00	0.00+/- 0.00	0.00+/- 0.00	0.00+/- 0.00	0.04+/- 0.01	0.00+/- 0.00	0	0.01+/- (0.01- 0.01)	
Inventory	0.00+/- -0.00	0.00+/- -0.01	0.00+/- -0.00	0.00+/- -0.00	0.00+/- -0.00	0.00+/- -0.00	0.04+/- -0.01	0.00+/- -0.00		0.01+/- (0.01- 0.01)	
182) New Caledonia	-0.01+/- 0.02	0.00+/- 0.00	0.00+/- 0.00	0.00+/- 0.00	0.00+/- 0.00	0.00+/- 0.00	0.04+/- 0.01	0.00+/- 0.00	0	0.00+/- (0.02- 0.03)	
Inventory	0.04+/- -0.03	0.00+/- -0.00	0.00+/- -0.00	0.00+/- -0.00	0.00+/- -0.00	0.00+/- -0.00	0.04+/- -0.01	0.00+/- -0.00		0.04+/- (0.03- 0.03)	
183) Vanuatu	0.01+/- -0.01	0.00+/- -0.00	0.00+/- -0.00	0.00+/- -0.00	0.00+/- -0.00	0.00+/- -0.00	0.04+/- -0.01	0.00+/- -0.00	0	0.01+/- (0.01- 0.01)	
Inventory	0.01+/- -0.01	0.00+/- -0.00	0.00+/- -0.00	0.00+/- -0.00	0.00+/- -0.00	0.00+/- -0.00	0.04+/- -0.01	0.00+/- -0.00		0.01+/- (0.01- 0.01)	
184) United States Virgin Islands	0.00+/- 0.00	0.00+/- 0.00	0.00+/- 0.00	0.00+/- 0.00	0.00+/- 0.00	0.00+/- 0.00	0.04+/- 0.01	0.00+/- 0.00	0	0.00+/- (0.00- 0.00)	
Inventory	0.00+/- -0.00	0.00+/- -0.00	0.00+/- -0.00	0.00+/- -0.00	0.00+/- -0.00	0.00+/- -0.00	0.04+/- -0.01	0.00+/- -0.00		0.00+/- (0.00- 0.00)	
185) British Virgin Islands	0.00+/- 0.00	0.00+/- 0.00	0.00+/- 0.00	0.00+/- 0.00	0.00+/- 0.00	0.00+/- 0.00	0.04+/- 0.01	0.00+/- 0.00	0	0.00+/- (0.00- 0.00)	
Inventory	0.00+/- -0.00	0.00+/- -0.00	0.00+/- -0.00	0.00+/- -0.00	0.00+/- -0.00	0.00+/- -0.00	0.04+/- -0.01	0.00+/- -0.00		0.00+/- (0.00- 0.00)	
186) Anguilla	0.00+/- -0.00	0.00+/- -0.00	0.00+/- -0.00	0.00+/- -0.00	0.00+/- -0.00	0.00+/- -0.00	0.04+/- -0.01	0.00+/- -0.00	0	0.00+/- (0.00- 0.00)	
Inventory	0.00+/- -0.00	0.00+/- -0.00	0.00+/- -0.00	0.00+/- -0.00	0.00+/- -0.00	0.00+/- -0.00	0.04+/- -0.01	0.00+/- -0.00		0.00+/- (0.00- 0.00)	
187) Montserrat	0.00+/- 0.00	0.00+/- 0.00	0.00+/- 0.00	0.00+/- 0.00	0.00+/- 0.00	0.00+/- 0.00	0.04+/- 0.01	0.00+/- 0.00	0	0.00+/- (0.00- 0.00)	
Inventory	0.00+/- -0.00	0.00+/- -0.00	0.00+/- -0.00	0.00+/- -0.00	0.00+/- -0.00	0.00+/- -0.00	0.04+/- -0.01	0.00+/- -0.00		0.00+/- (0.00- 0.00)	
188) Seychelles	0.00+/- 0.00	0.00+/- 0.00	0.00+/- 0.00	0.00+/- 0.00	0.00+/- 0.00	0.00+/- 0.00	0.04+/- 0.01	0.00+/- 0.00	0	0.00+/- (0.00- 0.00)	
Inventory	0.00+/- -0.00	0.00+/- -0.00	0.00+/- -0.00	0.00+/- -0.00	0.00+/- -0.00	0.00+/- -0.00	0.04+/- -0.01	0.00+/- -0.00		0.00+/- (0.00- 0.00)	
189) Saint Lucia	0.00+/- 0.00	0.00+/- 0.00	0.00+/- 0.00	0.00+/- 0.00	0.00+/- 0.00	0.00+/- 0.00	0.04+/- 0.01	0.00+/- 0.00	0	0.00+/- (0.00- 0.00)	
Inventory	0.00+/- -0.00	0.00+/- -0.00	0.00+/- -0.00	0.00+/- -0.00	0.00+/- -0.00	0.00+/- -0.00	0.04+/- -0.01	0.00+/- -0.00		0.00+/- (0.00- 0.00)	

Formatted: Font color: Dark Red

www.english-test.net

ANSWER

Formatted: Font color: Dark Red

ANSWER

[View all posts](#) | [View all categories](#)

ANSWER

Formatted: Font color: Dark Red

[View Details](#)

ANSWER

190) Cape Verde	0.00+/- 0.00	0.00+/- 0.00	0.00+/- 0.00	0.00+/- 0.00	0.00+/- 0.00	0.00+/- 0.00	0.04+/- 0.01	0.00+/- 0.00	0+/- (0.00- 0.00)
Inventory	0.00+/- -0.00	0.00+/- -0.00	0.00+/- -0.00	0.00+/- -0.00	0.00+/- -0.00	0.00+/- -0.00	0.04+/- -0.01	0.00+/- -0.00	0.00+/- (0.00- 0.00)
191) Martinique	0.00+/- 0.00	0.00+/- 0.00	0.01+/- 0.01	0.00+/- 0.00	0.00+/- 0.00	0.00+/- 0.00	0.04+/- 0.01	0.00+/- 0.00	0+/- (0.01- 0.01)
Inventory	0.00+/- -0.00	0.00+/- -0.00	0.01+/- -0.01	0.00+/- -0.00	0.00+/- -0.00	0.00+/- -0.00	0.04+/- -0.01	0.00+/- -0.00	0.00+/- (0.01- 0.01)
192) Barbados	0.00+/- 0.00	0.00+/- 0.00	0.00+/- 0.00	0.00+/- 0.00	0.00+/- 0.00	0.00+/- 0.00	0.04+/- 0.01	0.00+/- 0.00	0+/- (0.00- 0.00)
Inventory	0.00+/- -0.00	0.00+/- -0.00	0.00+/- -0.00	0.00+/- -0.00	0.00+/- -0.00	0.00+/- -0.00	0.04+/- -0.01	0.00+/- -0.00	0.00+/- (0.00- 0.00)
193) Guadeloupe	0.00+/- 0.00	0.00+/- 0.00	0.02+/- 0.01	0.00+/- 0.00	0.00+/- 0.00	0.00+/- 0.00	0.04+/- 0.01	0.00+/- 0.00	0+/- (0.01- 0.02)
Inventory	0.00+/- -0.00	0.00+/- -0.00	0.01+/- -0.01	0.00+/- -0.00	0.00+/- -0.00	0.00+/- -0.00	0.04+/- -0.01	0.00+/- -0.00	0.02+/- (0.01- 0.02)
194) Malta	0.00+/- -0.00	0.00+/- -0.00	0.00+/- -0.00	0.00+/- -0.00	0.00+/- -0.00	0.00+/- -0.00	0.04+/- -0.01	0.00+/- -0.00	0+/- (0.00- 0.01)
Inventory	0.00+/- -0.00	0.00+/- -0.00	0.00+/- -0.00	0.00+/- -0.00	0.00+/- -0.00	0.00+/- -0.00	0.04+/- -0.01	0.00+/- -0.00	0.01+/- (0.00- 0.01)
195) Maldives	0.00+/- 0.00	0.00+/- 0.00	0.00+/- 0.00	0.00+/- 0.00	0.00+/- 0.00	0.00+/- 0.00	0.04+/- 0.01	0.00+/- 0.00	0+/- (0.00- 0.00)
Inventory	0.00+/- -0.00	0.00+/- -0.00	0.00+/- -0.00	0.00+/- -0.00	0.00+/- -0.00	0.00+/- -0.00	0.04+/- -0.01	0.00+/- -0.00	0.00+/- (0.00- 0.00)
196) Reunion	0.00+/- 0.00	0.00+/- 0.02	0.03+/- 0.00	0.00+/- 0.00	0.00+/- 0.00	0.00+/- 0.00	0.04+/- -0.01	0.00+/- -0.00	0+/- (0.02- 0.02)
Inventory	0.00+/- -0.00	0.00+/- -0.02	0.03+/- -0.00	0.00+/- -0.00	0.00+/- -0.00	0.00+/- -0.00	0.04+/- -0.01	0.00+/- -0.00	0.03+/- (0.02- 0.02)
197) Mauritius	0.00+/- 0.00	0.00+/- 0.01	0.02+/- 0.00	0.00+/- 0.00	0.00+/- 0.00	0.00+/- 0.00	0.04+/- 0.01	0.00+/- 0.00	0+/- (0.01- 0.01)
Inventory	0.00+/- -0.00	0.00+/- -0.00	0.01+/- -0.01	0.00+/- -0.00	0.00+/- -0.00	0.00+/- -0.00	0.04+/- -0.01	0.00+/- -0.00	0.02+/- (0.01- 0.01)
198) Dominica	0.00+/- 0.00	0.00+/- 0.00	0.00+/- 0.00	0.00+/- 0.00	0.00+/- 0.00	0.00+/- 0.00	0.04+/- 0.01	0.00+/- 0.00	0+/- (0.00- 0.00)
Inventory	0.00+/- -0.00	0.00+/- -0.00	0.00+/- -0.00	0.00+/- -0.00	0.00+/- -0.00	0.00+/- -0.00	0.04+/- -0.01	0.00+/- -0.00	0.00+/- (0.00- 0.00)
199) Antigua and Barbuda	0.00+/- 0.00	0.00+/- 0.00	0.00+/- 0.00	0.00+/- 0.00	0.00+/- 0.00	0.00+/- 0.00	0.04+/- 0.01	0.00+/- 0.00	0+/- (0.00- 0.00)
Inventory	0.00+/- -0.00	0.00+/- -0.00	0.00+/- -0.00	0.00+/- -0.00	0.00+/- -0.00	0.00+/- -0.00	0.04+/- -0.01	0.00+/- -0.00	0.00+/- (0.00- 0.00)
200) Saint Kitts and Nevis	0.00+/- 0.00	0.00+/- 0.00	0.00+/- 0.00	0.00+/- 0.00	0.00+/- 0.00	0.00+/- 0.00	0.04+/- 0.01	0.00+/- 0.00	0+/- (0.00- 0.00)

Formatted: Font color: Dark Red

[View Details](#)

Formatted: Font color: Dark Red

Formatted: Font color: Dark Red

<u>Inventory</u>	0.00+/- 0.00	0.00+/- 0.00	0.00+/- 0.00	0.00+/- 0.00	0.00+/- 0.00	0.00+/- 0.00	0.04+/- 0.01	0.00+/- 0.00	0.00+/- (0.00- 0.00)
222) Bouvet Island	0.00+/- 0.00	0.00+/- 0.00	0.00+/- 0.00	0.00+/- 0.00	0.00+/- 0.00	0.00+/- 0.00	0.04+/- 0.01	0.00+/- 0.00	0.00+/- (0.00- 0.00)
<u>Inventory</u>	0.00+/- 0.00	0.00+/- 0.00	0.00+/- 0.00	0.00+/- 0.00	0.00+/- 0.00	0.00+/- 0.00	0.04+/- 0.01	0.00+/- 0.00	0.00+/- (0.00- 0.00)
223) Tokelau	0.00+/- 0.00	0.00+/- 0.00	0.00+/- 0.00	0.00+/- 0.00	0.00+/- 0.00	0.00+/- 0.00	0.04+/- 0.01	0.00+/- 0.00	0.00+/- (0.00- 0.00)
<u>Inventory</u>	0.00+/- 0.00	0.00+/- 0.00	0.00+/- 0.00	0.00+/- 0.00	0.00+/- 0.00	0.00+/- 0.00	0.04+/- 0.01	0.00+/- 0.00	0.00+/- (0.00- 0.00)
224) South Georgia and the South Sandwich Islands	0.00+/- 0.00	0.00+/- 0.00	0.00+/- 0.00	0.00+/- 0.00	0.00+/- 0.00	0.00+/- 0.00	0.04+/- 0.01	0.00+/- 0.00	0.00+/- (0.00- 0.00)
<u>Inventory</u>	0.00+/- 0.00	0.00+/- 0.00	0.00+/- 0.00	0.00+/- 0.00	0.00+/- 0.00	0.00+/- 0.00	0.04+/- 0.01	0.00+/- 0.00	0.00+/- (0.00- 0.00)
225) Niue	0.00+/- 0.00	0.00+/- 0.00	0.00+/- 0.00	0.00+/- 0.00	0.00+/- 0.00	0.00+/- 0.00	0.04+/- 0.01	0.00+/- 0.00	0.00+/- (0.00- 0.00)
<u>Inventory</u>	0.00+/- 0.00	0.00+/- 0.00	0.00+/- 0.00	0.00+/- 0.00	0.00+/- 0.00	0.00+/- 0.00	0.04+/- 0.01	0.00+/- 0.00	0.00+/- (0.00- 0.00)
226) Norfolk Island	0.00+/- 0.00	0.00+/- 0.00	0.00+/- 0.00	0.00+/- 0.00	0.00+/- 0.00	0.00+/- 0.00	0.04+/- 0.01	0.00+/- 0.00	0.00+/- (0.00- 0.00)
<u>Inventory</u>	0.00+/- 0.00	0.00+/- 0.00	0.00+/- 0.00	0.00+/- 0.00	0.00+/- 0.00	0.00+/- 0.00	0.04+/- 0.01	0.00+/- 0.00	0.00+/- (0.00- 0.00)
227) British Indian Ocean Territory	0.00+/- 0.00	0.00+/- 0.00	0.00+/- 0.00	0.00+/- 0.00	0.00+/- 0.00	0.00+/- 0.00	0.04+/- 0.01	0.00+/- 0.00	0.00+/- (0.00- 0.00)
<u>Inventory</u>	0.00+/- 0.00	0.00+/- 0.00	0.00+/- 0.00	0.00+/- 0.00	0.00+/- 0.00	0.00+/- 0.00	0.04+/- 0.01	0.00+/- 0.00	0.00+/- (0.00- 0.00)
228) Heard Island and McDonald Islands	0.00+/- 0.00	0.00+/- 0.00	0.00+/- 0.00	0.00+/- 0.00	0.00+/- 0.00	0.00+/- 0.00	0.04+/- 0.01	0.00+/- 0.00	0.00+/- (0.00- 0.00)
<u>Inventory</u>	0.00+/- 0.00	0.00+/- 0.00	0.00+/- 0.00	0.00+/- 0.00	0.00+/- 0.00	0.00+/- 0.00	0.04+/- 0.01	0.00+/- 0.00	0.00+/- (0.00- 0.00)

Formatted: Font color: Dark Red

1245 **9.0 References**

1246

1247 Alvarez, R. A., Zavala-Araiza, D., Lyon, D. R. and Allen et al, D. T.: Assessment of methane
1248 emissions from the US oil and gas supply chain, *Science*, 361, 186–188,
1249 doi:10.1126/science.aar7204, 2018.

1250 Bachewe, F. N., Minten, B., Tadesse, F. and Taffesse, A. S.: The evolving livestock sector in
1251 Ethiopia: Growth by heads, not by productivity. 2018.

1252 Bergamaschi, P., Houweling, S., Segers, A., Krol, M., Frankenberg, C., Scheepmaker, R. A.,
1253 Dlugokencky, E., Wofsy, S. C., Kort, E. A., Sweeney, C., Schuck, T., Brenninkmeijer, C., Chen,
1254 H., Beck, V. and Gerbig, C.: Atmospheric CH₄ in the first decade of the 21st century: Inverse
1255 modeling analysis using SCIAMACHY satellite retrievals and NOAA surface measurements,
1256 *Journal of Geophysical Research-Atmospheres*, 118(13), 7350–7369, doi:10.1002/jgrd.50480,
1257 2013.

1258 Bloom, A. A., Bowman, K. W., Lee, M., Turner, A. J., Schroeder, R., Worden, J. R., Weidner,
1259 R., McDonald, K. C. and Jacob, D. J.: A global wetland methane emissions and uncertainty
1260 dataset for, *Geosci. Model Dev.*, 1–16, doi:10.5194/gmd-10-2141-2017, 2017.

1261 Bloom, A. A., Palmer, P. I., Fraser, A., Reay, D. S. and Frankenberg, C.: Large-Scale Controls of
1262 Methanogenesis Inferred from Methane and Gravity Spaceborne Data, *Science*, 327(5963), 322–
1263 325, doi:10.1126/science.1175176, 2010.

1264 Bowman, K. W., Rodgers, C. D., Kulawik, S. S., Worden, J., Sarkissian, E., Osterman, G., Steck,
1265 T., Lou, M., Eldering, A. and Shephard, M.: Tropospheric emission spectrometer: Retrieval
1266 method and error analysis, *IEEE TRANSACTIONS ON GEOSCIENCE AND REMOTE
1267 SENSING*, 44(5), 1297–1307, 2006.

1268 Buchwitz, M., Reuter, M., Schneising, O., Boesch, H., Guerlet, S., Dils, B., Aben, I., Armante,
1269 R., Bergamaschi, P., Blumenstock, T., Bovensmann, H., Brunner, D., Buchmann, B., Burrows, J.
1270 P., Butz, A., Chedin, A., Chevallier, F., Crevoisier, C. D., Deutscher, N. M., Frankenberg, C.,
1271 Hase, F., Hasekamp, O. P., Heymann, J., Kaminski, T., Laeng, A., Lichtenberg, G., Maziere, M.,
1272 D., Noël, S., Notholt, J., Orphal, J., Popp, C., Parker, R., Scholze, M., Sussmann, R., Stiller, G.,
1273 P., Warneke, T., Zehner, C., Bril, A., Crisp, D., Griffith, D. W. T., Kuze, A., O'Dell, C.,
1274 Oshchepkov, S., Sherlock, V., Suto, H., Wennberg, P., Wunch, D., Yokota, T., and Yoshida, Y.:
1275 The Greenhouse Gas Climate Change Initiative (GHG-CCI): Comparison and quality assessment
1276 of near-surface-sensitive satellite-derived CO₂ and CH₄ global data sets, *Remote Sens Environ.*
1277 162, 344–362, https://doi.org/10.1016/j.rse.2013.04.024, 2015.

1278 Formatted: Font: Times, 12 pt

1279 Formatted: Font: Times

1279 Ciais, P., Sabine, C., Bala, G., Bopp, L., Brovkin, V., Canadell, J., Chhabra, A., DeFries, R.,
1280 Galloway, J., Heimann, M., Jones, C., Le Quéré, C., Myneni, R. B., Piao, S., and Thornton, P.:
1281 Carbon and Other Biogeochemical Cycles, in: *Climate Change 2013: The Physical Science*
1282 Basis, Contribution of Working Group I to the Fifth Assessment Report of the Intergovernmental
1283 Panel on Climate Change, edited by: Stocker, T. F., Qin, D., Plattner, G.-K., Tignor, M., Allen,

- 1284 S. K., Boschung, J., Nauels, A., Xia, Y., Bex, V., and Midgley, P. M., Cambridge University
 1285 Press, Cambridge, UK, New York, NY, USA, 2013.
- 1286 Connor, B. J., Boesch, H., Toon, G., Sen, B., Miller, C. and Crisp, D.: Orbiting Carbon
 1287 Observatory: Inverse method and prospective error analysis, *J. Geophys. Res.*, 113(D5), D05305,
 1288 doi:10.1029/2006JD008336, 2008.
- 1289 Crippa, M., Solazzo, E., Huang, G., Guizzardi, D., Koffi, E., Muntean, M., Schieberle, C.,
 1290 Friedrich, R. and Janssens-Maenhout, G.: High resolution temporal profiles in the Emissions
 1291 Database for Global Atmospheric Research, *Scientific Data*, 1–17, doi:10.1038/s41597-020-
 1292 0462-2, 2020.
- 1293 [Cusworth, D. H., Jacob, D. J., Varon, D. J., Miller, C. C., Liu, X., Chance, K., Thorpe, A. K.,
 1294 Duren, R. M., Miller, C. E., Thompson, D. R., Frankenberg, C., Guanter, L., and Randles, C. A.:
 1295 Potential of next-generation imaging spectrometers to detect and quantify methane point sources
 1296 from space, *Atmos Meas Tech.*, 12, 5655–5668, <https://doi.org/10.5194/amt-12-5655-2019>, 2019,](#)
 1297
- 1298 [Cusworth, D. H., Duren, R. M., Thorpe, A. K., Eastwood, M. L., Green, R. O., Dennison, P. E.,
 1299 Frankenberg, C., Heckler, J. W., Asner, G. P., and Miller, C. E.: Quantifying Global Power Plant
 1300 Carbon Dioxide Emissions With Imaging Spectroscopy, *Agu Adv.*, 2,
 1301 <https://doi.org/10.1029/2020av000350>, 2021,](#)
- 1302 [Cusworth, D. H., Bloom, A. A., Ma, S., Miller, C. E., Bowman, K., Yin, Y., Maasakkers, J. D.,
 1303 Zhang, Y., Scarpelli, T. R., Qu, Z., Jacob, D. J. and Worden, J. R.: A Bayesian framework for
 1304 deriving sector-based methane emissions from top-down fluxes, *Nature Communications Earth
 1305 and Environment*, 1–8, doi:10.1038/s43247-021-00312-6, 2021,](#)
- 1307 [Deng, Z., Ciais, P., Tzompa-Sosa, Z. A., Saunois, M., Qiu, C., Tan, C., Sun, T., Ke, P., Cui, Y.,
 1308 Tanaka, K., Lin, X., Thompson, R. L., Tian, H., Yao, Y., Huang, Y., Lauerwald, R., Jain, A. K.,
 1309 Xu, X., Bastos, A., Sitch, S., Palmer, P. I., Lauvaux, T., d'Aspremont, A., Giron, C., Benoit, A.,
 1310 Poulet, B., Chang, J., Petrescu, A. M. R., Davis, S. J., Liu, Z., Grassi, G., Albergel, C., and
 1311 Chevallier, F.: Comparing national greenhouse gas budgets reported in UNFCCC inventories
 1312 against atmospheric inversions, *Earth Syst Sci Data Discuss.*, 2021, 1–59,
 1313 <https://doi.org/10.5194/essd-2021-235>, 2021,](#)
- 1315 Dlugokencky, E. J., Nisbet, E. G., Fisher, R. and Lowry, D.: Global atmospheric methane:
 1316 budget, changes and dangers, *Philosophical Transactions of the Royal Society A: Mathematical,
 1317 Physical and Engineering Sciences*, 369(1943), 2058–2072, doi:10.1098/rsta.2010.0341, 2011.
- 1318 Duren, R. M., Thorpe, A. K., Foster, K. T., Rafiq, T., Hopkins, F. M., Yadav, V., Bue, B. D.,
 1319 Thompson, D. R., Conley, S., Colombi, N. K., Frankenberg, C., McCubbin, I. B., Eastwood, M.
 1320 L., Falk, M., Herner, J. D., Croes, B. E., Green, R. O. and Miller, C. E.: California's methane
 1321 super-emitters, *Nature*, 575(7781), 180–184, doi:10.1038/s41586-019-1720-3, 2019.

Formatted: Font: Times, 12 pt

Formatted: Font: Times

Formatted: Font: Times, 12 pt

Formatted: Font: Times

Formatted: Font: (Default) Times New Roman

Formatted: Space After: 0 pt, Adjust space between Latin and Asian text, Adjust space between Asian text and numbers, Tab stops: Not at 0.39" + 0.78" + 1.17" + 1.56" + 1.94" + 2.33" + 2.72" + 3.11" + 3.5" + 3.89" + 4.28" + 4.67"

Formatted: Font: Times

Deleted: Cusworth, D., A. A. Bloom, S. Ma, et al.: A Bayesian framework for deriving sector-based methane emissions from top-down fluxes, *Communications Earth and Environment* (accepted).

Formatted: Font: Times, 12 pt

Formatted: Font: Times

- 1326 Etiope, G., Ciotoli, G., Schwietzke, S. and Schoell, M.: Gridded maps of geological methane
1327 emissions and their isotopic signature, *Earth System Science Data*, 11, 1–22, doi:10.5194/essd-
1328 11-1-2019, 2019.
- 1329 Frankenberg, C., Meirink, J., Van Weele, M., Platt, U. and Wagner, T.: Assessing methane
1330 emissions from global space-borne observations, *Science*, 308(5724), 1010–1014,
1331 doi:10.1126/science.1106644, 2005.
- 1332 Fung, I., Prather, M., John, J., Lerner, J. and Matthews, E.: Three-dimensional model synthesis
1333 of the global methane cycle, *Journal of Geophysical Research - Atmospheres*, 96(D7), 13.033–
1334 13.065, 1991.
- 1335 Ganesan, A. L., Rigby, M., Lunt, M. F., Parker, R. J., Boesch, H., Goulding, N., Umezawa, T.,
1336 Zahn, A., Chatterjee, A., Prinn, R. G., Tiwari, Y. K., Schoot, M. and Krummel, P. B.:
1337 Atmospheric observations show accurate reporting and little growth in India's methane
1338 emissions, *Nat Commun*, 1–7, doi:10.1038/s41467-017-00994-7, 2017.
- 1339 Ganesan, A. L., Schwietzke, S., Poulter, B., Arnold, T., Lan, X., Rigby, M., Vogel, F. R., Werf,
1340 G. R., Janssens-Maenhout, G., Boesch, H., Pandey, S., Manning, A. J., Jackson, R. B., Nisbet, E.
1341 G. and Manning, M. R.: Advancing Scientific Understanding of the Global Methane Budget in
1342 Support of the Paris Agreement, *Global Biogeochemical Cycles*, 9(1), 53–38,
1343 doi:10.1029/2018GB006065, 2019.
- 1344 Ganesan, A. L., Stell, A. C., Gedney, N., Comyn-Platt, E., Hayman, G., Rigby, M., Poulter, B.
1345 and Hornbrook, E. R. C.: Spatially Resolved Isotopic Source Signatures of Wetland Methane
1346 Emissions, *Geophys. Res. Lett.*, 45(8), 3737–3745, doi:10.1029/2008GB003299, 2018.
- 1347 Hmiel, B., Petrenko, V. V., Dyonisius, M. N., Buijzer, C., Smith, A. M., Place, P. F., Harth, C.,
1348 Beaudette, R., Hua, Q., Yang, B., Vimont, I., Michel, S. E., Severinghaus, J. P., Etheridge, D.,
1349 Bromley, T., Schmitt, J., Faïn, X., Weiss, R. F. and Dlugokencky, E.: Preindustrial $^{14}\text{CH}_4$
1350 indicates greater anthropogenic fossil CH_4 emissions, *Nature*, 1–5, doi:10.1038/s41586-020-
1351 1991-8, 2020.
- 1352 Janardanan, R., Maksyutov, S., Tsuruta, A., Wang, F., Tiwari, Y. K., Valsala, V., Ito, A.,
1353 Yoshida, Y., Kaiser, J. W., Janssens-Maenhout, G., Arshinov, M., Sasakawa, M., Tohjima, Y.,
1354 Worthy, D. E. J., Dlugokencky, E. J., Ramonet, M., Arduini, J., Lavric, J. V., Piacentino, S.,
1355 Krummel, P. B., Langenfelds, R. L., Mammarella, I. and Matsunaga, T.: Country-scale analysis
1356 of methane emissions with a high-resolution inverse model using GOSAT and surface
1357 observations, *Remote Sensing*, 12(3), 375, doi:10.3390/rs12030375, 2020.
- 1358 Janssens-Maenhout, G., Crippa, M., Guizzardi, D., Muntean, M., Schaaf, E., Dentener, F.,
1359 Bergamaschi, P., Pagliari, V., Olivier, J. G. J., Peters, J. A. H. W., van Aardenne, J. A., Monni,
1360 S., Doering, U., Petrescu, A. M. R., Solazzo, E. and Oreggioni, G. D.: EDGAR v4.3.2 Global
1361 Atlas of the three major greenhouse gas emissions for the period 1970–2012, *Earth Syst. Sci.*
1362 Data, 11(3), 959–1002, doi:10.5194/essd-11-959-2019, 2019.

- 1363 Jiang, Z., Jones, D. B. A., Worden, H. M., Deeter, M. N., Henze, D. K., Worden, J., Bowman, K.
1364 W., Brenninkmeijer, C. A. M. and Schuck, T. J.: Impact of model errors in convective transport
1365 on CO source estimates inferred from MOPITT CO retrievals, *Journal of Geophysical Research-Atmospheres*, 118(4), 2073–2083, doi:10.1002/jgrd.50216, 2013.
- 1366
- 1367 Kirschke, S., Bousquet, P., Ciais, P., Saunois, M., Canadell, J. G., Dlugokencky, E. J.,
1368 Bergamaschi, P., Bergmann, D., Blake, D. R., Bruhwiler, L., Cameron-Smith, P., Castaldi, S.,
1369 Chevallier, F., Feng, L., Fraser, A., Heimann, M., Hodson, E. L., Houweling, S., Josse, B.,
1370 Fraser, P. J., Krummel, P. B., Lamarque, J.-F., Langenfelds, R. L., Le Quéré, C., Naik, V.,
1371 O'Doherty, S., Palmer, P. I., Pison, I., Plummer, D., Poulter, B., Prinn, R. G., Rigby, M.,
1372 Ringeval, B., Santini, M., Schmidt, M., Shindell, D. T., Simpson, I. J., Spahni, R., Steele, L. P.,
1373 Strode, S. A., Sudo, K., Szopa, S., van der Werf, G. R., Voulgarakis, A., van Weele, M., Weiss,
1374 R. F., Williams, J. E. and Zeng, G.: Three decades of global methane sources and sinks, *Nature Geoscience*, 1–11, doi:10.1038/ngeo1955, 2013.
- 1375
- 1376 Lu, X., Jacob, D. J., Zhang, Y., Maasakkers, J. D., Sulprizio, M. P., Shen, L., et al.: Global
1377 methane budget and trend, 2010–2017: complementarity of inverse analyses using in situ
1378 (GLOBALVIEWplus CH₄ ObsPack) and satellite (GOSAT) observations, *Atmos. Chem. Phys.*,
1379 21, 4637–4657, <https://doi.org/10.5194/acp-21-4637-2021>, 2021.
- 1380 Maasakkers, J. D., Jacob, D. J., Sulprizio, M. P., Scarpelli, T. R., Nesser, H., Sheng, J., Zhang,
1381 Y., Lu, X., Bloom, A. A., Bowman, K. W., Worden, J. R. and Parker, R. J.: 2010–2015 North
1382 American methane emissions, sectoral contributions, and trends: a high-resolution inversion of
1383 GOSAT observations of atmospheric methane, *Atmospheric Chemistry and Physics*, 21(6),
1384 4339–4356, doi:10.5194/acp-21-4339-2021, 2021.
- 1385 Maasakkers, J. D., Jacob, D. J., Sulprizio, M. P., Scarpelli, T. R., Nesser, H., Sheng, J.-X.,
1386 Zhang, Y., Hersher, M., Bloom, A. A., Bowman, K. W., Worden, J. R., Janssens-Maenhout, G.,
1387 and Parker, R. J.: Global distribution of methane emissions, emission trends, and OH
1388 concentrations and trends inferred from an inversion of GOSAT satellite data for 2010–2015,
1389 *Atmospheric Chemistry and Physics*, 19(11), 7859–7881, doi:10.5194/acp-19-7859-2019, 2019.
- 1390 Maasakkers, J. D., Jacob, D. J., Sulprizio, M. P., Turner, A. J., Weitz, M., Wirth, T., Hight, C.,
1391 DeFigueiredo, M., Desai, M., Schmeltz, R., Hockstad, L., Bloom, A. A., Bowman, K. W., Jeong,
1392 S. and Fischer, M. L.: Gridded National Inventory of U.S. Methane Emissions, *Environ. Sci.
1393 Technol.*, 50(23), 13123–13133, doi:10.1021/acs.est.6b02878, 2016.
- 1394 McNorton, J. R., Bousserez, N., Agustí-Panareda, A., Balsamo, G., Choulga, M., Dawson, A.,
1395 Engelen, R., Kipling, Z. and Lang, S.: Representing model uncertainty for global atmospheric
1396 CO₂ flux inversions using ECMWF-IFS-46R1, *Geosci. Model Dev.*, 13(5), 2297–
1397 2313, doi:10.5194/gmd-13-2297-2020, 2020.
- 1398 Melton, J. R., Wania, R., Hodson, E. L., Poulter, B., Ringeval, B., Spahni, R., Bohn, T., Avis, C.
1399 A., Beerling, D. J., Chen, G., Eliseev, A. V., Denisov, S. N., Hopcroft, P. O., Lettenmaier, D. P.,
1400 Riley, W. J., Singarayer, J. S., Subin, Z. M., Tian, H., Zürcher, S., Brovkin, V., van Bodegom, P.
1401 M., Kleinen, T., Yu, Z. C. and Kaplan, J. O.: Present state of global wetland extent and wetland

- 1402 methane modelling: conclusions from a model inter-comparison project (WETCHIMP),
1403 *Biogeosciences*, 10(2), 753–788, doi:10.5194/bg-10-753-2013, 2013.
- 1404 Miller, S. M., Michalak, A. M., Detmers, R. G., Hasekamp, O. P., Bruhwiler, L. M. P. and
1405 Schwietzke, S.: China's coal mine methane regulations have not curbed growing emissions, *Nat*
1406 *Commun*, 10(1), 1–8, doi:10.1038/s41467-018-07891-7, 2019.
- 1407 Pandey, S., Gautam, R., Houweling, S., van der Gon, H. D., Sadavarte, P., Borsdorff, T.,
1408 Hasekamp, O., Landgraf, J., Tol, P., van Kempen, T., Hoogeveen, R., van Hees, R., Hamburg, S.
1409 P., Maasakkers, J. D. and Aben, I.: Satellite observations reveal extreme methane leakage from a
1410 natural gas well blowout, *Proceedings of the National Academy of Sciences of the United States*
1411 *of America*, 116(52), 26376–26381, doi:10.1073/pnas.1908712116, 2019.
- 1412 Parker, R., Boesch, H., Cogan, A., Fraser, A., Feng, L., Palmer, P. I., Messerschmidt, J.,
1413 Deutscher, N., Griffith, D. W. T., Notholt, J., Wennberg, P. O. and Wunch, D.: Methane
1414 observations from the Greenhouse Gases Observing SATellite: Comparison to ground-based
1415 TCCON data and model calculations, *Geophys. Res. Lett.*, 38(15), L15807,
1416 doi:10.1029/2011GL047871, 2011.
- 1417 Poulter, B., Bousquet, P., Canadell, J. G., Ciais, P., Peregon, A., Saunois, M., Arora, V. K.,
1418 Beerling, D. J., Brovkin, V., Jones, C. D., Joos, F., Gedney, N., Ito, A., Kleinen, T., Koven, C.
1419 D., McDonald, K., Melton, J. R., Peng, C., Peng, S., Prigent, C., Schroeder, R., Riley, W. J.,
1420 Saito, M., Spahni, R., Tian, H., Taylor, L., Viovy, N., Wilton, D., Wiltshire, A., Xu, X., Zhang,
1421 B., Zhang, Z. and Zhu, Q.: Global wetland contribution to 2000–2012 atmospheric methane
1422 growth rate dynamics, *Environ. Res. Lett.*, 12(9), 094013, doi:10.1088/1748-9326/aa8391, 2017.
- 1423 Prather, M. J., Holmes, C. D. and Hsu, J.: Reactive greenhouse gas scenarios: Systematic
1424 exploration of uncertainties and the role of atmospheric chemistry, *Geophysical Research*
1425 *Letters*, 39(9), doi:10.1029/2012GL051440, 2012.
- 1426 Qu, Z., Jacob, D. J., Shen, L., Lu, X., Zhang, Y., Scarpelli, T. R., Nesser, H., Sulprizio, M. P.,
1427 Maasakkers, J. D., Bloom, A. A., Worden, J., Parker, R. J. and Delgado, A. L.: Global
1428 distribution of methane emissions: a comparative inverse analysis of observations from the
1429 TROPOMI and GOSAT satellite instruments, *Atmospheric Chemistry and Physics*,
1430 doi:10.5194/acp-21-14159-2021, 2021.
- 1431 Rodgers, C. D. and Connor, B. J.: Intercomparison of remote sounding instruments, *Journal of*
1432 *Geophysical Research-Atmospheres*, 108, 4116, doi:10.1029/2002JD002299, 2003.
- 1433 Rosentreter, J. A., Borges, A. V., Deemer, B. R., Holgerson, M. A., Liu, S., Song, C., Melack, J.,
1434 Raymond, P. A., Duarte, C. M., Allen, G. H., Olefeldt, D., Poulter, B., Battin, T. I. and Eyre, B.
1435 D.: Half of global methane emissions come from highly variable aquatic ecosystem sources,
1436 *Nature Geoscience*, 14(4), 225–230, doi:10.1038/s41561-021-00715-2, 2021.
- 1437 Saunois, M., Stavert, A. R., Poulter, B., Bousquet, P., Canadell, J. G., Jackson, R. B., Raymond,
1438 P. A., Dlugokencky, E. J., Houweling, S., Patra, P. K., Ciais, P., Arora, V. K., Bastviken, D.,
1439 Bergamaschi, P., Blake, D. R., Brailsford, G., Bruhwiler, L., Carlson, K. M., Carroll, M.,

1440 Castaldi, S., Chandra, N., Crevoisier, C., Crill, P. M., Covey, K., Curry, C. L., Etiope, G.,
1441 Frankenberg, C., Gedney, N., Hegglin, M. I., Höglund-Isaksson, L., Hugelius, G., Ishizawa, M.,
1442 Ito, A., Janssens-Maenhout, G., Jensen, K. M., Joos, F., Kleinen, T., Krummel, P. B.,
1443 Langenfelds, R. L., Laruelle, G. G., Liu, L., Machida, T., Maksyutov, S., McDonald, K. C.,
1444 McNorton, J., Miller, P. A., Melton, J. R., Morino, I., Müller, J., Murguia-Flores, F., Naik, V.,
1445 Niwa, Y., Noce, S., O'Doherty, S., Parker, R. J., Peng, C., Peng, S., Peters, G. P., Prigent, C.,
1446 Prinn, R., Ramonet, M., Regnier, P., Riley, W. J., Rosentreter, J. A., Segers, A., Simpson, I. J.,
1447 Shi, H., Smith, S. J., Steele, L. P., Thornton, B. F., Tian, H., Tohjima, Y., Tubiello, F. N.,
1448 Tsuruta, A., Viovy, N., Voulgarakis, A., Weber, T. S., van Weele, M., van der Werf, G. R.,
1449 Weiss, R. F., Worthy, D., Wunch, D., Yin, Y., Yoshida, Y., Zhang, W., Zhang, Z., Zhao, Y.,
1450 Zheng, B., Zhu, Q., Zhu, Q. and Zhuang, Q.: The Global Methane Budget 2000–2017, Earth
1451 Syst. Sci. Data, 12(3), 1561–1623, doi:10.5194/essd-12-1561-2020, 2020.

1452 Scarpelli, T. R., Jacob, D. J., Maasakers, J. D., Sulprizio, M. P., J-X, S., Rose, K., Romeo, L.,
1453 Worden, J. R. and Janssens-Maenhout, G.: A global gridded (0.1 degrees x 0: 1 degrees)
1454 inventory of methane emissions from oil, gas, and coal exploitation based on national reports to
1455 the United 2020.

1456 Schaefer, H., Fletcher, S. E. M., Veidt, C., Lassey, K. R., Brailsford, G. W., Bromley, T. M.,
1457 Dlugokencky, E. J., Michel, S. E., Miller, J. B., Levin, I., Lowe, D. C., Martin, R. J., Vaughn, B.
1458 H. and White, J. W. C.: A 21st century shift from fossil-fuel to biogenic methane emissions
1459 indicated by $^{13}\text{CH}_4$, Science, doi:10.1126/science.aad2705, 2016.

1460 Schwietzke, S., Sherwood, O. A., Bruhwiler, L. M. P., Miller, J. B., Etiope, G., Dlugokencky, E.
1461 J., Michel, S. E., Arling, V. A., Vaughn, B. H., White, J. W. C. and Tans, P. P.: Upward revision
1462 of global fossil fuel methane emissions based on isotope database, Nature, 538(7623), 88–91,
1463 doi:10.1038/nature19797, 2016.

1464 Shen, L., D. Zavala-Araiza, R. Gautam, M. Omara, T. Scarpelli, J. Sheng, M.P. Sulprizio, J.
1465 Zhuang, Y. Zhang, Z. Qu, X. Lu, S. Hamburg, and D.J. Jacob, *Unravelling a large methane*
1466 *emission discrepancy in Mexico using satellite observations*, Remote Sensing Environ.,
1467 260, 112461, 2021.

1468 Shindell, D. T., Faluvegi, G., Koch, D. M., Schmidt, G. A., Unger, N. and Bauer, S. E.:
1469 Improved Attribution of Climate Forcing to Emissions, Science, 326(5953), 716–718,
1470 doi:10.1126/science.1174760, 2009.

1471 Stavert, A. R., Saunois, M., Canadell, J. G., Poulter, B., Jackson, R. B., Regnier, P., Lauerwald,
1472 R., Raymond, P. A., Allen, G. H., Patra, P. K., Bergamaschi, P., Bousquet, P., Chandra, N.,
1473 Ciais, P., Gustafson, A., Ishizawa, M., Ito, A., Kleinen, T., Maksyutov, S., McNorton, J., Melton,
1474 J. R., Müller, J., Niwa, Y., Peng, S., Riley, W. J., Segers, A., Tian, H., Tsuruta, A., Yin, Y.,
1475 Zhang, Z., Zheng, B., and Zhuang, Q.: *Regional trends and drivers of the global methane budget*,
1476 *Global Change Biol.*, 28, 182–200, <https://doi.org/10.1111/gcb.15901>, 2022.

Formatted: Font: Times, 12 pt

1477 Tsuruta, A., Aalto, T., Backman, L., Hakkarainen, J., Laan-Luijkx, I. T. van der, Krol, M. C.,
1478 Spahni, R., Houweling, S., Laine, M., Dlugokencky, E., Gomez-Pelaez, A. J., Schoot, M. van
1479 der, Langenfelds, R., Ellul, R., Arduini, J., Apadula, F., Gerbig, C., Feist, D. G., Kivi, R.,

Formatted: Font: Times

Formatted: Font: Times, 12 pt

- 1481 [Yoshida, Y., and Peters, W.: Global methane emission estimates for 2000–2012 from](#)
1482 [CarbonTracker Europe-CH4 v1.0, Geosci Model Dev, 10, 1261–1289,](#)
1483 [https://doi.org/10.5194/gmd-10-1261-2017, 2017.](https://doi.org/10.5194/gmd-10-1261-2017)
- 1484 ↑ Turner, A. J., Frankenberg, C. and Kort, E. A.: Interpreting contemporary trends in atmospheric
1485 methane, Proceedings of the National Academy of Sciences of the United States of America,
1486 8(8), 201814297–9, doi:10.1073/pnas.1814297116, 2019.
- 1487 ↑ Turner, A. J., Frankenberg, C., Wennberg, P. and Jacob, D.: Ambiguity in the causes for decadal
1488 trends in atmospheric methane and hydroxyl. 2017.
- 1489 ↑ Turner, A. J., Fung, I., Naik, V., Horowitz, L. W. and Cohen, R. C.: Modulation of hydroxyl
1490 variability by ENSO in the absence of external forcing, Proceedings of the National Academy of
1491 Sciences of the United States of America, 115(36), 8931–8936, doi:10.1073/pnas.1807532115,
1492 2018.
- 1493 ↑ van der Werf, G. R., Randerson, J. T., Giglio, L., van Leeuwen, T. T., Chen, Y., Rogers, B. M.,
1494 Mu, M., van Marle, M. J. E., Morton, D. C., Collatz, G. J., Yokelson, R. J. and Kasibhatla, P. S.:
1495 Global fire emissions estimates during 1997–2016, Earth Syst. Sci. Data, 9(2), 697–720,
1496 doi:10.5194/acp-9-5785-2009, 2017.
- 1497 ↑ Varon, D. J., McKeever, J., Jervis, D., Maasakkers, J. D., Pandey, S., Houweling, S., Aben, I.,
1498 Scarpelli, T. and Jacob, D. J.: Satellite Discovery of Anomalously Large Methane Point Sources
1499 From Oil/Gas Production, Geophys. Res. Lett, 361(23), 186–10, doi:10.1029/2019GL083798,
1500 2019.
- 1501 ↑ [Wolf, J., Asrar, G. R., and West, T. O.: Revised methane emissions factors and spatially](#)
1502 [distributed annual carbon fluxes for global livestock, Carbon Balance Management, 12, 16,](#)
1503 [https://doi.org/10.1186/s13021-017-0084-y, 2017](https://doi.org/10.1186/s13021-017-0084-y)
- 1504 ↑ Worden, J. R., Bloom, A. A., Pandey, S., Jiang, Z., Worden, H. M., Walker, T. W., Houweling,
1505 S. and Röckmann, T.: Reduced biomass burning emissions reconcile conflicting estimates of the
1506 post-2006 atmospheric methane budget, Nat Commun, 1–11, doi:10.1038/s41467-017-02246-0,
1507 2017.
- 1508 ↑ Worden, J., Kulawik, S., Shepard, M., Clough, S., Worden, H., Bowman, K. and Goldman, A.:
1509 Predicted errors of tropospheric emission spectrometer nadir retrievals from spectral window
1510 selection, Journal of Geophysical Research-Atmospheres, 109(D9), D09308,
1511 doi:10.1029/2004JD004522, 2004.
- 1512 ↑ Yu, X., Millet, D. B., Wells, K. C., Henze, D. K., Cao, H., Griffis, T. J., Kort, E. A., Plant, G.,
1513 Deventer, M. J., Kolka, R. K., Roman, D. T., Davis, K. J., Desai, A. R., Baier, B. C., McKain,
1514 K., Czarnetzki, A. C. and Bloom, A. A.: Aircraft-based inversions quantify the importance of
1515 wetlands and livestock for Upper Midwest methane emissions, Atmospheric Chemistry and
1516 Physics, 21(2), 951–971, doi:10.5194/acp-21-951-2021, 2021.

Formatted: Font:

Formatted: Space After: 0 pt, Adjust space between Latin and Asian text, Adjust space between Asian text and numbers, Tab stops: Not at 0.39" + 0.78" + 1.17" + 1.56" + 1.94" + 2.33" + 2.72" + 3.11" + 3.5" + 3.89" + 4.28" + 4.67"

Formatted: Font: Times, 12 pt

Formatted: Font:

Formatted: Space After: 0 pt, Adjust space between Latin and Asian text, Adjust space between Asian text and numbers, Tab stops: Not at 0.39" + 0.78" + 1.17" + 1.56" + 1.94" + 2.33" + 2.72" + 3.11" + 3.5" + 3.89" + 4.28" + 4.67"

1519 Zavala-Araiza, D., Lyon, D. R., Alvarez, R. A., Davis, K. J., Harriss, R., Herndon, S. C., Karion,
1520 A., Kort, E. A., Lamb, B. K., Lan, X., Marchese, A. J., Pacala, S. W., Robinson, A. L., Shepson,
1521 P. B., Sweeney, C., Talbot, R., Townsend-Small, A., Yacovitch, T. I., Zimmerle, D. J. and
1522 Hamburg, S. P.: Reconciling divergent estimates of oil and gas methane emissions, Proceedings
1523 of the National academy of Sciences, 201522126, doi:10.1073/pnas.1522126112, 2015.

1524 Zhang, Y., Jacob, D. J., Lu, X., Maasakkers, J. D., Scarpelli, T. R., Sheng, J.-X., Shen, L., Qu,
1525 Z., Sulprizio, M. P., Chang, J., Bloom, A. A., Ma, S., Worden, J., Parker, R. J. and Boesch, H.:
1526 Attribution of the accelerating increase in atmospheric methane during 2010–2018 by inverse
1527 analysis of GOSAT observations, Atmospheric Chemistry and Physics, 21(5), 3643–3666,
1528 doi:10.5194/acp-21-3643-2021, 2021.

1529

Page 2: [1] Deleted **Microsoft Office User** **3/12/22 1:08:00 AM**

▼

Page 2: [2] Deleted **Microsoft Office User** **3/12/22 1:19:00 AM**

▼

▲